Two genes involved in trichome morphogenesis: Localisation and putative function of STI and At-CLASP in *A. thaliana.*

Inaugural-Dissertation

zur

Erlangung des Doktorgrades

der Mathematisch-Naturwissenschaftlichen Fakultät

der Universität zu Köln

vorgelegt von

Ullrich Herrmann

aus Frechen

Köln

2007

Table of Contents

Index of figures

Index of tables

Index of abbreviations

μ	micro
A. thaliana	*Arabidopsis thaliana*
Aa	amino acid(s)
At-CLASP	CLASP similar protein At2g20190
ATP	Adenosine Triphosphate
BiFC	Bimolecular Fluorescence Complementation
BLAST	Basic Local Alignment Tool
C. elegans	*Caenorhabditis elegans*
cDNA	complementary DNA
CFP	Cyan Fluorescent Protein
CPC	CAPRICE
CPR5	Constitutive Pathogen Response 5
D. melanogaster	*Drosophila melanogaster*
D. rerio	*Danio rerio*
DAPI	4',6-Diamidino-2-phenylindol
DNA	Desoxyribonucleic acid
EB1	END BINDING PROTEIN 1
EGL3	ENHANCER OF GLABRA 3
g	gramm
GFP	Green Fluorescent Protein
GL1	GLABRA1
H. sapiens	*Homo sapiens*
ICK	INHIBITOR OF CYCLIN DEPENDENT KINASES
KAK	KAKTUS
Kb	kilobase
kDa	kilo dalton
L*er*	Landsberg *erecta*
M	mol per litre
M. musculus	*Mus musculus*
M. truncatula	*Medicago truncatula*
min	minute
mRNA	messenger RNA
NLS	Nuclear localization signal
O. lucimarinus	*Ostreococcus lucimarinus*
O. sativa	*Oryza sativa*
O. tauri	*Ostreococcus tauri*
ORF	open reading frame
P. patens	*Physcomitrella patens*
PAGE	Polyacrylamide gel electrophoresis
PCR	Polymerase chain reaction
R. norvegicus	*Rattus norvegicus*
RFP	Red Fluorescent Protein
RNA	Ribonucleic acid
Rpm	rounds per minute
RT	Room Temperature
RT	room temperature
SDS	Sodiumdodecylsulfate
SIM	SIAMESE
SPR1	SPIRAL 1
STI	STICHEL
STI-HOM	STI homologous protein At1g14460
T-DNA	transfer DNA
TFC-A	TUBULIN COFACTOR A
TRY	TRIPTYCHON
TTG1	TRANSPARENT TESTA GLABRA 1
TUA4	TUBULIN 4
V. vinifera	*Vitis vinifera*
YFP	Yellow Fluorescent Protein

Abstract

Within the scope of this thesis two proteins were analysed whose mutant phenotype affects the branching of trichomes.

at-clasp mutant plants posses unbranched trichomes and the strength of the phenotype depends on the allele used. Sterility is observed in the strongest alleles. Furthermore it was shown that the *at-clasp* mutant phenotype is temperature dependant. Growth conditions with temperatures up to 16°C are permissive for normal growth of all alleles. To determine the localisation of At-CLASP, fusions to fluorescent proteins were constructed. It was shown that At-CLASP is localised to microtubules. Contrary to the data from *H. sapiens,* At-CLASP localisation was not restricted to the +end of microtubules but marks filaments almost entirely. To understand the binding properties of At-CLASP to microtubules, it was dissected into two fragments. The C-terminal region of the protein was localised to the cell-cortex or the plasma membrane. In contrast, the N-terminal region was sufficient to mediate the binding to microtubules as this fragment was hardly distinguishable from the entire protein. Despite the altered localisation of At-CLASP compared to *H. sapiens* CLASP, several orthologs of *H. sapiens* CLASP interaction partners were identified in the *A. thaliana* genome. These putative *A. thaliana* binding partners were tested for interaction with At-CLASP in direct Yeast-Two-Hybrid experiments. However, no interactions were detected. One postulated function of CLASP from *H. sapiens* is the stabilisation of subsets of microtubules. To test a similar function of the *A. thaliana* protein, the rescue of the *tfc-a* mutant under an increased dosage of At-CLASP was analysed. Preliminary results suggest that a stabilizing function of At-CLASP might be evolutionary retained.

Trichomes of strong s*tichel* alleles are completely unbranched. To improve the understanding of STI function plants expressing GFP:STI fusions were analysed further. GFP:STI fusion proteins mark the tip of emerging trichomes. As soon as a trichomes becomes visible by means of morphological criteria, GFP:STI can be detected in the tip of trichomes. Trichomes that initiate the second branch showed GFP:STI signal even before the branch was visible. Plasmolysis experiments demonstrated that GFP:STI is likely localised to the plasma membrane. In order to get a closer insight into which part of the STI protein is responsible for its specific localization, fragments were analysed for showing a comparable localisation pattern. Fusions of parts of the STI protein with YFP could not reveal the likely present motif for the described localisation. Nevertheless one longer fragment S1/AS3 and one shorter fragment S3/AS3 showed a strong dominant negative effect when overexpressed in wild-type. To increase the understanding about the molecular function of STI, possible binding partners of GFP:STI were identified by an immunoprecipitation assay.

Phospholipase Dα1 and one transcription factor of the MADS-box family were identified as candidates for interaction with STI. *A. thaliana* contains one gene (*STI-HOM*) which is very similar to STI. To test whether STI-HOM fulfils a comparable a role in trichome development T-DNA mutants were analysed. None of them showed a trichome phenotype. The analysis of a *sti sti-hom* double-mutant situation revealed no change in the *sti* mutant trichome phenotype. Promoter swapping experiments were performed to test whether both proteins are functionally exchangeable. However STI-HOM was not able to rescue the *sti* mutant trichome phenotype. Therefore STI and STI-HOM are likely functionally distinct.

Zusammenfassung

Im Rahmen dieser Dissertation wurden zwei Proteine untersucht, dessen mutanter Phänotyp eine gestörte Verzweigung von Trichomen ist. *at-clasp* mutante Pflanzen sind unterverzweigt und die Stärke des Phänotyps ist vom verwendeten Allel abhängig. Sterilität der Pflanzen wurde bei starken Allelen beobachtet. Weiterhin wurde gezeigt, dass der *at-clasp* mutante Phänotyp abhängig von der Temperatur ist. Wachstumsbedingungen mit Temperaturen von maximal 16°C erlauben normales Wachstum. Um die Lokalisierung von At-CLASP festzustellen wurden Fusionen mit fluoreszierenden Proteinen hergestellt. Es wurde gezeigt, dass At-CLASP an Mikrotubuli lokalisiert ist. Im Gegensatz zu den Daten von *H. Sapiens* ist At-CLASP nicht ausschließlich am +Ende von Mikrotubuli lokalisiert, sondern markiert vollständige Filamente. Um die Bindung von At-CLASP an Mikrotubuli besser zu verstehen wurde es in zwei Fragmente unterteilt. Der C-terminale Bereich des Proteins war am Zell-Cortex oder der Plasmamembran lokalisiert. Im Gegensatz dazu war der N-terminale Bereich ausreichend, um Mikrotubuli zu binden und konnte somit vom Lokalisierungsmuster des vollständigen Proteins kaum unterschieden werden. Abgesehen vom veränderten Lokalisierungsmuster von At-CLASP im Vergleich zu *H. sapiens* CLASP wurden verschiedene Orthologe von *H. sapiens* CLASP Bindungspartnern im Genom von *A. thaliana* identifiziert. Diese putativen Bindungspartner aus *A. thaliana* wurden auf Interaktion mittels des direktem Hefe-2-Hybrid Systems getestet. Jedoch konnte keine Interaktion festgestellt werden. Eine putative Funktion von CLASP aus *H. sapiens* ist die Stabilisierung von bestimmten Mikrotubuli Filamenten. Um eine ähnliche Funktion des *A. thaliana* Proteins zu überprüfen wurde versucht die *tfc-a* Mutante mit einer erhöhten Menge von At-CLASP zu retten. Vorläufige Ergebnisse deuten darauf hin, dass eine solche Funktion evolutionär erhalten geblieben sein könnte.

Trichome von starken *stichel* Allelen sind vollständig unverzweigt. Um das Verständnis über die Funktion von STI zu verbessern wurden GFP:STI Fusionen untersucht. GFP:STI Fusionsproteine markieren die Spitze von Trichomen. Sobald ein Trichome aufgrund von morphologischen Kriterien zu erkennen ist, kann GFP:STI in der Spitze detektiert werden. Trichome, die sich kurz vor der Einführung der zweiten Verzweigung befinden zeigen das GFP:STI Signal am Ort der Spitze der neuen Verzweigung bevor diese zu erkennen ist. Plasmolyse Experimente zeigten, dass GFP:STI wahrscheinlich in der Plasmamembran lokalisiert ist. Um festzustellen welcher Teil des STI Proteins notwendig ist, um diese spezifische Lokalisierung zu erreichen wurden Fragmente auf ein vergleichbares Lokalisierungsmuster untersucht. Jedoch konnten Fusionen von YFP mit verschiedenen Fragmenten keine möglicherweise vorhandenen Motive, welches erforderlich für die

3

Lokalisierung sein könnte, identifizieren. Interessanterweise zeigten ein längeres Fragment S1/AS3 und ein kürzeres Fragment S3/AS3 einen starken dominant negativen Effekt wenn sie im Wildtyp überexprimiert wurden. Um das Verständnis der molekularen Funktion von STI zu verbessern wurden mögliche Bindungspartner von GFP:STI über Immunopräzipitation identifiziert. Phospholipase Dα1 und ein Transkriptionsfaktor der MADS-box Familie wurden als Kandidaten für eine mögliche Interaktion mit STI identifiziert. *A. thaliana* enthält ein Gen (*STI-HOM*) welches sehr ähnlich zu *STI* ist. Um festzustellen ob STI-HOM eine vergleichbare Rolle in der Trichomentwicklung hat wurden T-DNA Mutanten untersucht. Keine davon zeigte einen Trichomphänotyp. Auch die Analyse von *sti sti-hom* Doppelmutanten zeigte keine Änderung des *sti* mutanten Trichomphänotyps. Außerdem wurden Experimente durchgeführt bei denen der Promoter von beiden Genen getauscht wurde, um festzustellen ob beide Proteine funktional austauschbar sind. Jedoch war STI-HOM nicht in der Lage den *sti* mutanten Trichomphänotyp zu retten. Somit ist es wahrscheinlich, dass STI und STI-HOM funktonal unterschiedlich sind.

❖ Clasp

1   Introduction

Any plant cell has organelles and compartments with a defined spatial and temporal organisation. Also any process related to growth or the reaction to mechanical stimuli is highly dependent onto the cytoskeleton. The plant cytoskeleton consists of three families of proteins, actin, tubulin and intermediate filaments. Actin filaments are polymers of single globular actins (G-actin) that form a slightly helical structure of approximately 8nm diameter. Actin and tubulin belong to gene-families with several members. The actin family consists of eight members which are separated into a vegetative class, expressed in almost every tissue, and a reproductive class that is expressed predominantly in reproductive organs (Kandasamy et al. 2002). Tubulin filaments are assembled from heterodimeric globular α- and β-tubulin. These filaments form a hollow structure of approximately 13 protofilaments whereas every protofilaments consists of tubulin dimers bound to their ends. A typical microtubule filament has a diameter of 25nm and is therefore wider than intermediate filaments (Hussey et al. 2002). Intermediate filaments have an intermediate diameter of 10 to 15nm when compared to actin or tubulin filaments (Buchanan et al. 2000). Important animal intermediate-filaments are for example keratins, nuclear lamins or neurofilament proteins. These filaments have a rod-forming α-helical domain flanked by diverse globular domains. Until now it is unknown whether intermediate-filaments in plants are present. Due to the absence of keratins and neurofilaments in plants and a different structural composition concerning signalling and stability of cells (a rigid cell-wall is present), intermediate-filaments might not be present in *A. thaliana*.

The functions of cytoskeletal filaments are diverse. They help to anchor organelles or macromolecules like polysomes with the help of additional proteins to the plasmamembrane (Figure 1A). In addition the cytoskeleton serves as track for motor proteins that transport cargo to different locations within the cell (Figure 1B). One especially important aspect of the cytoskeleton is the polarity. Tubulin and actin proteins itself are polar proteins in respect to their asymmetric structure. In addition tubulin filaments are derived by the association of α- and β-subunits providing further polarity. Actin filaments consist of actin monomers that bind each other through noncovalent bonds to yield a slender helical structure. Furthermore both ends of cytoskeletal filaments have different assembly/disassembly rates leading to a preferential growing +end during growth-phase. These different rates are possible thru binding of accessory proteins, in case of microtubule these are microtubule-associated proteins (MAPs). In particular these MAPs, important for this study, are plus-end-tracking proteins (+TIPs) as they are bound to the growing microtubule end and modulate

the dynamic assembly/disassembly mentioned above. The combination of these different properties enables a cell to define axes. For example a filament forming a spiral that moves to the right establishes a new axis, left to right (Figure 1C). Furthermore filaments can generate polarity to a cell by transporting cargo preferentially to one place within a cell for example the tip of a growing trichome branch (Figure 1D).

During the growth of any organism the amount of cell needs to be increased, a process which is depended on the replication of DNA that takes place during mitosis. Microtubules are essential to form the spindle-apparatus that provides the mechanical force for the separation of the sister chromatids (summarized by (Sitte et al. 1998). Microtubules connect both spindle poles, the kinetochores and are directed to the cell-periphery. Plants posses special microtubule containing structures which are unique to this kingdom. The preprophase band is assembled in preparation of the following mitosis. It marks the position of the future cell-plate and might alter the cell-wall properties locally (Mineyuki 1999; Wasteneys 2002). At the Anaphase-Telophase transition arrays of microtubule form the phragmoplast which is located between the two daughter nuclei. The phragmoplast supplies the "skeleton" which is necessary to direct all needed components to the place of cell-wall synthesis.

The usage of trichome cells as a model system for morphogenesis in cells with a complex structure, allowed the identification of several mutants affecting the cytoskeleton (Hulskamp et al. 1994; Marks 1997; Zhang et al. 2005). The following pages summarize the status quo of mutants and their effect *in planta*. Afterwards the current knowledge about +TIPs in other organisms, with the main focus on CLASP, is compiled.
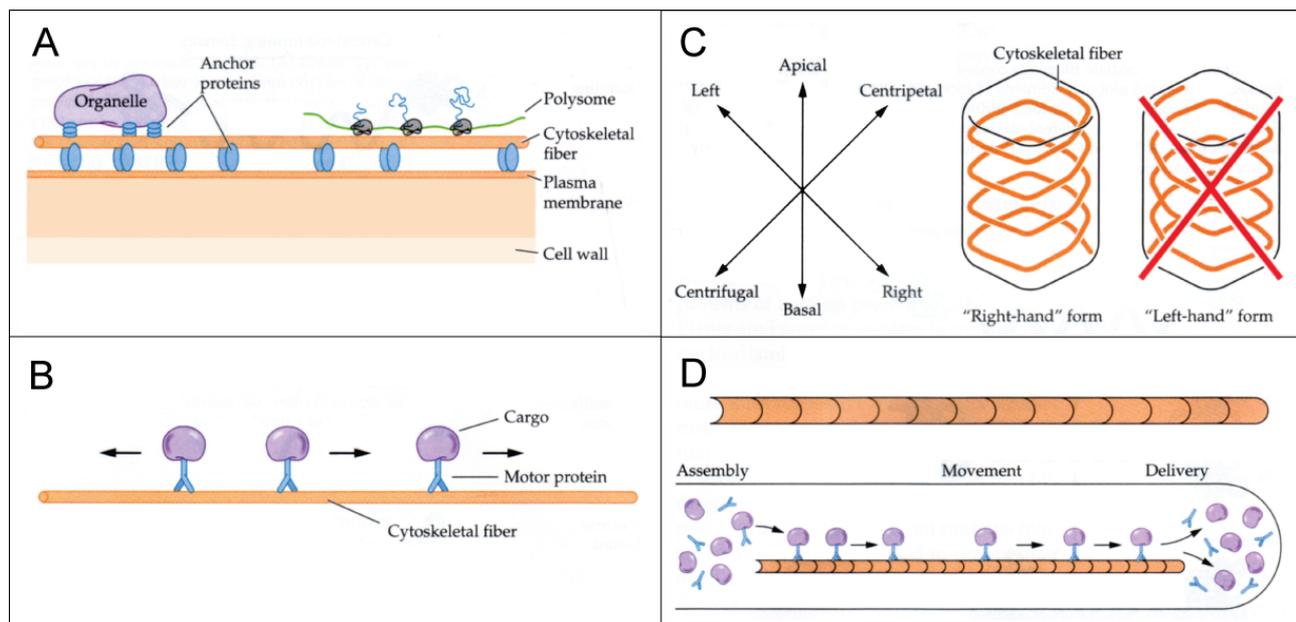
Figure 1: Different conceivable functions of the cytoskeleton.
(A) In connection with other plasma membrane embedded anchoring proteins, filaments can anchor organelles or macromolecules to the plasma membrane. **(B)** Motor proteins utilize filaments as tracks for the transport of cargo. **(C)** The cytoskeleton provides spatial cues to the structure of a cell. In addition to the apical- and basal- or centrifugal- and centripetal-direction a microfilament can provide a new axis (left and right in this example). **(D)** Cytoskeletal filaments are polar by virtue of the polarity of its subunits and the different assembly rates of both ends. By transporting a cargo along the filament a concentration gradient can be established.

Figure was modified and quoted from (Buchanan et al. 2000)

1.1   Trichome mutants with defects in the microtubule cytoskeleton

The development of any trichome can be divided in different steps as described in 4.1 (Figure 14). The involvement of the microtubule cytoskeleton is detected mainly during the process of branching. Many mutants with defects in branching are affected concerning the microtubule cytoskeleton. Although all mutants with an altered ploidy level are affected with respect to branching but they do not necessarily show abnormalities in the microtubule cytoskeleton. This paragraph will concentrate on the trichome mutants affected in both processes, branching and cytoskeleton morphology.

TUBULIN-FOLDING COFACTOR A (TFC-A) is a cofactor involved in the maintenance of the correct balance of assembly competent α- and β-tubulin (Kirik et al. 2002a), like TUBULIN-FOLDING COFACTOR C (TFC-C) (Kirik et al. 2002b). Mutants in both genes show pleiotropic effects like reduced total size, sterility and in addition reduced trichome branching. Not much is known about the processing of new α- and β-tubulin in plants, but much more information is available from the human research field. During biogenesis of α- and β-tubulin subunits a series of binding to chaperonins and other cofactors is necessary to allow the subunits to assemble (Cowan et al. 1999). Within this process TFC-A likely binds to β-tubulin and TFC-B to α-tubulin (Dhonukshe

et al. 2006). TFCs are most likely important for the maintenance of the correct concentrations of α- and β-tubulin demonstrated by the overexpression of α-tubulin in *tfc-a* mutant background that can rescue the mutant phenotype (Kirik et al. 2002a).

Another mutant with reduced branch-points belongs to the kinesin-like, calmodulin binding protein family (KCBP) which was named *zwichel (zwi)* (Oppenheimer et al. 1997). KCBPs are motor proteins that move along microtubules (Figure 1B). For the special case of ZWI it was shown that its activity is dependent on the Ca2+/Calmodulin concentration (Deavours et al. 1998). The *furca* class of mutants has a *zwi*-comparable phenotype (Luo et al. 1999). This class consists of four independent genes and the concerning mutants are entirely underbranched. Until now the molecular nature of these genes is not known. Another mutant with a comparable trichome phenotype is *angustifolia* (*an*) (Folkers et al. 2002a; Kim et al. 2002). Mutants in this locus are underbranched and show diverse additional phenotypes like a smaller leave size. AN belongs to the CtBP/BARs like proteins with diverse functions in development, differentiation and apoptosis (Corda et al. 2006). An additional phenotype *in planta* is the change of the microtubule cytoskeleton. Microtubules in the tip of wild-type trichomes are usually denser but *an* mutant trichomes show an even distribution of microtubules in the tip (Folkers et al. 2002a). A mutant which is strongly affected in branching is *sti* (Ilgenfritz et al. 2003). As a large part of this thesis deals with this mutant a more detailed introduction will be given in chapter 4.2 . In contrast to *an* mutants no defect in the cytosceletal organization was observed (Ilgenfritz et al. 2003), but the application of microtubule stabilizing drugs is able to rescue the branching phenotype (Mathur et al. 2000). A functional connection to the microtubule cytoskeleton is therefore likely.

Several other mutants were identified with defects in the microtubule cytoskeleton which do not always show a trichome phenotype. TONNEAU2 (TON2) is a putative protein phosphatase 2A. *ton2* mutant alleles showed dwarf growth, a missing preprophase-band and are sterile (Camilleri et al. 2002). The preprophase-band might mark the position of the division plane of the dividing cell (Mineyuki et al. 1990) and as a consequence hypocotyls cell of strong ton alleles loose their longish shape and are in majority rounder. The microtubule cytoskeleton in wild-type is usually oriented perpendicular to the leave growth axis but strong *ton* mutant alleles do not show any preferential direction (Camilleri et al. 2002).

An extremely dwarf growth phenotype is observed for another mutant important for the organization of the microtubule cytoskeleton, *microtubule organization 1 (mor1)*. Mutants in this locus showed extreme shortening of microtubule length under restrictive temperature as the allele described is temperature sensitive in consequence of a mutation in a HEAT repeat (Whittington et

al. 2001). MOR1 belongs to the family of MAP215 proteins which is well conserved between plants and animals (Gard et al. 2004). In vitro experiments showed, that members of the MOR1 family increase the tubulin polymerization significantly (Hamada et al. 2004). Presumably the function of MOR1 is the maintenance of microtubule length in developing cells.

To maintain the dynamic behavior of the microtubule cytoskeleton another class of proteins is needed which are able to severe microtubules enabling the repositioning of filaments (destabilizing function). This is done by the KATANIN proteins that consist of a smaller p60 subunit and a bigger p80 subunit. This heterodimer might by especially important during the cell-cycle where the distribution of microtubules is rapidly changed. The p60 subunit was identified in *A. thaliana* too (Burk et al. 2001; Bouquin et al. 2003). It turned out that mutants in this gene termed *lue1* were identified in a trichome mutant screen as *furca2* (*frc2*) (Luo and Oppenheimer 1999).

1.2   Trichome mutants with defects in the actin cytoskeleton

One class of mutants showed changes is the actin cytoskeleton that results in a changed trichome structure. This is the *distorted* class of mutants (Hulskamp et al. 1994). Trichomes of these mutant class e.g. *wurm* are branched but the clearly defined shape (Figure 14, Figure 17) is affected (distorted) (Mathur et al. 2003a). Several additional phenotypes are observed for some mutants of this class. Pavement and hypocotyls cells loose contact with neighbouring cells and root hairs are curled and occasionally branched. These pleiotropic effects are due to the molecular nature of the genes affected. Most of the eight members of the distorted class of mutants belong to the putative ACTIN RELATED PROTEIN 2/3 complex (ARP2/3) (Mathur 2005). The ARP2/3 complex consists of seven subunits and is present in different organisms (Pollard et al. 2002; Vartiainen et al. 2004). An active ARP2/3 complex binds to parent actin filaments to initiate branching. This branching generates an array of filamentous actin (F-actin). Arrays of F-actin are important for the regional growth of cells. Mutants of the distorted class showed changed or randomized distribution of F-actin leading to a distorted cell shape. This distorted cell shape can be phenocopied by the application of actin destabilizing drugs (Mathur et al. 1999; Szymanski et al. 1999). These experiments denoted again the connection of the *distorted* class of mutants to the actin cytoskeleton and an involvement of the ARP2/3 in trichome growth. In addition the organelle motility in some mutants of this class is affected as peroxisomes and golgi bodies are moving differently in comparison to wild-type (Mathur et al. 2003c). Recent reviews summarize the current knowledge about the putative ARP2/3 complex in *A. thaliana* (Deeks et al. 2003; Grennan 2005; Mathur 2005; Mathur 2006).

The actin cytoskeleton was no matter of investigation in this study. Due to the known importance of

the actin cytoskeleton for microtubules and well described interactions between both, future studies could investigate this issue.

1.3   The +end binding proteins CLASP and ORBIT

Microtubules are highly dynamic structures. Microtubules filaments change between phases of growth and shrinkage or even loose their dynamic by keeping the status quo. These processes are collectively termed dynamic instability. The change from growth to shrinkage is termed catastrophe and the opposite process rescue. As microtubules preferentially grow at one side it was termed the +end in contrast to the –end (Figure 2). (These different growth rates establish one matter of polarity in microtubules.) Dynamic instability is possible due to the polar nature of tubulin dimers itself and a large amount of microtubule associated proteins (MAPs).

The assembly of microtubules out of the α+β-tubulin pool is an energy dependent process. Only GTP-bound β-tubulin (red circle, Figure 2) bound to α-tubulin is incorporated into growing microtubules. In contrast to the –end, the +end contains α/β-tubulin dimers bound to GTP. The hydrolysis to GDP occurs temporally later and therefore the –end is devoid of GTP-bound dimers. The presence of GDP-bound tubulin dimers is one reason for the increased instability of the –end. In mammals this –end is bound in some cell types to Microtubule organising centres (MTOCs), which prevents the shrinkage of this filament at the –end. In addition posttranslational modifications increase the stability of microtubules (Bulinski et al. 1991).
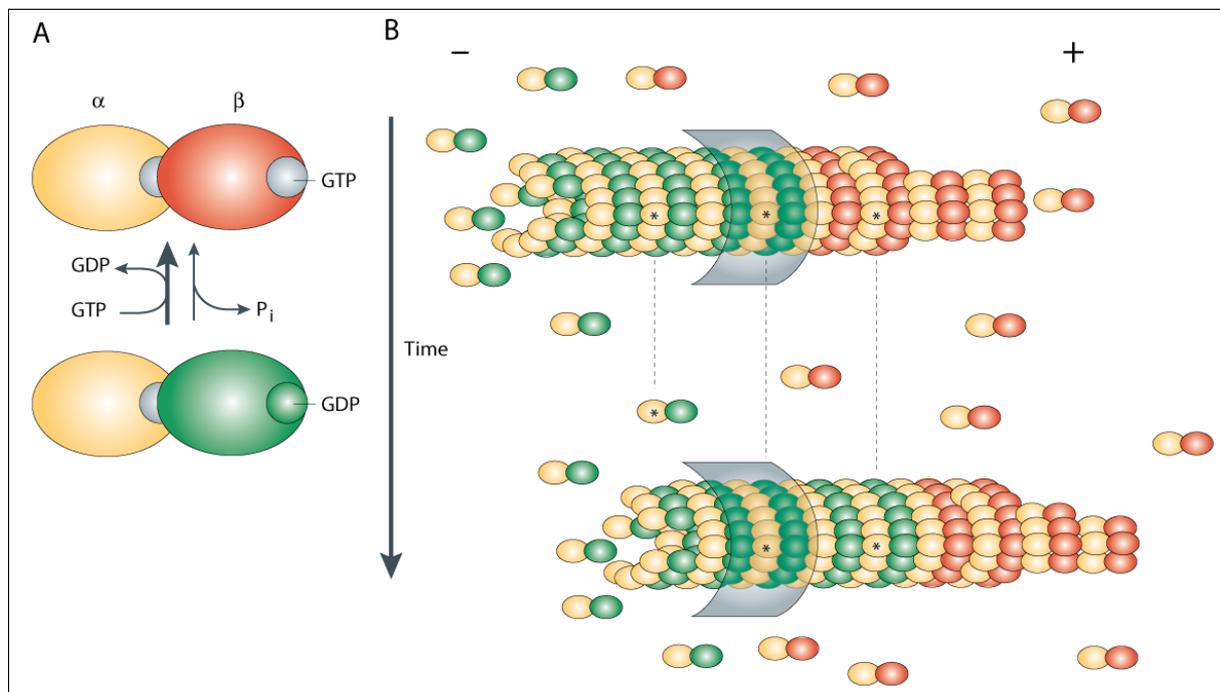
Figure 2: The ends of microtubules define growth and shrinkage.
(A) Tubulin dimers that are incorporated into the microtubule lattice are bound to GTP. GTP is bound only to β-tubulin.
(B) Microtubules preferentially grow at one site termed the +end in contrast to the –end. The left tubulin dimer marked

with an asterisk is not incorporated into the microtubule lattice any more (lower microtubule filament), demonstrating the shrinkage at the minus end. Over time the GTP bound to β-tubulin is hydrolysed to GDP.

This figure was quoted and modified from (Galjart 2005).

Furthermore a large number of MAPs regulate the stability of microtubules. CLASP 1/2 from *H. sapiens* and ORBIT from *D. melanogaster* are MAPs. CLASP1 from human is expressed ubiquitously whereas CLASP2 is expressed preferentially in the brain (Akhmanova et al. 2001). CLASP was identified in a two-hybrid screen as an interacting partner of CLIP170 (CYTOPLASMIC LINKER PROTEIN 170) and therefore termed CLIP ASSOCIATED PROTEIN (CLASP). CLIP170 is the first member of proteins that harbour the structural composition to bind microtubules and organelles. CLIP170 possesses an N-terminal microtubule binding motif and a C-terminal metal-binding motif which is needed for the binding to endocytic vesicles (Pierre et al. 1992) (Figure 3). CLIP170 is localised to prometaphase kinetochores (Dujardin et al. 1998) and to the end of growing microtubules (Perez et al. 1999). Like CLIP170, CLASP is localised to the end of growing microtubules (Akhmanova et al. 2001). CLASP1α is the longest isoform from *H. sapiens* and is most similar to ORBIT/MAST from *D. melanogaster* (Figure 4). CLASP1α has a length of 1538aa and differs from other mammalian isoforms at its N-terminus. The N-terminus shows similarity to proteins from the Dis1/TOG/MAP215 family of microtubule binding proteins (Figure 3B in green). Members of this family are present in most eukaryotes whereas MICROTUBULE ORGANIZATION 1 (MOR1) is a Dis1/TOG/MAP215 family related protein from *A. thaliana* (Gard et al. 2004). The middle part of CLASP1α is serine and arginine rich (Figure 3B in grey) and contains the domain responsible for the interaction with EB1 and microtubules (Mimori-Kiyosue et al. 2005). In addition recent studies showed the presence of an actin binding motif within this region (Tsvetkov et al. 2007). The C-terminal part of the CLASP1α protein is responsible for the binding to different CLIPs, the cell-cortex and the Golgi apparatus (Akhmanova et al. 2001) . HEAT repeats are distributed over the whole length of the protein (Figure 3B dotted lines). HEAT repeats are tandemly repeated sequences of around 50 aa. Proteins with heat repeats have very diverse functions but many mediate the interaction to other proteins (Andrade et al. 1995; Andrade et al. 2001). *MOR1* from *A. thaliana* showed a mutant phenotype with point mutations in a predicted HEAT repeat (Whittington et al. 2001). Nevertheless the function of this repeat is not known so far.
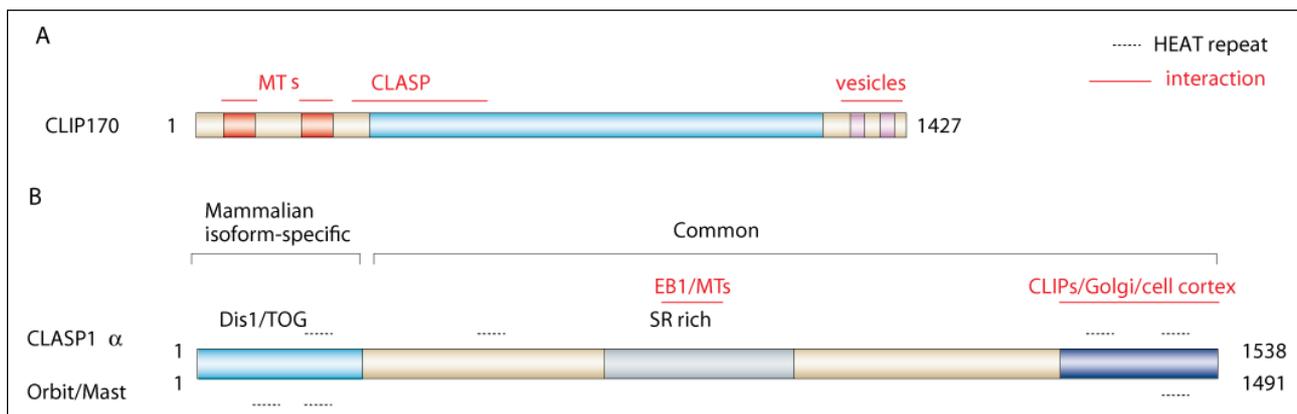
Figure 3: The structure of CLIP170 and CLASP1α/ORBIT
(A) CLIP170 consists of several domains. An N-terminal microtubule binding region (red) is followed by the CLASP interaction region. At the C-terminal part of CLIP170 contains zinc knuckles (pink) important for the binding to different other proteins, not mentioned and to endocytic vesicles. **(B)** CLASP1α consists of an N-terminal region variable in several mammalian isoforms. The homology to proteins of the DIS/TOG family is found in this region. In the middle part of the protein a serine rich region is located (grey) which is important for the binding to microtubules. At the C-terminal part of the protein interaction with CLIPs, Golgi and the cell-cortex was detected (blue). HEAT-repeats are always indicated as dotted lines. Interaction of a certain part of the protein is indicated with red lines and a description in red.
          Figure was quoted and modified after (Galjart 2005).

Mutants in the CLASP related protein s*tu1p* from *S. cerevisiae* showed that it is important for the mitotic spindle. Preanaphase spindles collapse as STU1p is likely to be important in generating the pulling force applied to interpolar microtubules that connect the spindle-pole bodies (Pasqualone et al. 1994; Yin et al. 2002). Similar importance for mitosis was observed for ORBIT/MAST from *D. melanogaster*. *Orbit/mast* mutant cell-lines showed impaired chromosome segregation, defective centrosome separation and generally disrupted spindles (Inoue et al. 2000; Lemos et al. 2000). ORBIT is localised to centrosomes, centromeres and spindle microtubules. In contrast to the organisms described so far, two ORBIT similar proteins a present in *H. sapiens*. Like in the *H. sapiens* genome two *CLASP* genes are present in *M. musculus*, too. The analysis of *M. musculus clasp2* knock-out lines showed that *clasp2* and *clasp1* have largely overlapping functions (Pereira et al. 2006). H. sapiens CLASP1 is localised to the +end of microtubules and the Golgi apparatus (Akhmanova et al. 2001). This localisation reflects the stabilisation function of CLASP on certain microtubules especially at the cortex or the spindle (Mimori-Kiyosue et al. 2005; Mimori-Kiyosue et al. 2006).

Aim of the work:

This work focuses on the initial characterization of an unknown protein from *A. thaliana*. It shows similarity to CLASP1/2 from *H. sapiens* and ORBIT from *D. melanogaster*. It is located on chromosome two (At2g20190). So far no publication describes its function in *A. thaliana* but a lot is known from other organisms. The main function of CLASP in *H.sapiens* is the stabilisation of microtubules, reviewed by (Galjart 2005). This is possible through its localisation as a +Tip binding protein and a set of known interacting proteins like EB1 or CLIP170.

The characterization of the mutant phenotype from different available alleles should be the starting point of this study. Fusions to fluorescent proteins should be generated to examine the localisation of this unknown protein in *A. thaliana*. Fragments of the cDNA should be tested in a similar fashion whether or not the domain architecture of this unknown protein is conserved to e.g. *H. sapiens* CLASP. Interacting proteins of *H. sapiens* CLASP are already known. Therefore similarity searches should be performed to identify putative orthologs in *A. thaliana*. These potential interactors should be tested in direct Yeast Two-Hybrid assays for interaction.

2   Results

2.1   *A. thaliana* At2g20190 has sequence similarity to human CLASP1

The knowledge about CLASP related proteins from other organisms, summarised in the introduction, lead to a reverse genetic approach to identify candidate genes for CLASP in *A. thaliana*. BLAST analysis (Altschul et al. 1990) revealed that there is only one gene in *A. thaliana* with similarity to CLASP related proteins. The similarity within the plant kingdom is the highest. Pairwise alignments showed that *A. thaliana* At2g20190 and *O. sativa* Os04g0507500 contain 62,2 % identical AS whereas *A. thaliana* compared with *M. truncatula* ABE89955 (NCBI locus number) share 55,8 % identical AS. The similarity between *A. thaliana* and *H. sapiens* decreases to 19 % identical AS for CLASP1 versus 15,6 % identical AS for CLASP2.

BLAST analysis is a suitable tool to detect similarities between proteins. Nevertheless to determine the evolutionary distance between several proteins different algorithms have to be utilized. The "PAUP" program (http://paup.csit.fsu.edu/index.html) was used to determine the evolutionary distance with the "Parsimony" and "Neighbor-joining" algorithms. 19 proteins were compared to At2g20190 and the evolutionary distance was displayed by a phylogram (Figure 4). Most branches in the phylogram were supplemented by two values describing the significance for the presence of this branch. The first value was generated by the Neighbor-joining algorithm and the second by Parsimony. The phylogram shows that plants and algae belong to an own branch which is separated from the animals. *At2g20190* is a single copy gene which is comparable to *M. truncatula* and *V. vinifera*. By contrast, *P. patens* and *O. sativa* contain one paralogous gene. Animals contain usually two *CLASP* genes which are located in two different branches. Interestingly *M. musculus* and *R. norvegicus* CLASP1/2 are located in a separate branch within the CLASP1/2 branch. In contrast to *M. musculus, R. norvegicus* and *H. sapiens* the CLASP similar proteins from *C. elegans* are located on an independent branch. Furthermore three different CLASP similar proteins are present in *C. elegans.*

At2g20190 is annotated in the last Annotation (V6) of the AGI (Arabidopsis Genome Initiative) as an unknown protein with similarity to the CLIP-associated protein CLASP2 from *R. norvegicus* (NCBI locus NP_849997). Due to sequence similarity and the analysis of the evolutionary distance At2g20190 will be named At-CLASP in this work. Within the protein sequence the carboxy-terminal part of the CLASP-proteins is mostly conserved between the organisms while most of the protein shows only low similarity (Figure 6C).
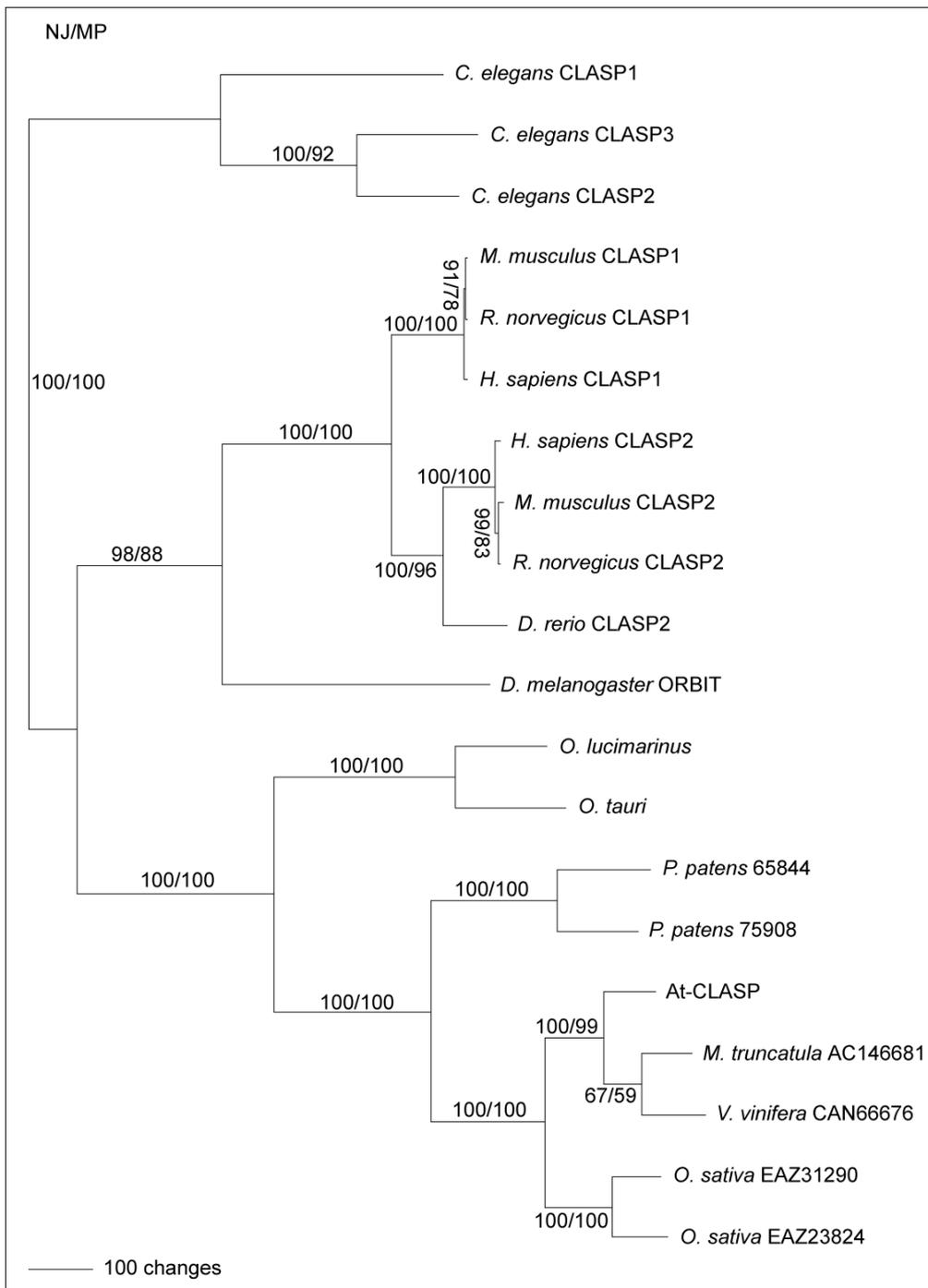
Figure 4: Evolutionary distance of At-CLASP and orthologs.
The evolutionary distance of At-CLASP and several orthologs was displayed by a phylogram. Proteins from the plant kingdom and the animals are located on different branches. In addition *C. elegans* proteins are evolutionary distant and form the third branch. CLASP1 and CLASP2 are located in different branches whereas plants usually contain only one copy of CLASP. Exceptions are *O. sativa* and *P. patens* which contain at least one paralogous gene.

NJ= Neighbor-joining algorithm; MP=Parsimony algorithm

2.2 Genomic structure and domain organisation

At-CLASP is located on chromosome 2 and is found on the end of BAC T2G17 and F11A3. It consists of 20 exons and 19 introns. The total size of all introns and exons is about 7kb (Figure 5). According to the AGI (Arabidopsis Genome Initiative) the AGI code of *At-CLASP* is At2g20190.

Most of the exons are small in size (< 160bp) but two are larger than 300bp and only one has a size of almost 1800bp (Figure 4). The gene-structure was verified by the availability of a full-length cDNA which showed that *At-CLASP* is encoded by the annotated exons. The cDNA used in this study came from the Riken Institute and the corresponding clone-number is RAFL09-38-C02 (Seki et al. 2002). Previous computer derived annotations of the exon/intron structure proposed a much smaller total gene size (Figure 10) but by the availability of the new cDNA this annotation has to be denoted as wrong.
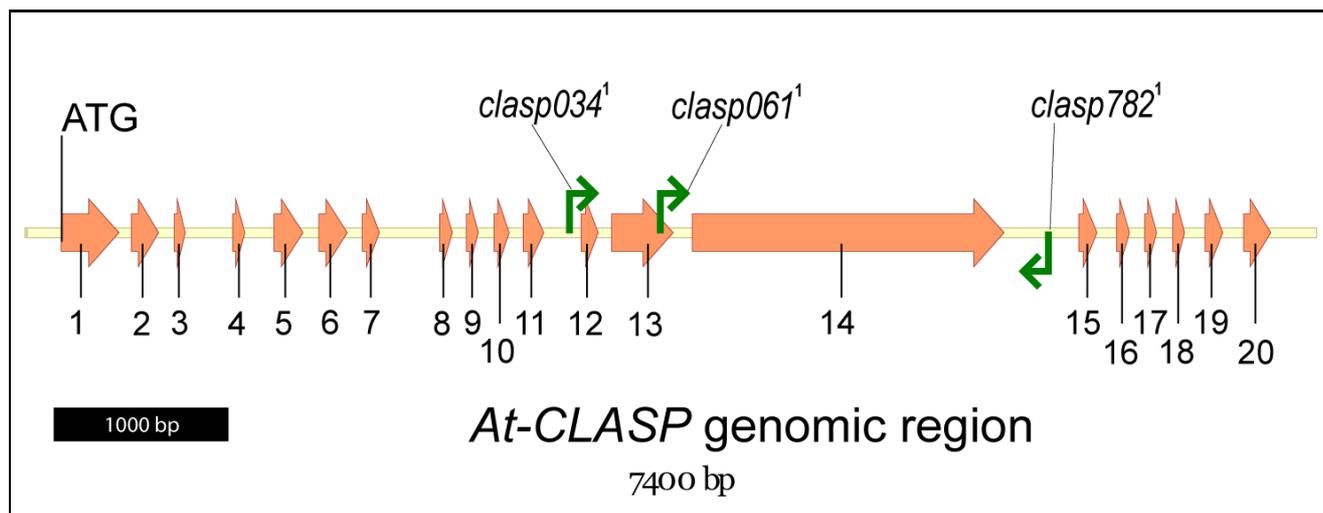
Figure 5: Genomic structure of Clasp.
The distribution of exons (orange arrows) and the insertion of T-DNAs (green arrows) within the Clasp genomic region are depicted in this figure. The individual exons are numbered beginning from the ATG that indicates the translational start.
    [1] *clasp034*, *clasp061* and *clasp782* correspond to the name of the T-DNA insertion.

The At-CLASP protein encodes a protein of 1439 aa. At-CLASP and its orthologs from animals are evolutionary distinct (Figure 4) and only one domain is present in all proteins. The carboxy-terminal Mast-C domain which plays a general role in microtubule binding and organisation of the mitotic spindle (Lemos et al. 2000). This domain in At-CLASP was identified by the Conserved Domain Database (CDD) (http://www.ncbi.nlm.nih.gov/Structure/cdd/cdd.shtml). Additional conserved domains were not identified for At-CLASP, but it is possible that parts of the protein are functionally conserved however a detection by sequence comparison is not feasible. Therefore a closer look onto the structure of known CLASP orthologs is needed.

CLASP1 from *H.sapiens* and Orbit from *D.melanogaster* share some common features concerning their structural composition and function. The C-terminal part of the protein contains sequences that are found in proteins of the Dis1/TOG family which are mediating the stabilization of microtubules. In the middle part of the protein is a Serin and Arginin rich region needed for the binding to Microtubules and EB1 (Figure 6A). The C-terminal part of human CLASP mediates the binding to

CLIP, Golgi and the cell cortex (Galjart 2005). This domain has been termed MAST (Figure 6A). Distributed over the entire protein are HEAT repeats, predicted by bioinformatic means, which can form a helical structure that might function in protein-protein interaction.

So far At-CLASP is annotated as unknown protein. The verification of parts of its structural composition is the aim of this study, but few similarities can be detected by bioinformatical methods. HEAT repeats are distributed over the entire protein. (REP http://www.embl-heidelberg.de/~andrade/papers/rep/search.html). A putative PEST sequence that can mediate protein degradation was found in the C-terminal part of At-CLASP too (detected by PESTfind https://emb1.bcc.univie.ac.at/toolbox/pestfind/pestfind-analysis-webtool.htm). PEST sequences can trigger the rapid degradation of proteins (Rechsteiner et al. 1996). In contrast no PEST-sequence with a high enough score was detected for human CLASP1. The MAST domain that seems to be a general motif of CLASP proteins was detected in the C-terminal part by the Conserved Domain Database from NCBI (features summarised in Figure 6B).
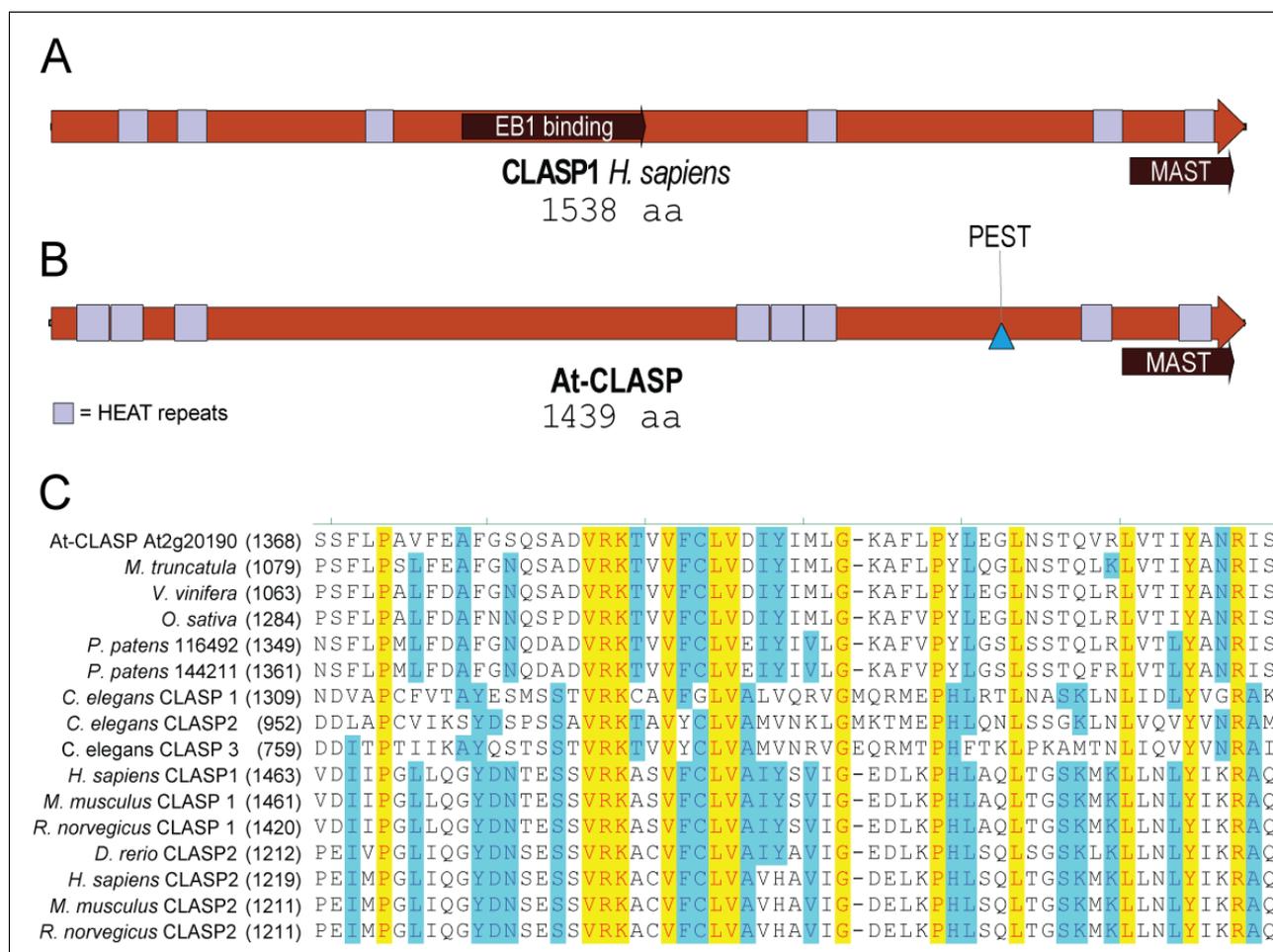
Figure 6: Protein domain organisation of human CLASP1 and At-CLASP.
(A) illustrates the CLASP1 protein from *H.sapiens*, with some of its domains. The Serin-Arginin rich region in the middle of the protein mediates the binding to microtubules an EB1 via few conserved residues. The C-terminal part of CLASP1 contains the MAST-C domain that mediates the binding to CLIP, Golgi or the cell cortex. Distributed over the protein are HEAT repeats in grey. (B) The At-CLASP structure is until now only predicted but it shows some

similarities compared to CLASP1 from humans. HEAT repeats (grey boxes) are distributed all over the protein and the MAST-C domain in the C-terminal part of At-CLASP. **(C)** Alignment of the C-terminal region of different CLASP similar proteins. This region contains the putative MAST domain and is most similar among the analysed proteins.

2.3   The *at-clasp* mutant has a pleiotropic phenotype

The analysis of the CLASP ortholog in *D.melanogaster* ORBIT revealed that it is affected in mitotic spindle formation. Consequently different cell types of hypomorphic alleles have an increased mitotic index whereas amorphic alleles of *orbit* show late lethality (Inoue et al. 2000). R106.7 from *C.elegans* is an ortholog of ORBIT and has a defect in positioning the spindle. Disturbing the function of this gene by an RNAi approach leeds to embryonic lethality (Gönczy et al. 2000).

To determine whether *A. thaliana* mutants show similar defect, lines with insertions in the At-CLASP locus At2g20190 were analysed. The large size of At2g20190 and the position in the genome yielded several insertion lines. Three alleles of *at-clasp* have been analysed in more detail. These are *clasp061* (SALK_120061*)*, *clasp034* (SALK_083034) and allele *clasp782* (SALK_049782*)*, all of them are derived from the SALK collection (Alonso et al. 2003). Two of these insertions are located within an intron, one is located in exon 3 (Figure 5). The border sequences have been confirmed by PCR and subsequent sequencing. Insertions within AT-*CLASP* result in different phenotypes. An obvious phenotype is the reduction in branch number. About 20 % of the trichomes have only one branch point whereas Col wild type has less than 2% (Table 1). In addition the overall height of all mutant alleles analysed is reduced. For example allele *clasp061* has approximately only 25% of the height when compared to wild-type (Figure 8A). In addition *at-clasp* mutant plant rosette leaves are oriented in spirals (Figure 8G) like observed elsewhere (Sedbrook et al. 2004). An even more severe phenotype is observed in the reproductive organs. At-clasp mutant alleles are unable to produce intact siliques at temperatures above 25°C. Below this temperature *at-clasp* siliques are indistinguishable from wild type. Not all alleles show the same penetrance concerning the silique phenotype. Allele *clasp782* is able to produce few siliques (Figure 8E) but allele *clasp034* or *clasp061* cannot produce any. Probably allele *clasp782* is hypomorphic. The analysis of *At-Clasp* transcript in the three mutant alleles revealed differences in comparison to wild-type (Figure 7). After 33 cycles of amplification Col wild-type presents a clear band of the expected size. Some residual transcript is observed in allele *clasp034* which has an insertion in intron 11. Both other alleles do not produce any product after 33 amplification cycles. The primers used for the detection of the transcript cover almost the complete At-CLASP cds (433+434). Control amplifications with EF1 primers, like used elsewhere (Kirik et al. 2002a*)*; show that comparable amounts of cDNA were used.

Table 1: Branching in *at-clasp* mutants
The trichomes of allele *clasp034*, *clasp061* and *clasp782* were analysed concerning to the number of branch points. The position of the insertions is shown in Figure 5. Allele *clasp061* is inserted within an exon and is showing the strongest phenotype.

Branching in at-*clasp*-mutant alleles compared to wild-type

allele	trichome branch-points [1]			N
	1	2	3	
Col	0,71	89,67	9,62	707
clasp034	20,65	76,09	3,26	460
clasp061	23,11	74,48	2,41	623
clasp782	18,73	78,4	2,87	801

[1] trichomes counted on leave 3 and 4. (percentage values)

1= EF1 25 cycles
2= Clasp full-length 33 cycles
Primer 433+434=3787bp
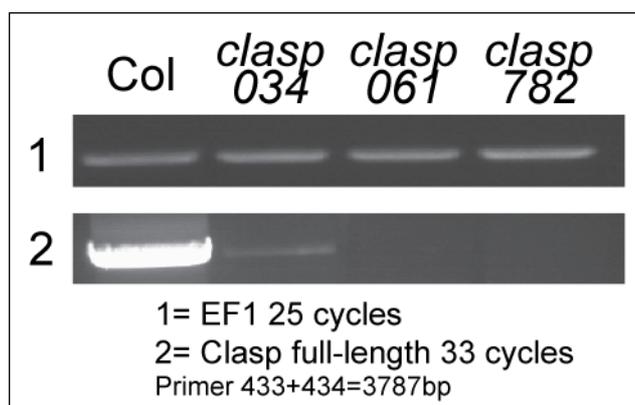
Figure 7: Expression of At-CLASP in mutant alleles.
After 33 cycles of amplification Col wild-type shows a clear signal for the At-CLASP transcript. In at-clasp mutant backgrounds only *clasp034* mutant alleles present residual transcript after 33 cycles of amplification. Both further alleles are devoid of transcript under the conditions analysed. Primers 433+434 were used for this experiment which amplify almost the complete CDS of At-CLASP. The control amplification with primers for EF1 confirms similar amounts of cDNA.
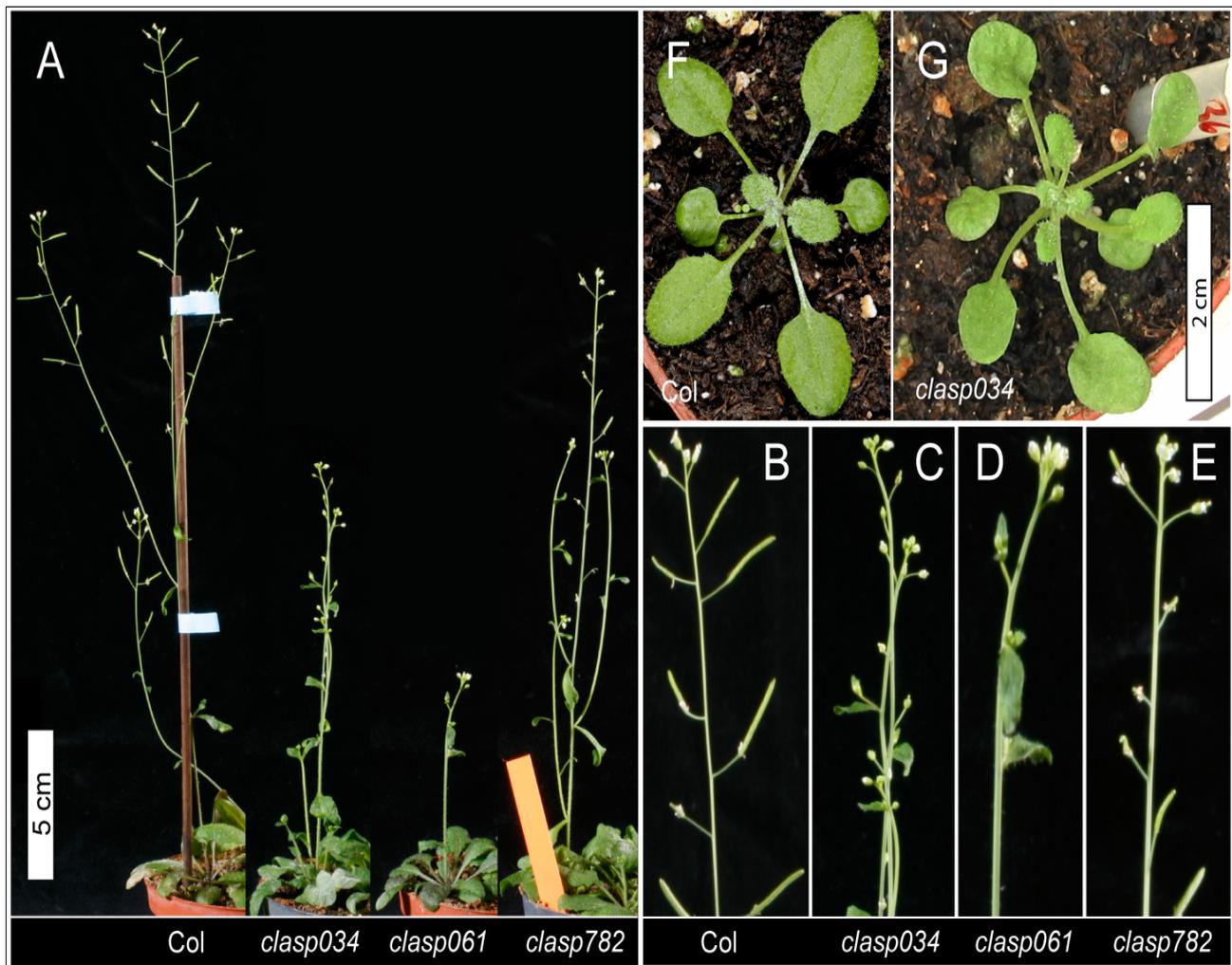
Figure 8 Different phenotypes of *at-clasp* mutant alleles.
(A) *At-clasp* mutants and Col wild-type are imaged at the same time with identical magnification. All mutant alleles analysed showed a retarded growth phenotype and a reduced fertility. **(B-E)** These magnifications show the inflorescence of the mutants analysed in A. **(C+D)** Both alleles do not produce any intact siliques even in later stages. **(E)** Allele *clasp782* is most likely not a complete loss of function and can produce few siliques. **(F+G)** In addition a twisting phenotype is observed which is exemplary shown for *clasp034*.

2.4   Expression Analysis of *CLASP*

The spatial and temporal correct expression pattern of any gene is necessary for its function. Independent of all further regulation steps concerning the transcript or the subsequent protein a RNA transcript needs to be present. A protein like CLASP in *H.sapiens* or *D.melanogaster* is most likely present in most tissues and time points because its function is essential for every growing cell (Inoue et al. 2000). At-CLASP is evolutionary most distant from the species analysed (Figure 4A) therefore it needs to be validated whether the expression of At-CLASP is detectable in most tissues.

The presence of the *At-CLASP* transcripts in wild-type leaves, which present the trichome phenotype, should be confirmed. *At-CLASP* transcripts should be detected by PCR on cDNA

libraries of Col wild-type. To determine the expression levels in different organs and tissues of *A. thaliana* the commonly available database with expression data derived from microarray experiments should be used. They allow a qualitative and quantitative analysis of the transcripts detected in a selected tissue. The use of microarray data allows in addition a comparative analysis of all genes detected by the chip. By comparing the *At-CLASP* expression to the expression of all other genes, candidates might be detected, that are expressed at similar time-points and in the same tissues. Genes with a comparable expression pattern are termed coregulated and might be important in a similar process *in planta*. Several known proteins were identified as regulated similar to *At-CLASP* (Table 2).

The promoter of any gene limits the expression of its gene to be expressed in selected tissues and different time points. By analysing the transcript levels by the methods mentioned above only a "snapshot" of the current expression level in a heterogeneous tissue is available. How the transcript is expressed in different cell types and during the development of the plant can be visualized indirectly. Fusions of the putative *At-CLASP* promoter and the GUS (β-glucoronidase) reporter gene allow the visualisation of the promoter activity (Jefferson 1989). The construct used for this assay is described in Figure 11.

The *At-CLASP* transcript (detected with primer 433/434 covering almost the complete cDNA) is detected in Col wild-type after 33cycles of amplification in cDNA libraries of rosette leaves. The expression of the putative promoter of *At-CLASP* driving the *GUS* gene shows that *At-CLASP* is indeed expressed in leaves (Figure 9B+C). The expression is higher in younger tissue (detectable in all epidermal cell-types) and is reduced to a selective expression in the vascular tissue of older leaves. Stomata and trichomes are stained too but the signal in trichomes is not detectable in older stages any more.

The results from the genevestigator website (Figure 9D) confirm the expression in leaves. In addition they show that *At-CLASP* is expressed in similar levels in all major organs of *A. thaliana*. Surprisingly both probe sets used for detecting the RNA level of *At-CLASP* do not show the same expression level at all. The probe set 265576_at which is located at the end of the *At-CLASP* transcript shows expression level almost 10 times higher than the probe set at the beginning of the transcript.
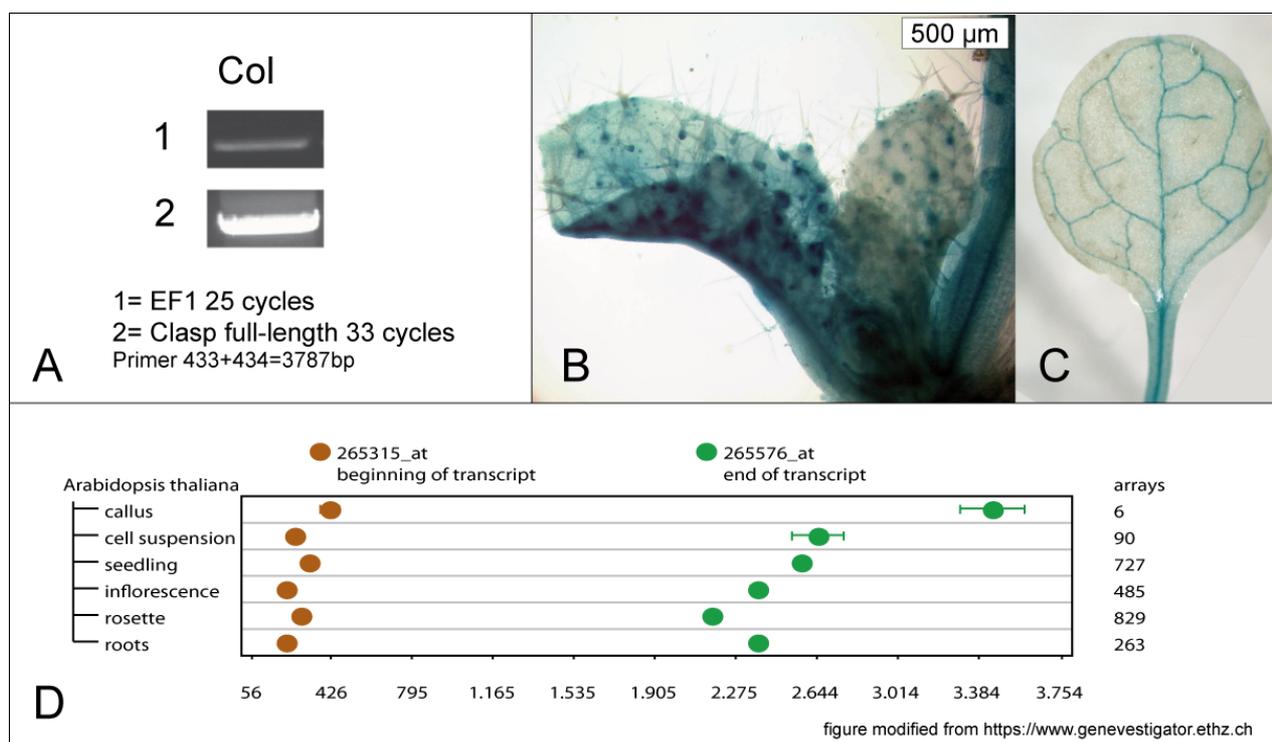
Figure 9: Expression analysis of *At-CLASP*.
(A) The full length cDNA of *At-CLASP* is expressed in Col wild-type. The *EF1 (Elongation Factor 1)* gene was amplified as a control for equal amounts of cDNA. **(B+C)** The activity of the Clasp-promoter construct used to rescue the *at-clasp*-mutant (Figure 10). The expression of the Gus gene was most prominent in young leaves where stomata, trichomes and the vascular tissue are stained. The expression of the reporter in older parts of the plant is only visible in the vascular-system. **(D)** Microarray expression data with two probe sets representing At-CLASP show the expression levels in different organs. (Zimmermann et al. 2004). Interestingly these probes differ seriously in expression.

Table 2: Genes coregulated with At-CLASP.
This table list all genes that show similar expression level in different tissues and upon certain stimuli. To achieve that, expression databases from chip experiments are queried by the "Expression Angler" program from the University of Toronto. Labelled in grey are known proteins with publications. Candidate At4g15930 was found previously in a Yeast-Two-Hybrid screen (Table 16). The r-value is the Pearson correlation coefficient that numeralizes the similarity of gene expression (Toufighi et al. 2005).

AGI	r-value	name or similarity of the protein
At2g20190	1	At-CLASP
At5g18410	0,894	PIR (PIR of plants), PIROGI, KLUNKER
At5g12370	0,836	Exocyst complex component 5
At3g51850	0,823	CPK13 (calcium-dependent protein kinase 13)
At5g08100	0,822	L-asparaginase / L-asparagine amidohydrolase
At4g15930	0,818	dynein light chain, putative | found in Two-Hybrid as putative STI interactor
At5g18580	0,811	FASS (FASS 1), tonneau 2 (TON2)
At4g24390	0,810	F-box family protein (FBX14)
At4g02610	0,807	tryptophan synthase, alpha subunit
At2g35110	0,807	Protein NAP1, (NAP of plants), GNARLED
At5g01020	0,805	protein kinase family protein
At1g28440	0,804	HSL1 (HAESA-LIKE 1, ATP binding / kinase/ protein serine/threonine kinase
At5g09810	0,798	Actin-7 (Actin-2)
At3g43740	0,793	leucine-rich repeat family protein
At2g37050	0,792	leucine-rich repeat family protein
At3g24040	0,789	glycosyltransferase family 14 protein
At4g16340	0,788	SPK1 (SPIKE1) GTP binding / GTPase binding / guanyl-nucleotide exchange factor

2.5 Rescue of the *at-clasp* mutant phenotype

The T-DNA insertions of all three alleles of *at-clasp* were verified by PCR and subsequent sequencing of the PCR products. To exclude that a second site insertion at a different position in the genome is the cause of the phenotype observed, different insertion lines for *at-clasp* were analysed. All three lines analysed showed a consistent phenotype and no additional cosegregating phenotype. As a final prove to be the cause of the mutant phenotype rescue attempts for the different mutant lines were performed.

Three different approaches were used to rescue the mutant phenotype. First the full-length cDNA from the Riken Institute (Seki et al. 1998) was introduced into a ubiquitous expressing 35S vector (Figure 12). Second it might be possible that *At-CLASP* expressed under an artificial and ubiquitously expressing promoter is not reflecting the endogenous situation *in planta*. The temporal and spatial expression pattern as well as the total amount of transcript generated by this promoter might not fully rescue the mutant phenotype. Therefore a 2.4kb Fragment upstream of the *At-CLASP* translational start was amplified and introduced into a vector replacing the original promoter (Figure 10). Two vectors were generated that allowed the translational fusion of YFP to both ends of the cDNA. These vectors driving the *At-CLASP* gene were used to rescue the mutant phenotype. Third the sequence similarity between *H. sapiens* CLASP1 and At-CLASP is low (Figure 4) but the function might be still conserved. Therefore *H. sapiens CLASP1* under the control of the 35S promoter was used to rescue *at-clasp* mutants too.

At-clasp mutants can be rescued by introducing the full-length cDNA under control of the 35S promoter (for construct design refer to Figure 12). More than 50 lines carrying translational fusions of At-CLASP:YFP or YFP:At-CLASP were generated that are able to rescue the mutant phenotype. The second rescue attempt under the putative endogenous promoter yielded a total number of 76 primary transformants for the fusion of YFP to the carboxterminus of At-CLASP (Cl::Cl:YFP) and 50 transformants for the aminoterminal fusion (Cl::YFP:Cl). The rescue efficiency was not uniform among the transformed lines and four different classes of rescue were observed. The rescue was scored based on the ability to form siliques under restrictive temperature. Class one showed siliques indistinguishable from wild-type and was considered as complete rescue. In the second class siliques are wild-type, but the plants are generally smaller compared to the previously described class. Class three is reduced in size but additionally the number of siliques is reduced too. Class four harbours the rescue construct but shows the mutant phenotype. 25% of Cl::Cl:YFP showed a complete or partial rescue, whereas 30 % of the other fusion Cl::YFP:Cl rescued the *at-clasp*

mutant phenotype (Table 3). The analysis was performed onto a heterozygous segregating T2 generation. In conclusion both vectors used to rescue the mutant phenotype could rescue at comparable rates. The position of the YFP fusion was not affecting the recue of the mutant phenotype.

To check a possible functional conservation of *H. sapiens* CLASP1 it was transformed into *at-clasp* mutant plants. None of the 30 primary transformants was able to rescue the mutant (data not shown).
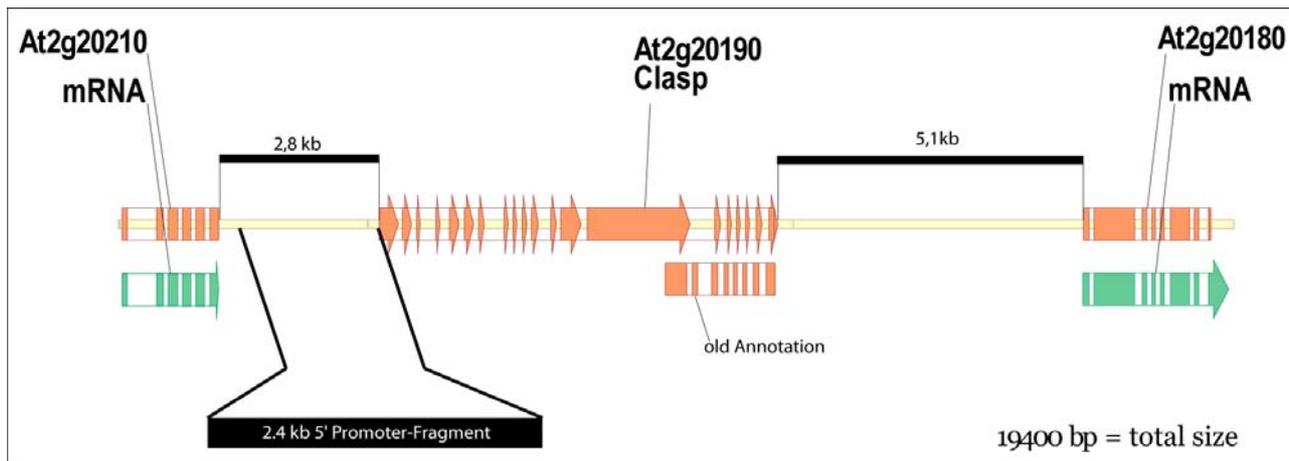
Figure 10: The genomic region around the *At-CLASP* gene.
The region in front of the transcriptional start was chosen for the construction of the vector. This region covers almost the complete distance to the next gene upstream of *At-CLASP* suggesting that this part of the genomic region contains sufficient information to rescue the mutant. The next gene downstream of *At-CLASP* is more than 5kb distant. In an initial attempt to rescue the mutant; this part was not included into the construct. Below the *At-CLASP* gene the old computer derived annotation is listed which suggests a much smaller transcript.
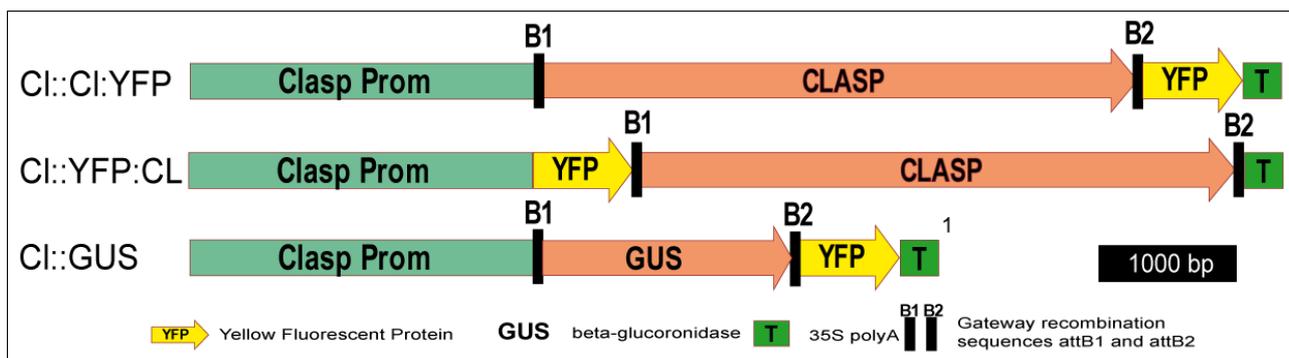
Figure 11: Promoter constructs used to rescue the *clasp* mutant phenotype.
The 2.4kb 5' prime region of Clasp as depicted in Figure 10 was used to construct three different vectors. Cl::Cl:YFP and Cl::YFP:Cl were used to resuce the mutant phenotype. Cl::GUS was constructed to analyse the promoter expression pattern *in planta*.

[1] the YFP in this vector is not expressed due to a stop codon in the GUS gene.

Table 3: The rescue efficiency of *At-CLASP* constructs under endogenous promoter.
The T1 generation of both constructs was analysed at a minimal temperature of 25°C for rescue of *clasp034*. This generation of the transformants is heterozygous and must not necessarily express *At-CLASP* at wild type comparable levels. The phenotype of every transformant was scored as described in the legend an acquired in total lines per phenotypic class. The rescue efficiency (percentage) was assembled from class ++,++- and +-.

Analysis of the T1 from CI::CI:YFP and CI::YFP:CI in *clasp034*[1]

construct	++[2]	++-[3]	+-[4]	-[5]	N	Re [%][6]
CI::CL:YFP	4	9	6	57	76	25
CI::YFP:CL	7	6	2	35	50	30

[1] rescue scored onto the ability to form siliques
[2] plants are completety rescued
[3] plants are rescued but reduced in size
[4] plants are severe reduced in size, only few silques
[5] no rescue, plants are very small and do not form siliques
[6] rescue efficiency

2.6 At-CLASP localises to microtubules

The localisation of CLASP1+2 from *H .sapiens* or its ortholog ORBIT from *D. melanogaster* were analysed by others in detail. CLASPs are localised to the end of growing microtubules and therefore they are termed +end tracking proteins (+TIPS) (Akhmanova et al. 2001) . The main function of CLASPs seems to be the local stabilisation of microtubules at the growing end which is especially important in mitosis. ORBIT the *D. melanogaster* ortholog of CLASP is needed in maintaining the length of the microtubules connecting kinetochore and spindle pole (Maiato et al. 2005). Binding to microtubules or binding to the cell cortex is mediated thru special parts of the protein. The C-terminal part of the cDNA is essential for binding to the cortex, whereas the middle part mediates the binding to microtubules or to EB1.

The main question is whether the function of At-CLASP is conserved in *A. thaliana* and the presence of domains required for this function is conserved in addition. This question is of outstanding interest as At-CLASP is most distinct from the At-CLASP similar proteins analysed so far. To access this question the localisation of the At-CLASP-protein fused to YFP was analysed. Two additionally fragments of the cDNA were fused to YFP to get more information about the function of the domains within this protein (A+B (1-3514 bp) and Cortex (3493-4320bp)). The orientation of both fragments is depicted in Figure 12. The full length cDNA was fused without untranslated regions two YFP before the translational- start or -stop.
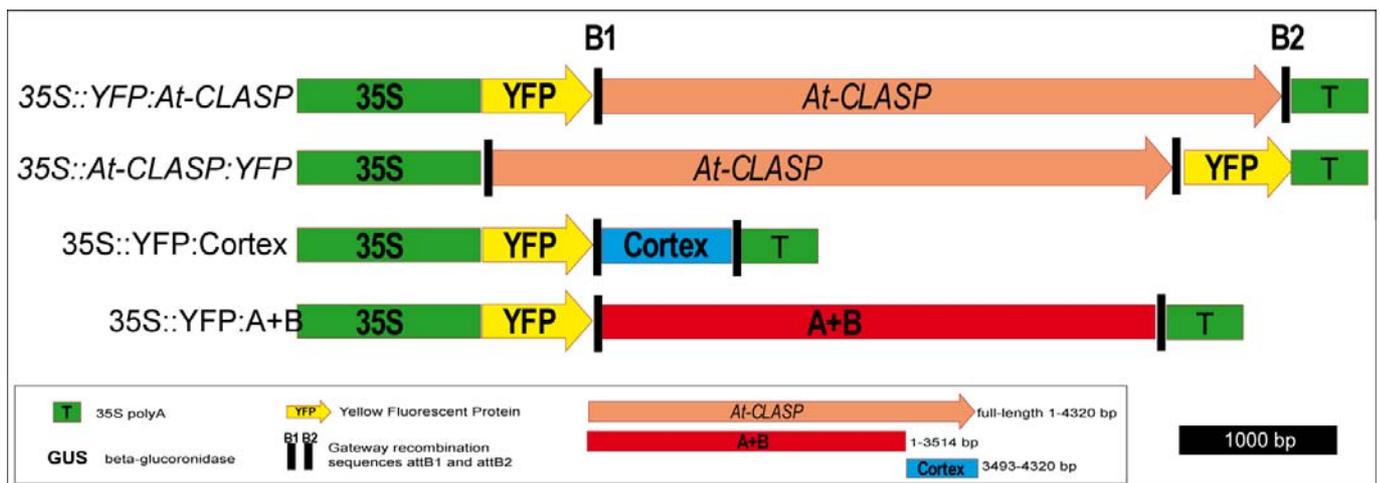
Figure 12: The constructs used for the analysis of the localisation of the CLASP-YFP fusion.
(A) Four different constructs were used to analyse the localisation of the fusion protein. All of them contain the 35S promoter four ubiquitous expression in all tissues. **(B)** The position of the cDNA fragments used for a rough mapping of the different parts of the protein.

Filamentous structures are labelled by the constructs *35S::YFP:At-CLASP* and *35S::At-CLASP:YFP* harbouring the full length cDNA (Figure 13). At-CLASP similar proteins from mammals are bound to microtubules and termed therefore "Microtubule Associated Proteins" (MAPs). To analyse the hypothesis that microtubule binding might be conserved in *A. thaliana*, we made use of the knowledge that EB1 (End binding Protein 1) is a +TIP that binds to microtubules (Mathur et al. 2003b). EB1-B (At5g62500) was fused to CFP-Cerulean in a modified vector, similar as for *35S::YFP:At-CLASP* depicted in Figure 12A. Cerulean is a CFP variant with increased quantum-yield (Rizzo et al. 2004) which was used because CFP is usually more sophisticated to detect. This new construct *35S::Cerulean:EB1-B* was transformed into the *35S::YFP:At-CLASP* lines showing the labelled filamentous structures. After simultaneous excitation of both fusion proteins it was obvious that At-CLASP labels filaments that are decorated by EB1-B (red) arguing that At-CLASP labels microtubules (green) (Figure 13G). An overlap of both signals was only occasionally visible (white arrow heads).

The localisation of the full length constructs *35S::YFP:At-CLASP* and *35S::At-CLASP:YFP* is visible in hypocotyl-, epidermal pavement- and stomata cells (Figure 13A+B+D). The overall signal strength is higher for the fusion of YFP at the amino terminus of the cDNA (*35S::YFP:At-CLASP*). The orientation of the microtubule network is variable. Microtubules of neighbouring cells show a change in orientation from left to right (Figure 13A). No clear preference for the orientation of microtubules is detectable. The signal of the fusion protein is distributed equally within the cells. Some cell types like stomata show an increased signal at the porus possibly due to higher microtubule bundling frequency (Figure 13D).

The analysis of fragments should shed some light onto the functions of different parts of the At-CLASP protein. The end of human CLASP1 is responsible for the binding to the cell cortex and to CLIP170 (Figure 6). Fusion of the Cortex fragment to YFP (35S::YFP:Cortex 3493-4320bp) resulted in a very strong signal, much brighter than in any other construct tested. The localisation of the fusion protein is different than the full length cDNA, as it is not marking any filamentous structure any more but the cell margins. Possibly the structure labelled is the plasma membrane or the cytoplasm. The moving cytoplasm is labelled in addition (unpublished observation, Figure 13C+F). The fusion protein is not located to the cell-wall as no signal was detected between two neighbouring cells (Figure 13I).

The localisation of fragment A+B (*35S::YFP:A+B,* 3493-4320bp) differs from the full-length cDNA and the cortex fragment localisation. Exemplary for the localisation of fragment A+B an epidermal cell (Figure 13E) and a trichome (Figure 13H) is depicted. Comparable to the localisation of the full length constructs it is detected in filamentous structures which are likely again microtubules. But the overall signal intensity is elevated in comparison to the construct harbouring the complete CDS. In addition the A+B fragment marks microtubules differently, since the number of labelled structures appeared to be reduced (Figure 13E). In addition small stretches of microtubules show increased signal intensity. Furthermore the signal intensity of fragment A+B in trichomes is clearly increased (Figure 13H). In contrast to the A+B fragment the fusion protein with the complete CDS is showing only a faint signal which is hardly detectable in trichomes (data not shown).

In summary the full length constructs and fragment A+B are labelling filamentous structures which are most likely microtubules. These microtubules are labelled over the complete length and not exclusively at the tips. The carboxy terminal part of At-CLASP (Cortex fragment) is decorating the plasma membrane and/or the cytoplasm in every cell-type analysed, but cannot bind to filamentous structures any more.
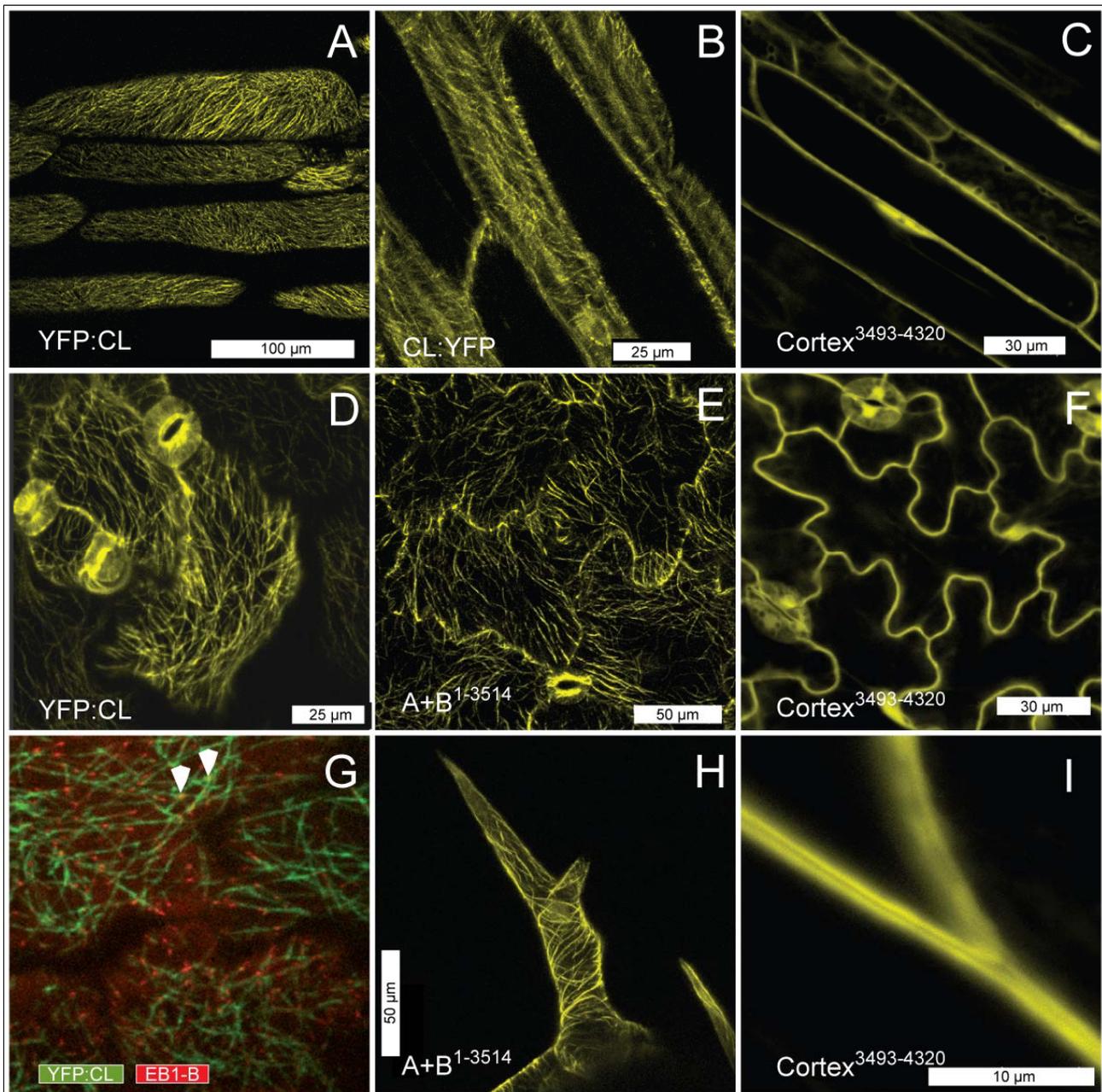
Figure 13: Localisation of At-CLASP and fragments of the cDNA.
(A-C) The full-length fusions to YFP and the Cortex fragment are detected in hypocotyls cells. **(D-F)** The localisation of both fragments and the full-length cDNA is also detected in epidermal cells. **(G)** To determine whether At-CLASP is localised to microtubules plants were analysed harbouring the *EB1-B* construct fused to CFP and At-CLASP fused to YFP. A single scan from epidermal cells shows the EB1-B:CFP fusion protein in red and 35S::YFP:CLASP in green. Colocalisation is observed not frequently (white arrow heads). **(H)** Fragment A+B is located to trichomes. **(I+F+C)** The cortex fragment fused to YFP is found in epidermal pavement-cells **(F)** and hypocotyls cells **(C+I).**

2.7 Analysis of putative CLASP interacting proteins

To identify interactors of At-CLASP a candidate approach was chosen. The orthologs of At-CLASP are members of a complex network of proteins regulating the dynamics of microtubule growth. For instance the binding between *H. sapiens* END BINDING PROTEIN 1 (EB1) and *H. sapiens* CLASP1 or 2 was demonstrated to be mediated via the middle part of the protein (Mimori-Kiyosue et al. 2005). The main interactor of CLASP that gave the name to it is CYTOPLASMIC LINKER

PROTEIN 170 (Clip170) and is not present in *A. thaliana*. Nevertheless other candidates are present which are the three members of the END BINDING PROTEIN 1 (EB1) family. One of the three members of the At-EB1 family was analysed previously in more detail (Mathur et al. 2003b), where it was shown that At-EB1-B is indeed a +end binding protein (+Tip). To determine whether At-CLASP interacts with *A. thaliana* orthologs of known interacting animal proteins from CLASP, a direct Yeast-Two-Hybrid was performed. One +end-binding protein from *A. thaliana* called SPIRAL1 (SPR1) (Sedbrook et al. 2004) was tested too. TUBULIN4 (TUA4) was used as a candidate with most likely positive interaction. The proteins used are listed in Table 4.

At-CLASP was transferred into the bait and prey vector and tested with the candidates into both directions (Table 5). None of the proteins was interacting with At-CLASP. All combinations grew normally after double transformation on the plates selective for the presence of both constructs and the transformation efficiency was reasonably high.

Table 4: Genes and corresponding AGI-codes used for the direct interaction tests.

Genes used for the interaction tests		
EB1-A	END-Binding-Protein 1-A	At3g47690
EB1-B	END-Binding-Protein 1-B	At5g62500
EB1-C	END-Binding-Protein 1-C	At5g67270
SPR1	SPIRAL 1	At2g03680
TUA4	Tubulin alpha-2/alpha-4 chain	At1g04820

Clasp direct interaction matrix				
Bait	CLASP prey		CLASP bait	prey
EB1-A	-		-	EB1-A
EB1-B	-		-	EB1-B
EB1-C	-		-	EB1-C
SPR1	-		-	SPR1
TUA4	-		-	TUA4

Table 5 CLASP direct interaction matrix.
At-CLASP and putative interactors were tested in a direct Yeast Two-Hybrid system. No interaction was observed between At-CLASP and the EB1 homologs, SPIRAL1 (SPR1) and TUBULIN4 (TUA4).

As a second approach to test At-CLASP properties to interact with the proteins of the At-EB1 family new constructs were generated. At-EB1-B and C were transferred into an amino-terminal

CFP-fusion vector similar to the constructs generated in Figure 12. To visualize simultaneously both proteins, At-EB1 and At-CLASP, the *At-EB1* vector was transformed into preselected At-CLASP-YFP plants. More than 50 independent lines were generated for both constructs. At-EB1-B is found on the likely +end of the microtubules labelled in red whereas the At-CLASP signal is green. No overlap was observed between both labelled proteins. Occasionally only few positions marked with an arrow head in Figure 13G showed random overlap.

2.8   Overexpression of *At-CLASP* stabilises microtubules

One of the putative functions of CLASP from *H. sapiens* is the stabilization of the microtubule cytoskeleton (Drabek et al. 2006). The necessity to stabilize microtubules is obvious for example when observing the mutant phenotype of *orbit* the CLASP similar protein from *D.melanogaster*. Microtubules are directed to kinetochores during mitosis by stabilizing grows at the plus end by ORBIT (Maiato et al. 2005). Knockouts in this gene are lethal in later stages of development (Inoue et al. 2000).

To determine whether At-CLASP stabilises microtubules *in planta*, At-CLASP was overexpressed in *tfc-a* mutant background. In *tfc-a* mutants the balance of α/β-tubulin monomers is affected (Kirik et al. 2002a) (refer to chapter 1.1). This imbalance causes phenotypes similar to those observed in mutants with impaired microtubule function. If At-CLASP stabilises microtubules the severe *tfc-a* mutant phenotype might be attenuated by increasing the total amount of At-CLASP. Therefore the 35S:CLASP construct was transformed into *tfc-a* mutant plants. By determining the amount of rescued and unrescued plants in conjunction with PCR genotyping it should be possible to detect a putative general stabilization function of At-CLASP.

As homozygous *tfc-a* mutant lines do not produce seeds, heterozygous plants were transformed. The offspring of a heterozygous generation should segregate into 25% plants showing *tfc-a* mutant phenotype and 75% plants with wild-type appearance. In total 55 primary transformants (T1) were generated and analysed. Six plants (11%) showed the *tfc-a* mutant phenotype and did not produce any seeds. Compared to the expected amount of 25% (=14 plants) in case At-CLASP does not affect the tfc-a mutant. The genotype of all T1 plants was tested by PCR genotyping. Three different parameters were tested. The presence of the T-DNA causative for the *tfc-a* mutant phenotype, the presence of a wild-type allele in this locus to detect heterozygosity and the presence of the newly introduced At-CLASP overexpression construct.

The PCR-analysis showed, that 62% of the T1-generation had a wild-type copy of the TFC-A gene and were therefore wild-type or heterozygous for TFC-A. For the remaining 38% only the *tfc-a* T-

DNA insertion could be detected but no TFC-A wild-type allele. These lines were genotyped for the presence of the newly introduced *At-CLASP* overexpression construct. Unfortunately due to time constraints no further experiments were performed to verify these findings independently.

3   Discussion

The cytoskeleton is a major component of any cell. It is responsible for the establishment and maintenance of the shape, polarity of the cell and transport of cargo and organelles (Figure 1). Changes in the stability of cytoskeletal filaments allow the cell to grow or even to move in respond to certain cues, what is observed for example in fibroblast cells (Small et al. 2002). The variability in stability is achieved by different means (refer to the introduction on page 10). One reason for changes in filament dynamics are associated proteins e.g. MAPs at the ends of filaments. *H. sapiens* CLASP1α is one of these MAPs which is located to the +end of microtubules and functions as a stabilising protein. Proteins of this class prevent the depolymerisation of certain microtubules.

Nevertheless until now no protein from *A. thaliana* was described that showed similarity to CLASP1α from *H. sapiens*.

3.1   The similarity and structural composition of At-CLASP and *H. sapiens* CLASP1α

Similarity searches with *H. sapiens* CLASP1α revealed one candidate in *A. thaliana* At2g20190 (chapter 2.1). This candidate was likely to be CLASP of *A. thaliana* because of several reasons. The total length of the *H. sapiens* CLASP1α is 1538aa in comparison to 1439aa for the candidate protein. In addition HEAT-repeats which are distributed over the *H. sapiens* CLASP1α protein are also found in the *A. thaliana* candidate (Figure 6). The C-terminal part of the protein was most conserved and allowed the detection of the MAST domain in both proteins. This is the only domain which is conserved between these proteins. This inability to detect more conserved domains might be due to the evolutionary distance of both proteins (Figure 4A). Phylogenetic analysis showed that plants, animals and nematodes (represented by *C. elegans*) are located on different branches which were detected with high confidence by to different algorithms. According to these algorithms both representatives of the dicots (*M truncatula* and *V. vinifera*) are closer related to At-CLASP, although the significance for this classification was only 67 respectively 59%. Both *O. sativa* paralogous genes were found in a separate branch, although the amount of similarity on amino-acid level compared to *M. truncatula* and *V. vinifera* is related. Nevertheless the positioning of this monocot proteins (*O. sativa*) in a separate branch was expected due to the evolutionary distance of monocots and dicots. Representatives of mosses (*P. patens*) and green-algae (*O. lucimarinus* and *O. tauri*), in that order, are At-CLASP related proteins. This order is consistent with current knowledge. Most animal organisms contain two CLASP proteins. The only exception is found in *C. elegans*. *C. elegans* contains three different CLASP proteins which are evolutionary distant from plants and the other animal organisms. Likely *C. elegans* CLASP2 and 3 developed in a later

duplication event. By contrast, *M. musculus, R. norvegicus* and *H. sapiens* contain only two *CLASP* genes. It is conceivable that both genes were duplicated at an early time point in evolution. Interestingly CLASP1 or 2 from *M. musculus* and *R. norvegicus* are located on a separate branch which is supported by a significant score. Both proteins are therefore closer related. *D. melanogaster* still clusters with the animal branch. However it is evolutionary most distinct which is supported by the 100% significance value from both algorithms.

This information discussed above showed similarities between *H. sapiens* CLASP1α and the *A. thaliana* candidate At2g20190 which therefore was termed At-CLASP.

3.2 *at-clasp* mutant plants show pleiotropic phenotypes

Alleles with insertions in the *At-CLASP* locus are reduced in fertility, show underbranched trichomes and rosette leaves are oriented in spirals, if grown under restrictive temperatures (Table 1, Figure 8). Three T-DNA insertion lines were subject of analysis (Figure 5). *clasp034* and *clasp782* have a T-DNA insertion within an intron. Both alleles are most likely hypomorphic as a correct splicing of the final transcript is feasible. Only allele *clasp061* has a T-DNA in an exon and is probably devoid of a complete transcript. Homozygous plants harbouring the *clasp061* T-DNA insertion are likely amorph alleles.

Further evidence that *clasp061* could be a hypomorphic allele came from the analysis of trichome branching on leave three and four (Table 1). Allele *clasp061* is most effected as 23% of the trichomes had only one branch-point in comparison to 0,9% in the corresponding Col wild-type. Furthermore the production of siliques is affected in all three alleles analysed like observed for the branching frequency in trichomes. Allele *clasp061* could not produce any siliques (Figure 8) like allele *clasp034* at 25°C or above. Only allele *clasp782* produced siliques and showed the weakest branching phenotype. Under growth conditions with temperatures below 25°C all three alleles produced siliques indistinguishable from wild-type. Probably all alleles analysed led to a temperature sensitive phenotype, which was observed for another *A. thaliana* mutant MAP mutant, termed *mor1* (Whittington et al. 2001).

In addition growth of the *at-clasp* mutants at temperatures higher than 25°C changed the orientation of the leaves. Leaves were oriented in spirals. This phenotype was observed for the +end MAP *sku6* (Sedbrook et al. 2004) and might be a common phenotype for mutant MAPs. Due to the changed microtubule dynamic the growth of structures like leaves is disturbed and they change their straight growth to spirals. Further support for different severeness of the phenotypes in all alleles analysed came from RT-PCR experiments. Only allele *clasp034* showed residual full-length transcript after 33 amplification cycles. The same primer pair detected the *At-CLASP* transcript in Col wild-type

(Figure 9). As the T-DNA insertion in *clasp034* is located in an intron it might be that the pre mRNA is spliced partially accurate resulting in a weak mutant phenotype. The phenotypically weakest *clasp782* allele was devoid of any full-length transcript. Nevertheless it is conceivable that 75% of the transcript is present as the insertion was found after 75% of the gene. Likely the insertion effects the stability of the full-length transcript which is therefore not detectable any more. The residual transcript in *clasp782* mutant plants might be enough to show a weak mutant phenotype. Primers amplifying the transcript before the insertion in *clasp782* do detect a transcript (data not shown). Therefore it is likely that a truncated transcript is present in clasp782 explaining the weak phenotype.

3.3 *At-CLASP* is expressed in almost any tissue

PCRs on leaf cDNA-libraries revealed that *At-CLASP* is expressed in leafs (Figure 9A), supported by the trichome branching phenotype. The putative *At-CLASP* promoter driving the expression of the GUS-reporter gene revealed a comparable result (Figure 9B+C). Nevertheless the promoter was more active in younger tissue. As this promoter driving the expression of the *At-CLASP* cDNA is able to rescue the mutant phenotype it is likely that the GUS expression pattern observed is reflecting the *in planta* expression situation. In addition RNA microarray hybridisation experiments, collected by the Genevestigator website, showed that the *At-CLASP* transcript is detected at comparable levels in most tissues (Figure 9D). Only probe set 265315_at which is located at the beginning of the transcript, showed the expression levels described above. The second probe set (265576_at) which should detect the end of the transcript yielded much higher signal intensity (more than 10 fold). As one would expect comparable signal intensity for two probes binding the same transcript, different scenarios might explain this finding. The probe set used might bind not specifically the *At-CLASP* transcript detecting other transcripts as well. However BLAST similarity searches identified only *At-CLASP* as similar to the transcript sequence. A further possibility could be a wrong gene annotation resulting in a different transcript. But up to now the presence of a full-length *At-CLASP* cDNA from Riken is not supporting this hypothesis. But no further cDNAs are available to verify the sequence information generated by the Riken institute. As differential splicing of *H. sapiens CLASP* was observed (Galjart 2005) in certain tissues, this possibility cannot be excluded. MAPs are regulating the dynamic of microtubules and differential splicing allows the generation of different proteins with different properties. Therefore splicing could generate an additional way to regulate microtubule dynamics. Whether differential splicing is present for the *At-CLASP* transcript is not clear and remains to be analysed in more detail.

By the availability of microarray hybridisation data a more sophisticated analysis is possible. Genes

important for a special process e.g. the regulation of microtubule dynamic must be expressed at the same time point and tissue. Not necessarily the total amount of transcript is identical but the timely activation and repression of transcription must show overlaps. Algorithms used for example by the "Expression Angler" website normalize the total expression levels and compare the timing as described above. Interestingly several known genes are coregulated with *At-CLASP* (Table 2): KLUNKER (KLK) is the gene with the best coregulation score (0,894) and belongs together with GNARLED (GRL; 0.807) to the regulators of ARP2/3 dynamic (Mathur 2005) . Interestingly ACTIN7 and *At-CLASP* are coregulated genes. Interactions between the microtubule- and actin-cytoskeleton are well known in mammalian cells (Watanabe et al. 2004). Recently the direct interaction between *H. sapiens* CLASP 1/2 and the actin-cytoskeleton was shown too (Tsvetkov et al. 2007). Therefore it is conceivable that similar interactions between the actin and microtubule cytoskeleton are also present *in planta*. Nevertheless the *in planta* importance of these At-CLASP coregulated genes has to be shown in later experiments. In addition three proteins related to microtubule dynamic were found to be coregulated with *At-CLASP*. The first candidate, the putative light chain of dynein was not analysed in *A. thaliana* so far. But the mammalian dynein/dynactin is an important microtubule +end binding protein complex interacting with CLIP170 (Lansbergen et al. 2004). This complex allows microtubules to slide along the cell cortex and can produce pulling forces (Dujardin et al. 2002). As vital processes are often conserved between many species it is conceivable that plants are no exception, but further experiments are needed to test this hypothesis. In addition one has to mention that until now no CLIP170 similar protein was identified in *A. thaliana*. More interestingly this dynein light chain like protein was also found as a putative STI interactor in Yeast Two-Hybrid (Table 16). As the microtubule cytoskeleton is important for STI function (*sti* mutant trichomes can be rescued by the application of microtubule stabilizing drugs (Mathur and Chua 2000)) a possible link between At-CLASP/dynein and STI/dynein needs to be tested.

The second candidate which is coregulated with *At-CLASP* is *TONNEAU2 (TON2)*. TON2 is a protein phosphatase 2A subunit and the corresponding mutant showed no preprophase band, misaligned phragmoplasts and dwarf growth (Camilleri et al. 2002). It is conceivable that phosphorylation is one way to regulate microtubule dynamic in addition to the diverse MAPs like At-CLASP. Other studies showed that direct modifications of the tubulin dimer can effect the stability of the complete filament (Bulinski and Gundersen 1991). Whether the target of this phosphatase is tubulin itself or certain accessory proteins is unknown, but the importance of TON2 for microtubule organisation/dynamic is striking with respect to the phenotypes observed. The third candidate gene was identified to be coregulated, even if the score is the weakest for all genes

included. This is SPIKE1 (SPK1) a protein with sequence similarity to a *H. sapiens* adapter protein needed to integrate signals leading to cytoskeletal reorganisation. *spk1* mutants have strongly deformed cotyledons and are only viable under 100% humidity as cells loose contact to each other. In addition trichomes are unbranched and *spk1* mutant plants grown under the conditions described above are sterile. Possibly SPK1 is a candidate for an upstream protein regulating MAPs like At-CLASP. Nevertheless possible interaction scenarios mentioned above are speculative and need further support of experimental data which is not yet present. In summary the analysis of coregulated genes identified a number of interesting genes. Surprisingly many identified genes showed a direct connection to the cytoskeleton excluding the possibility that this method is not suitable to identify genes important in the same pathway. Nevertheless the identification of these coregulated genes does not necessarily imply a physical interaction but it means that both compared genes are switched on and off at comparable time-points and tissues. Furthermore all gained information has to be proven by experimental data as the information described in this paragraph is generated mostly *in silico*.

3.4   Rescue and localisation of At-CLASP in mutant background

Two different attempts were used to rescue the *at-clasp* mutant phenotype. The full length *At-CLASP* cDNA (without UTRs) was expressed under the control of the 35S promoter (Figure 12) or under the control of the putative *At-CLASP* promoter (Figure 11). Both 35S constructs with YFP fused to the C-terminus or N-terminus of *At-CLASP* were able to rescue all analysed aspects of the *at-clasp* mutant phenotype. Likely the expression level of the 35S- and the *At-CLASP*-promoter is comparable (not analysed).

Mammalian CLASP1 is localised to the +end of growing microtubules (Akhmanova et al. 2001). The 35S construct mentioned above was used to visualize the At-CLASP protein *in planta* (Figure 13). The At-CLASP fusion protein was found in all cell types analysed. At-CLASP fusions to YFP are found along filamentous structures. Previously it was shown, that *A. thaliana* END-BINDING PROTEIN 1B (EB1-B) binds to microtubules (Mathur et al. 2003b). The colocalisation analysis of EB1B and At-CLASP showed that both proteins are bound to identical filaments and it was concluded, that At-CLASP is a microtubule binding protein (Figure 13G). Interestingly an overlap between both signals was usually not observed and seemed to occur only by random overlap of two microtubule filaments. This observation also implied that the ends of growing microtubules in the cells analysed were devoid of At-CLASP. By contrast *H. sapiens* CLASP1α is localised to the +end of growing microtubules (Akhmanova et al. 2001). Several reasons are conceivable explaining the altered localisation pattern. First it might be that the evolutionary distance to e.g. the well analysed

H. sapiens CLASP1α is sufficient for major changes in the At-CLASP properties. The localisation *in planta* might not be the +end anymore or further accessory proteins might be necessary to localise At-CLASP to the +end under special developmental situations for example the switch to mitosis. The At-CLASP similar protein ORBIT from *D. melanogaster* is important for mitosis because amorph alleles of *orbit* are defective in chromosome segregation (Inoue et al. 2000). DAPI stained nuclei did not show any apparent deviation from wild-type in leaf epidermal cells (data not shown). The altered localisation pattern might be to a functional diversification of At-CLASP properties during evolution. Other plant proteins might substitute several functions that are intrinsic to CLASP proteins from other organisms. Furthermore the observed localisation pattern might be due to the changed expression levels by the usage of the 35S promoter. High levels of *At-CLASP* transcript increase likely also the amount of the At-CLASP protein. An increased amount of At-CLASP could bind the microtubule cytoskeleton unspecifically leading to a change of its endogenous localisation pattern.

To characterize the binding properties of At-CLASP in more detail YFP-Fusion to fragments of the *At-CLASP* cDNA were analysed. Previous studies with *H. sapiens* CLASP1α showed microtubule binding activity in the middle part of the protein (Figure 3). Therefore constructs harbouring the beginning of the cDNA (termed A+B) and the end of the cDNA (termed cortex) were fused to YFP (Figure 12). The A+B$^{1-3514}$ fusion protein was localised to filamentous structures similar to the full-length construct. The observed binding to microtubules is consistent with the data from other researchers (Mimori-Kiyosue et al. 2005). Due to the localisation of the microtubule binding protein EB1-B and At-CLASP to the same filament the structure where the A+B fragment was bound to is likely the microtubule cytoskeleton again. But in contrast to the full-length construct the overall signal intensity of the A+B fusion protein was increased. For example a much stronger signal could be detected in trichomes (Figure 13H). Nevertheless the total amount of labelled microtubules seemed to be decreased. Consistent with the data from other researches (Mimori-Kiyosue et al. 2005) the first part of the protein is localised to microtubules. Nevertheless the fragment used covers 75% of the protein. The usage of smaller parts of the protein might narrow down the necessary binding sites. The increased signal intensity might be due to unspecific binding to microtubules. The missing part in fragment A+B is responsible (in *H. sapiens*) for the binding to different CLIP proteins (CLIP170 is not present in *A. thaliana*), the Golgi apparatus and the cell-cortex (Figure 3+Figure 12). In addition changes in the protein stability of the fragment might be responsible for the changed signal intensity.

Until now the binding properties of the C-terminal part of At-CLASP were unknown. Therefore a fusion between the end of the cDNA (3493-4320bp) the cortex fragment and YFP were used. Plants

expressing this fragment showed no labelling of filamentous structures any more but a very bright signal, stronger than all other constructs used, in the cytoplasm or the plasmamembrane (Figure 13C+F+I). Only the cell wall was devoid of any fusion protein (Figure 13I). The cortex fragment is therefore not responsible for the binding to microtubules, but might mediate the binding of the At-CLASP protein to the cell cortex. This finding is consistent with the data from other researchers (Mimori-Kiyosue et al. 2005). Unfortunately with the localisation pattern observed it cannot be excluded that the fusion protein is located by default to the cytoplasm. Due to the strong signal intensity a tethering to the cell-cortex or a general localisation to the cytoplasm is not distinguishable.

The putative *At-CLASP* promoter, driving the expression of the At-CLASP cDNA, is able to rescue the *at-clasp* mutant phenotype (Table 3). Only 25% (YFP fusion at the C-terminal part of At-CLASP) or 30% of the transformed plants (N-terminal fusion) were able to rescue the mutant phenotype in the T1 generation. Only 4% respectively 7% of the plants rescued all aspects of the mutant phenotype in T1 generation. Several possible reasons could explain the rescue efficiency observed. First it is conceivable that the YFP which is fused to the cDNA might disturb the correct expression or later folding of the protein. However this possibility is not very likely as the same cDNA under control of the 35S promoter is able to rescue the *at-clasp* mutant phenotype. Second, the putative promoter might be incomplete. Several regulatory motifs needed might not be present. In addition regulatory sequences in the intronic region, which were not present in this construct, might increase the total amount of transcript expression like observed elsewhere (Hong et al. 2003). The third scenario assumes an expression-level threshold below no rescue is observed. As the heterozygous T1 generation was scored for rescue it is possible that two copies of *At-CLASP* under its endogenous promoter are needed to rescue the mutant phenotype assuming that the expression level of the 35S promoter is higher with no need for two copies to be present. This could be tested by crossing one mutant allele e.g. *clasp061* to Col wild-type and the analysis of the F1 generation for the presence of any *at-clasp* related phenotype. In addition the analysis of not- and worse-rescued lines under the putative endogenous promoter (they were shifted to lower temperatures to generate seeds) will allow finding rescued homozygous lines in T2 if this hypothesis is true. So far the hypothesis of a dosage effect seems to be more probable as completely rescued plants were found in T1 generation. This might be due to several insertions of the T-DNA in the genome of these rescued T1 lines. In addition several plants showed rescue only in some aspects of the *at-clasp* mutant phenotype, suggesting again a dosage effect. Unfortunately the lines mentioned above were generated latest in this study. Therefore a detailed analysis of the localisation of the At-CLASP-YFP fusion under its putative promoter was not possible.

3.5 At-CLASP is not interacting with known binding partners

H. sapiens CLASP1/2 was shown to interact with *H. sapiens* EB1 and CLIP170 were CLASP derived its name from. CLIP170 is not present in *A. thaliana* judged by similarity searches but *H. sapiens* CLIP170 still showed some properties like microtubule when introduced into *A. thaliana* (Dhonukshe et al. 2003). The interaction between *H. sapiens* CLASP1/2 and EB1 is conserved in most organisms analysed (Lansbergen et al. 2006). *H. sapiens* EB1 is localised to the +end of microtubules like CLASP1/2 and promotes microtubule polymerization. The utilization of the yeast two-hybrid system allowed direct interaction tests between all candidates (Table 4+Table 5). Interestingly no interaction was observed. One possibility is that the yeast Two-Hybrid system is not suitable for testing interactions between these proteins. The researchers describing the interaction between *H. sapiens* CLASP1/2 and EB1 used immunoprecipitation for their experiment (Mimori-Kiyosue et al. 2005). The folding of At-CLASP and its putative interactors might be not accurate in *S. cerevisiae* or certain *A. thaliana* specific modifications are not incorporated into the protein rendering it unable to interact. On the other hand *S. cerevisiae* contains an EB1 similar protein termed BIM1p. As the EB1 interactions are conserved in many organisms no binding partner might be left to interact with the Gal4 fused proteins if *S. cerevisae* BIM1p has the ability to bind to At-CLASP. As a result the reporter might not be activated even if binding between EB1 and At-CLASP is possible. In contrast to this hypothesis independent experiments did not reveal colocalisation of EB1-B and At-CLASP *in planta* (Figure 13G). An overlap between both signals of the differentially tagged proteins was detected only if microtubules cross randomly. Usually the At-CLASP signal was clearly separated from the EB1-B signal on the same filament. So far this data suggests that At-CLASP is not localised to the +end but it might depend on the developmental situation of the cell (refer to chapter 3.4). Remembering the localisation pattern of At-CLASP, it is questionable that the +end binding protein SPR1 is a binding partner in the test-system. Nevertheless SPR1 was tested by yeast Two-Hybrid and not by an *in vivo* system comparable to the EB1-B and At-CLASP localisation described before. The binding of At-CLASP to microtubules was shown in the localisation chapter therefore the binding to one α-tubulin (TUA4) was designed as a positive control. Again no interaction was observed in yeast Two-Hybrid. As several α- and β-tubulins exist in *A. thaliana* instead of few in mammals (Kopczak et al. 1992; Snustad et al. 1992) it might be possible that the presence of this variety reflects an additional way of regulation of microtubule dynamic. Maybe TUA4 is not recognized by At-CLASP but other α-tubulins are. Furthermore it is conceivable that a single tubulin is not sufficient to bind At-CLASP but several subunits are needed like in a filament.

An additional explanation for the missing expected interactions might be the evolutionary distance

of At-CLASP and *H. sapiens* CLASP1/2 (Figure 4). Plant CLASPs and animal CLASPs are located on different branches emphasizing the evolutionary distance. Interestingly only the C-terminal part of all CLASP similar proteins showed a higher degree of conservation (Figure 6C). This region of the protein is important for the binding to CLIP170, which is not present in the *A. thaliana* genome. In addition the middle part of the human CLASP1 protein which is important for the binding to EB1 is even less conserved in *A. thaliana*. Finally it might be that At-CLASP acquired different interacting proteins during evolution, therefore explaining the interaction tests.

Previous studies suggested that CLASP1/2 (Drabek et al. 2006) or ORBIT (Maiato et al. 2005) might have a general stabilizing function. According to these authors subsets of microtubules like kinetochore directed microtubules are stabilized by ORBIT. This stabilization is essential for progression of mitosis in *D. melanogaster*. In an initial attempt to test this function *At-CLASP* was overexpressed in *kisT1* mutant plants. These mutants have a disturbed cytoskeleton and show dwarf growth with sterility in homozygous lines. The PCR analysis of The T2 generation revealed 13 plants (25%; page 30) harbouring the overexpression construct and the T-DNA responsible for the *kisT1* phenotype. The presence of this phenotypic class suggested that At-CLASP might have stabilizing function. But due to time constraints no further experiments were performed to verify this hypothesis. Therefore this hypothesis has to be termed speculative.

3.6 Outlook

The characterization of At-CLASP in this study indicated several differences and similarities in comparison to data obtained in other organisms. This study showed that the full-length cDNA used is able to rescue the *at-clasp* mutant phenotype. Furthermore the putative *At-CLASP* promoter is also able to rescue the mutant phenotype. Consistent with observations from *H. sapiens* At-CLASP binds microtubules like fragment A+B. The cortex fragment showed no microtubule binding similar to observations in *H. sapiens*. Future studies could focus on the further analysis of differences between At-CLASP and *H. sapiens* CLASP. So far the cause for the pleiotropic phenotypes observed in *at-clasp* mutants is unknown. The sterility observed for the more penetrant alleles of *at-clasp* might be due to a defect within the reproductive organs. Whether the male or female part is affected or the loss of At-CLASP function is a more general process needs to be clarified. Until now the At-CLASP localisation was never observed exclusively at the +end of growing microtubules. The analysis of different stages e.g. in dividing cells should allow a decision whether At-CLASP does not localise to the +end of microtubules or only at specific stages. Cell culture might be especially suitable as they can be synchronised for the presence of special developmental stages. Furthermore the analysis of YFP fusions to At-CLASP under its putative endogenous promoter might show whether the promoter is a matter for the previously observed localisation using the 35S promoter.

Until now the analysis of interactions revealed no interaction of At-CLASP with the *A. thaliana* members from known mammalian interactors. Especially EB1 is one of the key players for interactions with the microtubule cytoskeleton and these interactions were observed in almost any eukaryotic organism except plants. Therefore interactions between At-CLASP and the three members of EB1 in *A. thaliana* should be retested by different techniques closer to the *in planta* situation like Bimolecular Fluorescence Complementation (BiFC). One major interactor of *H. sapiens* CLASP is not present in the *A. thaliana* genome up to the current knowledge which is CLIP170. As similarity did not reveal any candidate different approaches like yeast Two-Hybrid or co-immunoprecipitation assays might identify the major interactors of At-CLASP. A protein with a similar function like CLIP170 might be identified, if it is present.

The function of *H. sapiens* CLASP is not completely understood but might be the stabilisation of certain microtubules to allow for example cell-division. Whether a comparable function in *A. thaliana* is present should be also tested. The further evaluation of the At-CLASP overexpression in *tfc-a* mutant plants might help to solve this question.

At-CLASP coregulated genes already supported a function of At-CLASP in the regulation of

microtubule dynamics. But until now the *in vivo* importance of these genes is elusive. The analysis of mutant and double mutant combinations might help to understand the relevance of this finding.

❖ Stichel:

4   Introduction

Plants are constituted of a variety of cell types, which differ in shape and function. Understanding the adaption of cell fate during development of a whole organism like *A. thaliana* is a very complex process. Due to the complexity of this process only a subset of cell types of A. *thaliana* has been analyzed in the past. The epidermal cells of leaves and roots are among the best analyzed plant tissues, although many aspects of cell fate determination are still only poorly understood. Epidermal cells have many functions like perception of and integration of environmental stimuli. In addition, they present a physical barrier against water loss. Leave epidermal cells are divided into three subtypes. Leave hairs (trichomes) pavement cells and stomata. Stomata develop in a well understood manner (Bergmann et al. 2007). Trichomes grow peripendicular to the epidermal surface and are big single cells. The function of trichomes is probably the protection against insects, UV-light and loss of water (Johnson 1975; Mauricio et al. 1997). Nevertheless, under controlled environmental conditions, trichomes are dispensable which facilitates screens for loss of function mutants. Several screens were performed to identify genes involved in trichome development (Marks et al. 1992; Hulskamp et al. 1994; Folkers et al. 1997). The phenotypes of the mutants found in these screens were compared to the wild-type trichome development. Now it was possible to dissect different steps in trichome development and thereby to determine the function of mutants within the developmental cascade (Figure 14).
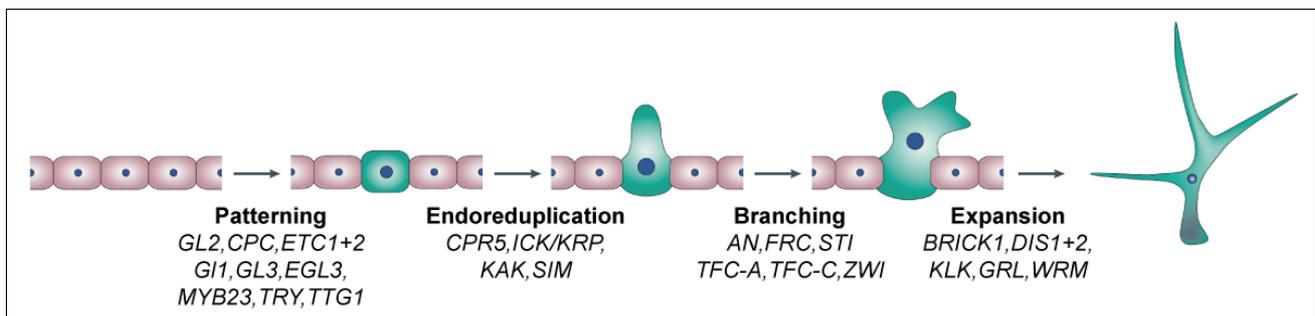
Figure 14: Trichome development can be separated in different steps
Trichome development can be divided into four different processes. By the so called patterning genes an initially equivalent epidermal cell is selected to become a trichoblast. Afterwards this cell expands rapidly its volume in conjunction with several endoreduplikation rounds. Branching genes establish the characteristic branch-points found in any wild-type trichome. Finally several proteins are required to mediate the expansion grows up to its adult stage. Figure was modified from (Hulskamp 2004).

4.1   Trichome development

The first step of trichome development is the selection of a precursor cell out of the epidermal cell-layer (Figure 14). This selection process is carried out through *de novo* pattern formation and is not

due to a position dependent mechanism, like it is found in roots (Schellmann et al. 2007). *De novo* patterning requires at least two components with different physical properties, an activator and an inhibitor. The activators of trichome fate determination are initially expressed everywhere. The activator simultaneously enhances its own transcription as well as the expression of inhibitory components. Thus, random fluctuations in the level of the activator lead to an enhancement of both components. The inhibitory proteins can spread faster to the adjacent cells than the activator proteins and as a consequence the trichome fate in the neighboring cell is inhibited. This general mechanism of pattern formation was described also by a mathematical model (Meinhardt 1982; Meinhardt 1994). Mutant screens identified a number of positive regulators of trichome pattering. These mutants are characterized by reduced trichome numbers or complete absence of trichomes. Among this class of mutants are *transparent testa glabra 1 (ttg1)*, *myb23*, *glabra1 (gl1)*, *glabra3 (gl3)* and *enhancer of gl3 (egl3)* (Koornneef 1981; Koornneef et al. 1982; Payne et al. 2000; Kirik et al. 2001b; Zhang et al. 2003). By contrast loss of negative regulators of trichome development results in an increased number of trichomes. The members of this class are TRIPTYCHON (TRY), CAPRICE (CPC), as well as at least two TRY homologous proteins termed ENHANCER OF TRY AND CPC 1 (ETC1*)* and ETC2 (Wada et al. 1997; Schellmann et al. 2002; Kirik et al. 2004a; Kirik et al. 2004b). e*tc1* or *etc2* alone do not show any patterning defect, but triple mutants like *try cpc etc1* are almost completely covered with trichomes (Kirik et al. 2004a).

Most proteins mentioned above are transcription factors, GL1 and MYB23 belong to the myb family, like TRY and its homologs. In contrast to GL1, the transactivation domain in TRY and its homologs is absent. They might be functionally limited to the binding of target genes without the subsequent activation of transcription. GL3 and its homologue EGL3 belong to the family of basic helix-loop-helix (bHLH) transcription factors (Toledo-Ortiz et al. 2003). TTG1 is the only mutant not encoding for a transcription factor. It belongs to the WD40 proteins that participate in diverse biological processes like gene transcription or cell division (Neer et al. 1994; Smith et al. 1999). Recent studies revealed that several proteins described above might build up a complex that regulates trichome fate. This putative complex can either promoter or inhibit the trichome fate of a single epidermal cell, depending on its composition. This complex has so far not been isolated but several studies identified interaction partners by Yeast Two-Hybrid experiments (Payne et al. 2000; Zhang et al. 2003; Kirik et al. 2005). According to these interaction studies GL3 and EGL3 can interact with TTG1 and GL1, but TTG1 and GL1 do not interact. A complex of these proteins, GL3, EGL3, TTG1, GL1 and MYB23 can promote the trichome fate (Figure 15). The suppression of trichome fate is likely achieved via competition of the inhibitory proteins (TRY,CPC,ETC1,ETC2) against the activating proteins for binding to GL3 (Esch et al. 2003) and the proposed but not yet

proven faster diffusion rate of the inhibitory proteins into the neighboring cells. It is assumed that GL1 is replaced by the inhibitory proteins in cells with epidermal fate (Figure 15). To inhibit the acquisition of trichome fate, inhibitory proteins like CPC have to be non cell-autonomous and need to move between cells faster than activating proteins. CPC has a dual function in root- and trichome-epidermis and it was shown that a CPC::GFP fusion is able to move in root-epidermis. This fusion was found in trichoblast and atrichoblast of the root, whereas *CPC* is expressed exclusively in atrichoblast (Wada et al. 2002; Kurata et al. 2005).

At the last step of trichome fate determination GL2 is activated, thereby triggering the expression of further genes required for trichome development (Rerie et al. 1994; Di Cristina et al. 1996; Szymanski et al. 1998; Fyvie et al. 2000).
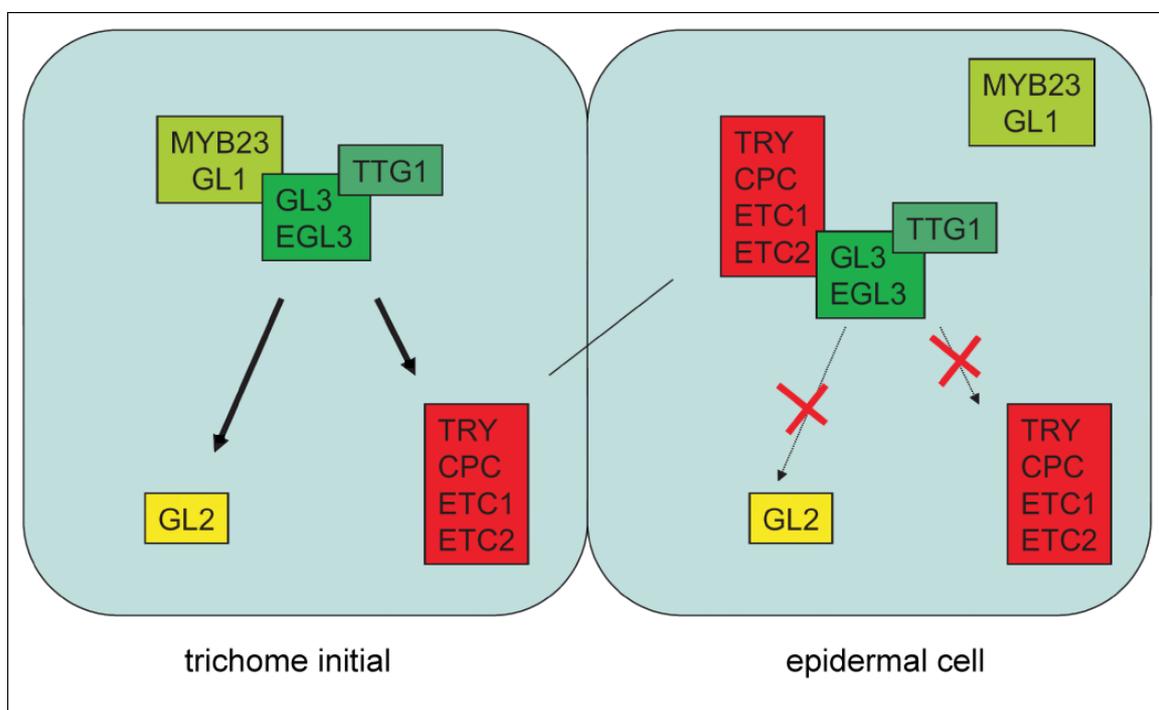
Figure 15: The putative protein-complex present in trichome-initials and epidermal cells.
Trichome initials contain a protein complex of at least five activators (green). The inhibitory proteins (red) are replaced from the complex by GL1/MYB23 and are able to move to neighbouring cells. Now all subsequent genes are expressed by the action of the HD-Zip transcription factor GL2 (arrows indicate expression of target genes), additionally the expression of the inhibitory genes is increased too. All adjacent cells acquire higher levels of the inhibitory proteins and compete for binding to GL3/EGL3. As a consequence GL1/MYB23 cannot bind any more and the inhibitory complex is present.
         Figure was modified from (Schellmann et al. 2005).

After establishment of the trichome pattern the trichome precursor cells increase in size and DNA content, a process called endoreduplication (Figure 14, reviewed by (Edgar et al. 2001)). Several proteins are known to regulate this process. These are SIAMESE (SIM) (Walker et al. 2000; Churchman et al. 2006), KAKTUS (KAK) (El Refy et al. 2003), INHIBITOR/INTERACTOR OF CYCLIN DEPENDEND KINASES/ KIP-RELATED PROTEINS (ICK/KIP) (Schnittger et al.

2003) and CONSTITUTIVE PATHOGEN RESPONSE 5 (CPR5) (Kirik et al. 2001a). *sim* mutant plants have multicellular trichomes with different nuclei showing a reduced DNA content. SIM encodes a 14 kD protein of unknown function. The presence of putative cyclin binding motifs and similar motif also found in ICK/KRP proteins suggest a function in cell-cycle regulation (Churchman et al. 2006). g*l3* mutant trichomes show decreased ploidy levels whereas *try* mutant trichomes exhibit higher degrees of ploidy (Hulskamp et al. 1994). Changes in ploidy level (rounds of endoreduplication) are mostly correlated with changes in trichome branch number. Increased ploidy level can lead to overbranched trichomes with supernumerary branches, like it is observed for *try* mutant trichomes. By contrast reduced ploidy levels are often causative for underbranched trichomes, what is observed in *gl3* mutant trichomes. Beside the endoreduplication phenotype the following mutants also show other pleiotropic effects. *kaktus (kak)* mutant trichomes are overbranched and show an increased DNA content (El Refy et al. 2003). KAK belongs to a completely different class of than the others proteins described before as it encodes a putative ubiquitin E3-ligase, which might be involved in protein degradation. Apparently endoreduplication is affected by the action of cell-cycle related proteins like (ICK/KIP). Trichome specific overexpression of this protein decreases the ploidy level and can induce cell-death (Schnittger et al. 2003). Furthermore cell-death is observed in *constitutive pathogen response 5 (cpr5),* a mutant that mimics pathogen response in absence of any pathogen. *cpr5* mutant trichomes are underbranched, glassy, show a reduced DNA content and die upon maturation (Kirik et al. 2001a).

Followed by enlargement of the cell volume branching genes are establishing the branch-points. Mutants affected in this process can be divided in early or late acting proteins. Proteins which are important at an early step of branch formation might not establish all branch-points showing no branches in the worst case. In contrast, late acting proteins might show only a reduction of branch-point formation STICHEL (STI) is acting at an early time point of trichome branching, since amorph alleles do not branch at all (Ilgenfritz 2000; Ilgenfritz et al. 2003; Bouyer 2004). *Angustifolia (an)* mutants are defective in the initiation of the second branch point (late acting) and present trichomes with one branch point only (Folkers et al. 2002a; Kim et al. 2002). *an* mutant trichomes accumulate actin filaments in the tip of trichomes. Additional phenotypes are changes in leaf shape and epidermal cell complexity (Kim et al. 2002). ZWICHEL (ZWI) interacts with AN in the yeast two-hybrid system and shares a similar branching phenotype (Oppenheimer et al. 1997). Nevertheless an *in planta* interaction was not shown until now. ZWI shows homology to kinesin motor proteins which are supposed to move along microtubule tracks.

Cytoskeleton associated proteins play an important role in the establishment of the 3-dimensional structure of a trichome. Regulators of the actin cytoskeleton are mainly involved in the last step of

trichome development. The proteins involved (Figure 14) will be explained in the introduction of the AtCLASP part because of the closer topical relevance.

4.2   Stichel a branching specific gene

This study focuses on the characterization of STI a protein with, up to now, specific function in trichome branching. Nevertheless the STI assigned function is so far unknown. In contrast to STI several other genes involved in trichome branching have functions beyond the regulation of trichome development. *tfc-a* mutant plants for example are almost unbranched, stunted and sterile (Kirik et al. 2002a). Several STI related studies were performed (Ilgenfritz 2000; Ilgenfritz et al. 2003; Bouyer 2004). *STI* was cloned by Hilmar Ilgenfritz by determining recombination event frequency between L*er* and Col (Ilgenfritz 2000). *STI* is located on chromosome two and "The Arabidopsis Genome Initiative" (AGI) (AGI 2000) assigned At2g02480 to its locus. The cDNA revealed that the annotation of the genomic sequence was accurate and the 3,6 kb long cDNA is assembled from six exons and five introns. The STI protein has a predicted length of 1218 aa and a conserved domain with similarity to the prokaryotic DNA-Polymerase III γ-subunit. DNA-Polymerase III mediates the replication of the genomic DNA in prokaryotes. Functionally related proteins from eukaryotes belong to the Replication factor C (RF-C) group. The similarity of STI to other proteins is detected only in the domain between position aa 449-799. Four genes in *A. thaliana* show similarity within this domain but only one, At1g14460, is closely related (Figure 16, red circle). The comparison of the STI conserved domain to different γ–subunits of DNA-Polymerase III from bacteria (Figure 16 green circle) revealed that they are closer related to STI than the RF-C domain containing proteins (blue circle). Only one member from *A. thaliana* with a putative RF-C domain is similar to proteins from eukaryotes containing this conserved domain (blue circle).
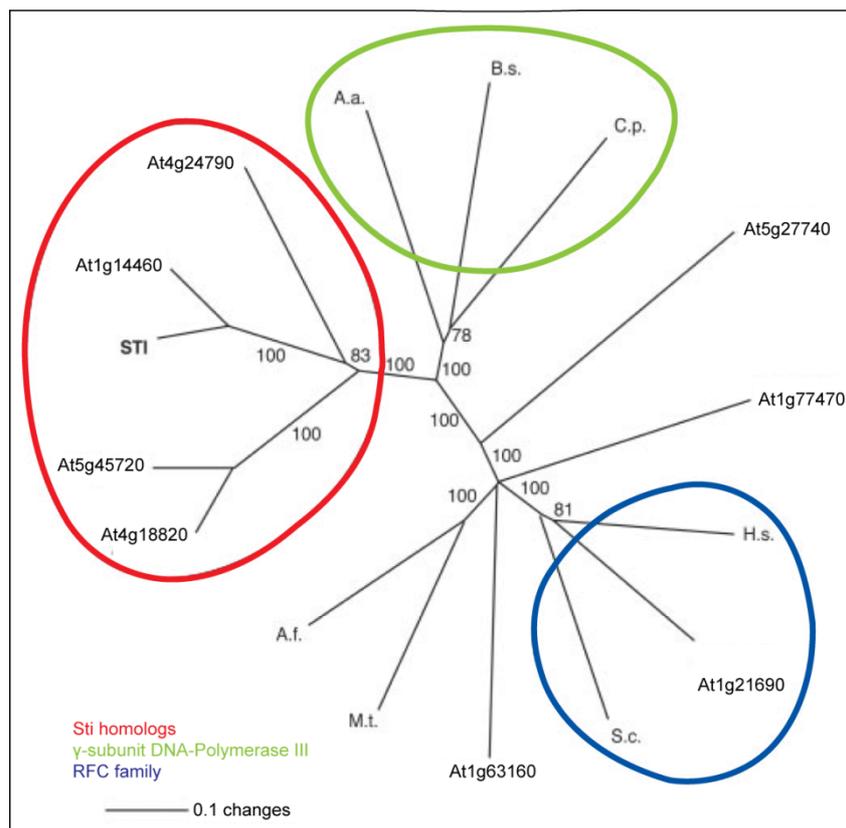
Figure 16: Similarity between STI and proteins from other organism sharing this conserved domain.
The STI sequence contains a conserved domain (aa 449-799). Four different proteins from *A. thaliana* show different similarity when compared to this domain (red circle). The γ-subunit from three analysed bacteria clades (green circle) is more similar to STI than the RF-C domain (blue circle). Four members of *A. thaliana* with a putative RF-C domain were analysed (At5g27740, At1g77470, At1g62160 and At1g21690), only the last one At1g21690 is similar enough to cluster with the group of eukaryotic RF-C containing proteins (blue circle). Similar proteins from Archaebacteria (A.f + M.t) are to distantly related and do not belong to either of the groups.
(A.a.=*Aquifex aeolicus*; C.p.= *Chlamydophila pneumoniae*; B.s.= *Bacillus subtilis*; H.s.= *Homo sapiens*; S.c.=*Sacharomyces cerevisiae*; A.f.= *Archaeoglobus fulgidus*; M.t.= *Methanothermobacter thermautotrophicus*)
　　　　Figure was modified and quoted from (Ilgenfritz et al. 2003).

The trichomes of *sti* mutant plants are unbranched or show up to one branch-point (Figure 17B), depending on the severity of the mutation. The first publication about STI described seven alleles in this locus (Ilgenfritz et al. 2003). Only a mutation that likely affects the splicing of the transcript shows a weaker branching phenotype (*sti40* Figure 17C), 78% of the trichomes have only one branch-point. The weak phenotype is likely due to an effect onto the splicing of the *STI* transcript (Ilgenfritz et al. 2003). The *sti40* mutation is located to position 2372 counted from the ATG start-codon (Table 6). *sti47* mutant plants, that harbour a stop codon after 111bp, exhibit a more severe phenotype than *sti40* (Ilgenfritz et al. 2003). Such an early stop-codon presumes a strong phenotype but the analysis by Ilgenfritz showed only a weak mutant phenotype. The same study shows that mutations more distant from the ATG cause a severe mutant phenotype, like alleles *emu* and *em1*. Since *sti* mutant trichomes are unbranched it is likely that STI is involved in an early step of trichome development. To access this question crosses with almost all trichome mutants were

performed (Folkers et al. 1997; Ilgenfritz et al. 2003). The analysis of these double-mutant combinations showed that the *sti* mutant phenotype is penetrant in almost all crosses analysed. Only the combination between *sti* and *nok* (*noeck*) indicated a different result. *nok* mutant trichomes are overbranched with up to seven branch-points (Folkers et al. 1997). In addition, to the first description of Folkers and co-workers, it was shown that one *nok* allele (*nok-gb*) is able to modify the phenotype of *cpr5* (Brininstool 2003). Double mutant combinations showed glassy trichomes reaching only have of the size of *cpr5* mutant trichomes. Recently the molecular nature of this gene has been clarified. NOK is a transcription factor of the MYB family and the AGI assigned At3g01140 to this locus (personal communication M. Jacoby and N. Platz). Trichomes from a cross between a week allele of *sti* (sti40) and *nok* have two branch-points (90% of all trichomes, Figure 17D), whereas *sti40* mutant trichomes are posses mainly one branch-point. A similar cross with a strong allele of *sti* is still branched but showed mostly only two branch-points (83%, Figure 17E). This observation suggests that *nok* is able to rescue *sti* mutant trichomes. It is likely that branching is controlled about independent pathways, one might involve the main action of STI and the other one mainly NOK.

triptychon (try) mutant trichomes are overbranched similar to *nok,* but they appear to be clustered in addition. Unlike *nok*, *try* mutants cannot rescue the *sti* branching phenotype. The *try* mutation is addititive as clusters appear in double-mutant combinations (Figure 17 F). One interesting attribute for STI is observed in this cross (*sti40 try-EM1*), as dependent on the dose of STI some rescue of the mutant phenotype is observed (Figure 17F). This might be due to the fact, that *sti40* itself is likely hypomorph and branching is not completely abolished. If the crossing between *try-EM1* and a putative amorph allele of *sti* (*sti-EMU*) were repeated, no rescue concerning the trichome branch-point number was observed (Folkers et al. 1997).

These previous experiments suggest that the dose of STI is important for the mutant rescue, supported also by the different *sti* mutant alleles. Additionally overexpression constructs, generated by D.Bouyer showed a broad spectrum of branched trichomes when transformed into a *sti* knockout line. The trichome rescue frequency showed the complete spectrum from underbranched to overbranched trichomes (Bouyer 2004).
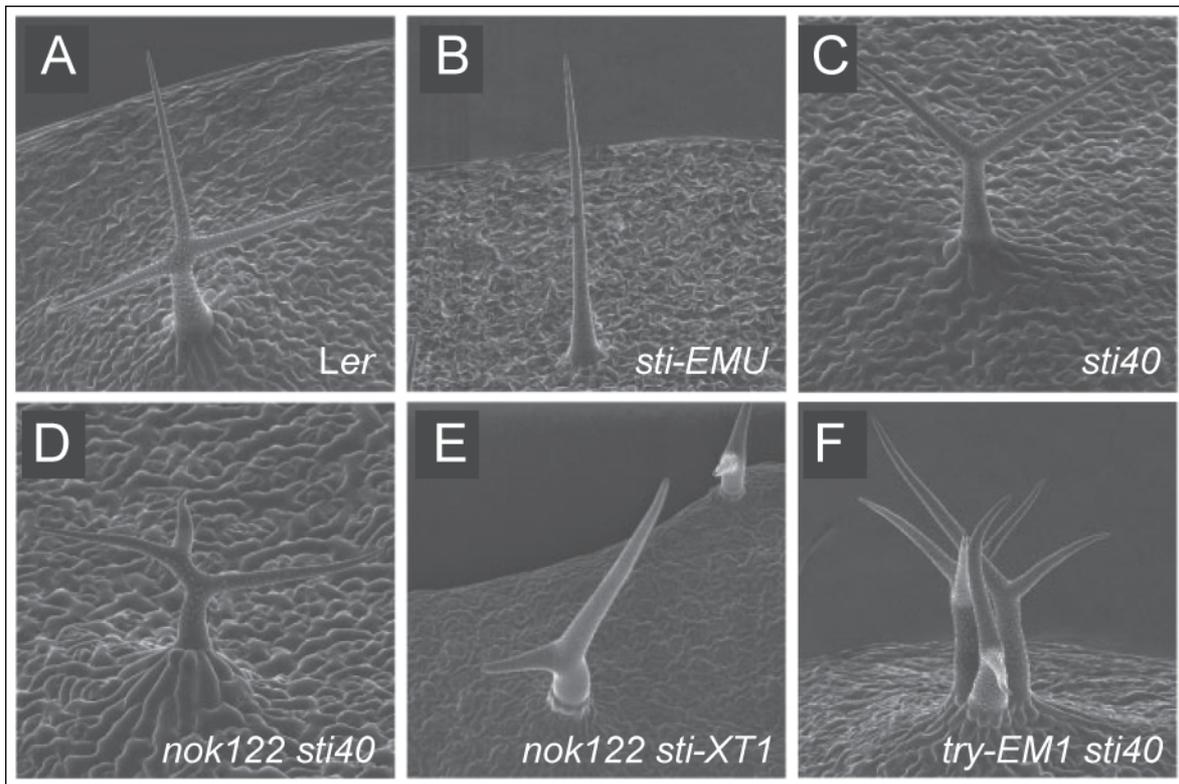
Figure 17: Mutant phenotypes of *sti* and double-mutants with *sti*.
(A) A wild-type trichome with two branch-points. **(B)** 97% of *Sti-EMU* trichomes are unbranched. **(C)** The weakest *sti* allele *sti40* shows 78% of the trichomes with one branch-point. **(D)** The double-mutant between *sti40* and *nok-122* is still branched. **(E)** The double-mutant combination between *sti-XT1* and *nok-122* is reduced concerning to branch-points. **(F)** *try-EM1* and *sti40* double-mutant lines show clustered trichomes, like in *try*, and reduced branching like in *sti40*.
        Figure was modified and quoted from (Ilgenfritz et al. 2003).

Considering the specific effect of *sti* mutants on trichome branching the subcellular localisation of the mRNA or the protein is of outstanding interest. Northern-blot analysis of different *A. thaliana* tissues resulted in comparable expression levels (Ilgenfritz et al. 2003). In addition *STI* expression was detected in *gl1* mutant tissues which are devoid of trichomes. Nevertheless the presence of a gene with high similarity to *STI* (At1g14460) doesn't exclude the possibility of cross-hybridisation to both transcripts.

The localisation of the STI protein was analysed by a fusion to GFP. The expression of the GFP:STI fusion protein under the control of the 35S promoter is able to rescue the mutant phenotype and this fusion protein is located to the tip of trichomes (Bouyer 2004).

Aim of the work:

STICHEL is a protein with important function in trichome branching. Nevertheless the molecular function of STI is still unknown. Therefore the focus of this study is the detailed analysis of the GFP:STI fusion protein localisation which was found at the tip of emerging trichomes (Bouyer 2004). Constructs harbouring only parts of the cDNA fused to a fluorescent protein should be generated and analysed in *sti* mutant and wild type background. By using these fragments it should be possible to narrow down the position of the localisation signal which is sufficient to resemble the original localisation in the tip of trichomes. Furthermore these constructs should be analysed for their rescue ability in *sti* mutant background. The expression pattern of the putative endogenous promoter should be analysed by fusion to a reporter to elucidate its temporal and spatial expression. To understand the differences between STI and the close homolog STI-HOM, both putative promoters should be exchanged. These experiments together with the expression pattern of the putative *STI-HOM* promoter might help to understand the function of this homologous gene. Finally a search for new interactors of STI might improve the understanding about this protein with unknown molecular function.

5   Results

5.1   Structure of STICHEL

STICHEL (STI) is a protein with unknown molecular function. Nevertheless it contains regions similar to other proteins. The most prominent among these domains is the gamma/tau subunit of DNA-Polymerase III which is located in the central part of the protein (Figure 18). In addition STI contains a potential AAA-ATPase domain which overlaps with the gamma tau subunit. The AAA-ATPase domain contains the p-loop motif which is required for ATP binding (Saraste et al. 1990). *In silico* analysis revealed that the STI protein also harbors two putative pest sequences (http://emb1.bcc.univie.ac.at/toolbox/pestfind/). Pest sequences are found in proteins which are subject of rapid degradation (Rogers et al. 1986; Rechsteiner and Rogers 1996). Finally STI displays a nuclear localization signal (NLS) in its N-terminal region. The NLS has been identified by "PREDICT NLS" (http://cubic.bioc.columbia.edu/cgi/var/nair/resonline.pl). According to "PREDICT NLS" more than 99% (262) of the proteins with a similar NLS are located to the nucleus and have the capability to bind DNA.
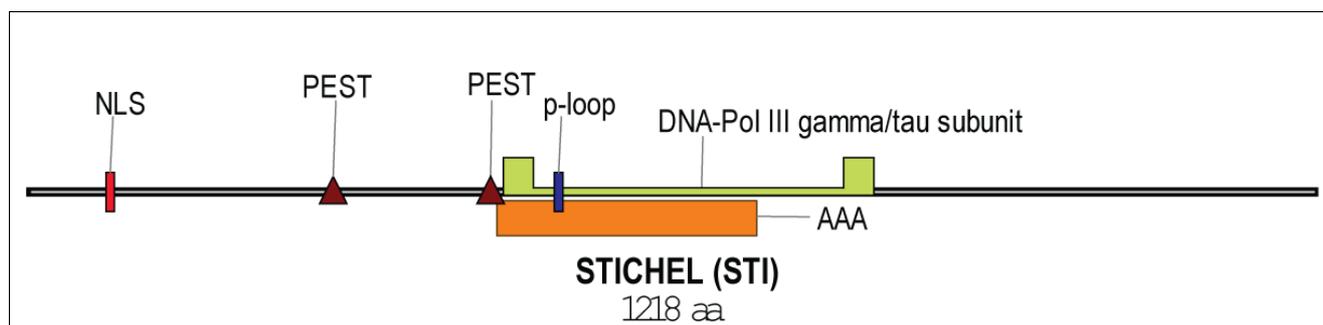
Figure 18: The structure of the STICHEL protein.
In silico analysis revealed several putative motifs. One nuclear localisation signal (NLS) is located in the N-terminal region of the protein. Two possible PEST signals which might be a motif for protein degradation are also located in the N-terminal region. In the middle of STICHEL is the gamma or tau subunit of DNA-Polymerase III located. The beginning of the DNA-Polymerase domain includes the AAA-ATPase domain with the p-loop aa. These aa are essential for binding ATP (Saraste et al. 1990).

5.2   The *sti* mutant has a trichome phenotype

The analysis of *sti* mutants might help to determine the function of the protein, provided that partial or complete loss of *sti* function leads to a visible phenotype. To access the function of STI, several mutant alleles have been analysed in more detail. Previous studies already identified a number of *sti* alleles (Ilgenfritz et al. 2003). The position of an insertion or a premature stop codon might give some insight into the importance of parts of the final protein for STI function. Until now alleles in

e.g. Columbia background are not available. New alleles in different backgrounds allow crossings to other mutants without mixing different ecotypes, which is especially important when analysing branching. Crossings between a mutant gene of interest and a suitable *sti* allele in the same ecotype allow the analysis of branching without the interference of branching- and patterning-effects due to a different ecotype. Furthermore insertions or mutations likely change the expression level of the affected gene or the expression is abolished completely. Therefore PCRs on cDNA banks of certain mutant alleles were also analysed.

sti mutants exhibit trichomes without branches, depending on the position of the mutation. Strong alleles like *sti01* and *sti146* are almost completely unbranched (Figure 20 F+G). Weak alleles like *sti40* present trichomes with mostly two branches in contrast to wild-type trichomes with three to four branches (Figure 20 H). EMS induced mutations in the Landsberg *erecta* (L*er*) ecotype are *sti01*, *sti40, sti47* and *sti146* (Table 6). The mutation in s*ti01* leads to a premature stop codon and therefore to a truncated transcript. Until now the position of the mutation responsible for the trichome phenotype in allele *sti146* is unknown. In addition to the trichome phenotype this line showed a second phenotype cosegregating with the trichome phenotype. This second mutation impairs growth of the root leading to an overall slower growth of the plant (data not shown). Both alleles described before show a strong *sti* mutant phenotype whereas the last Ler allele, *sti40* is most likely hypomorph. 78% of the trichomes have one branch point and only 22% are unbranched (Folkers et al. 1997) in comparison to strong alleles that do not produce branched. The mutation in *sti40* affects likely the splicing of the transcript, but obviously residual amounts of functional transcript are still present. Various databases comprise a number of insertions in the STI locus which are depicted blue in Figure 19. In this study three of these were analysed for the presence of a trichome phenotype. Line *stiCol* which has an insertion in exon 3 shows the strongest trichome phenotype (Figure 20 C; "WiscDsLox T-DNA Lines" generated by the University of Wisconsin). Trichomes are completely unbranched comparable to allele *sti01* and *sti146*. Line N808861 is an insertion in the 3'UTR and has no visible phenotype (Alonso et al. 2003). An insertion in the promoter region, like in line N811194 showed a weak phenotype (Figure 20 B). From the insertions in Wassilevskija ecotype only one was used in further experiments. This is line FLAG.019E04 (Brunaud et al. 2002) which has an insertion in exon one with the result of a complete loss of trichome branching (Figure 20 D).

Strong mutant alleles of sti did not show any expression after 40 amplification cycles (*sti01*, Figure 21). In contrast to *sti01,* N811194 presented a weak phenotype but no detectable change in transcript amount in comparison to an allele without phenotype (N808861) or Col wild-type.
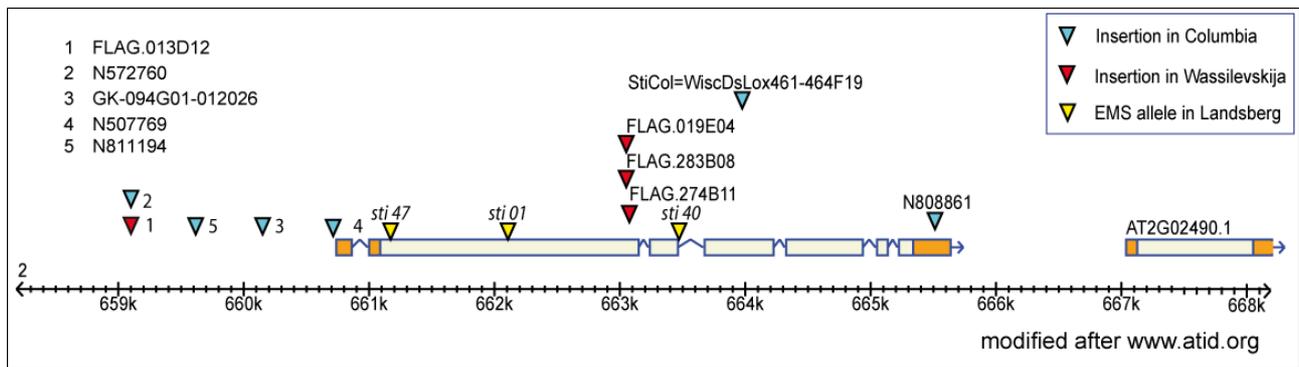
Figure 19: Summary of insertions within the *STICHEL* genomic area.
Blue triangles show insertions in the Columbia (Col) background while red triangles represent insertion in the Wassilevskija (Was) ecotype. Yellow triangles show the position of the mutation in Landsberg *erecta* (L*er*) background. Table 6 collects information on the different types and effects of the insertions.
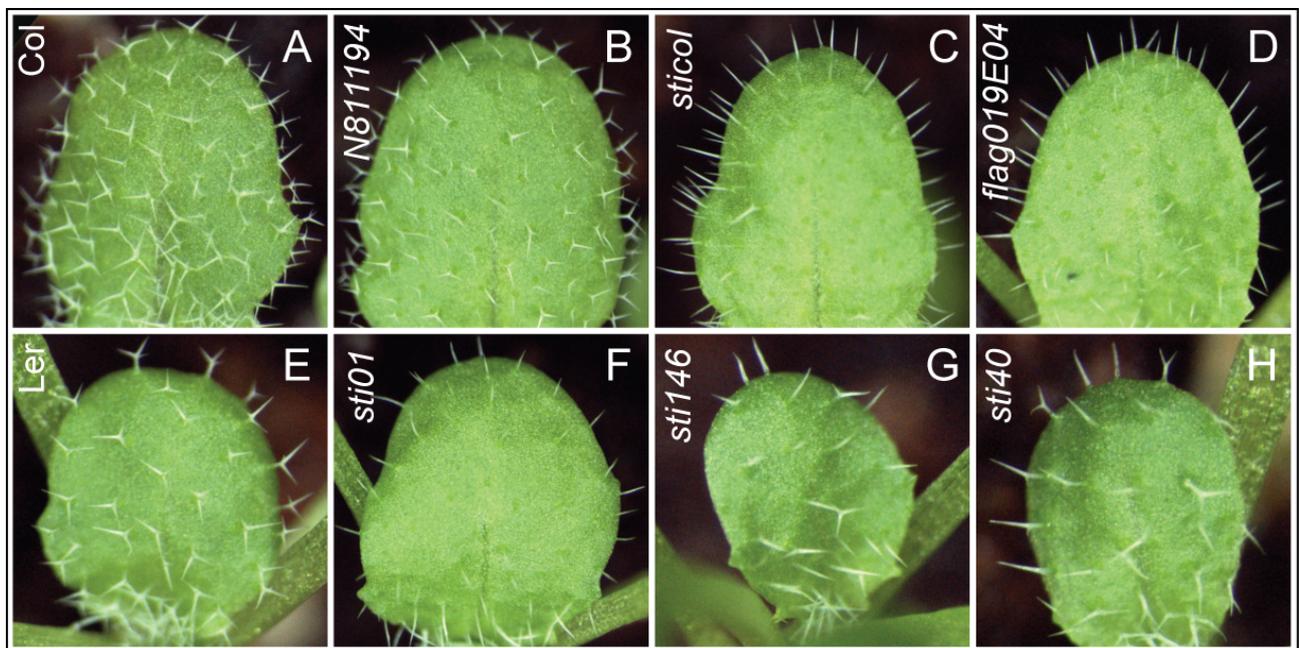
Figure 20: Trichome phenotypes of different *sti* mutant alleles.
(A) Col wild-type leaves have a majority of trichomes with two branch-points. **(B)** Allele *N811194* shows a minor reduction in trichome branch number. **(C)** *StiCol* alleles are unbranched. **(D)** The allele *flag019E04* in Wassilevskija background is unbranched too. **(E)** L*er* wild-type plants are the reference for the EMS mutants generated in this background. Trichomes in L*er* are slightly reduced in branch-point number. **(F+G)** *Sti01* and *sti146* are almost devoid of branched trichomes. **(H)** Trichomes in s*ti40* mutant plants are weak alleles as the majority of trichomes have one branch-point.

Table 6: Characterisation of *sti* mutant alleles.
This table summarises the different alleles used in this study and the position of the mutation or insertion. Position 1 is the ATG of the translational start. The reference column indicates the first description/analysis of this mutation or insertion.

allele	ecotyp	position	effect [2]	type	phenotyp	reference
sti40	L*er*	2372	G to A	EMS	weak	(Ilgenfritz et al. 2003)
sti47	L*er*	111	G to A	EMS	weak	(Ilgenfritz et al. 2003)
sti01	L*er*	939	G to A	EMS	strong	this study
sti146	L*er*				strong	this study
stiCol	Col	2883 AS	Exon 3	T-DNA	strong	this study
flag019E0	WS-4	1963 AS	Exon 1	T-DNA	strong	this study
N808861	Col	4412	3' UTR	T-DNA	no	this study
N811194	Col	-1527	Prom	T-DNA	weak	this study

[1] position of the mutation with the ATG as start; AS indicates that the insertion is on the antisense strand
[2] "Splice" is a mutation in the splicing donor or acceptor site
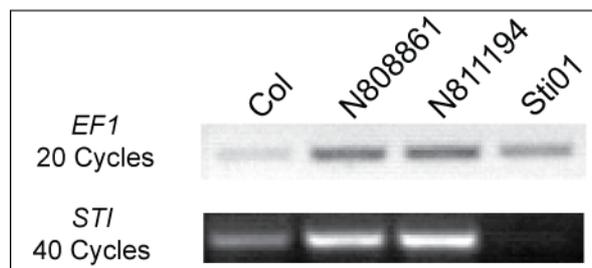
Figure 21: STI expression in *sti* mutant alleles.
STI is expressed in the weakest mutant allele available (N811194) and the expression level is not distinguishable from N808861 which showed no mutant phenotype. The strong sti allele *sti01* showed no amplificate after 40 amplification cycles. Control amplifications with EF1 presented comparable cDNA amounts. Only Col (derived from protoplasts) and *sti01* cDNA showed a reduction in transcript.

5.3 Expression analysis

The analysis of its spatial-temporal expression pattern is important for the characterization of any gene. First it allows determining whether a gene is expressed in the analysed tissue or not. Second the approximate amount of transcript in relation to a control can be determined. Third the acquisition of transcript level data over time and in different tissues facilitates to understand the function of the associated gene during the development of the organism analysed. Previous studies analysed the expression levels of *STI* in some mutant situations and tissues (summarized in chapter 4.2). D. Bouyer and co-workers showed that *STI* is expressed in every analysed tissue. But the expression level of the GFP:STI line and several tissues was unclear up to now like the temporal and spatial expression of *STI*.

Different techniques have been utilised in this study to get information about the expression levels of the *STI* transcript. PCR was performed onto cDNA libraries (Figure 22). The expression levels of the GFP:STI marker line was included too. An analysis of the Genevestigator website (https://www.genevestigator.ethz.ch/) provided information about the expression levels of *STI* and

its homolog *STI-HOM* in various tissues (this website is collecting and displaying data from microarray hybridisation experiments). To determine the spatial and temporal expression pattern of *STI* a reporter construct was generated. This reporter construct was comprised of the putative *STI* promoter followed by the *GUS* reporter gene. Promoter Gus fusions visualise the promoter activity *in planta* (Jefferson 1989).

30 cycles of amplification are not enough to amplify the endogenous transcript of *STI* (Figure 22 A). At least 40 amplification cycles were needed to detect *STI* in Col wild-type cDNA banks (Figure 21). The GFP:STI line which was used for the localisation studies showed a strong increase in transcript amount because it was detectable after 30 cycles of amplification. The hybridisation of labelled RNA to whole genome chips generates quantitative and qualitative data about every gene spotted onto the chip. *STI* and its homolog *STI-HOM* (Figure 21 B) are expressed at comparable levels. The expression of *STI* in undifferentiated cell-suspension culture is increased by factor five. Callus and root tissue showed increased levels of *STI* transcript, nevertheless the expression level is increased only by factor two. The putative *STI* promoter driving the expression of the GUS gene was introduced into plants. The analysis of the T1 generation revealed 82 primary transformants. Ten T1 plants were analysed for GUS activity and Figure 22 C-E shows representative pictures of the putative *STI* promoter activity. The promoter activity was highest in young leaves where it was detected ubiquitously in all epidermal cells. Older leave stages showed GUS-activity in trichomes and no or only few staining in other epidermal cells Figure 22 D+E.

Concerning to the expression of *STI* the current knowledge increased substantially. Initially the cDNA of STI was assembled from smaller parts (Ilgenfritz et al. 2003). Recently the Riken Institute submitted a full length cDNA for Stichel (AK229470) which is significantly different from the one predicted by computational methods (NM_126303). The length of the coding region known so far and used in this study is 3657 bp instead of 1905 bp for the cDNA isolated by the Riken institute. In contrast to the cDNA from Riken the lab of D. Marks submitted sequence oft the STI mRNA (AF264023) which supports the predicted cDNA and not the sequence submitted by Riken.

Additionally new information about the structure of the transcript is available. According to the new cDNA sequences available, the 5'UTR contains an intron that is spliced out in the final transcript.
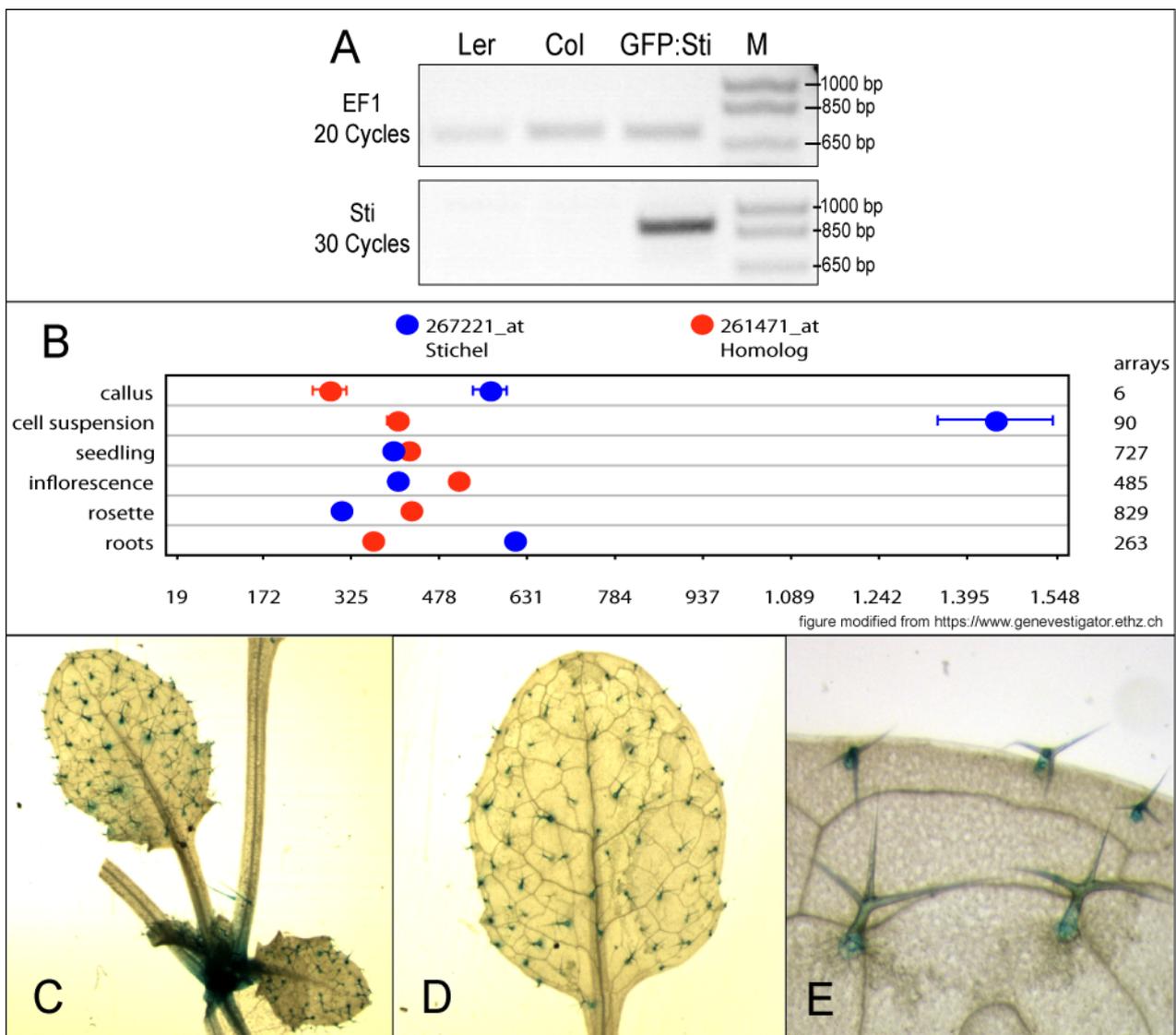
Figure 22: Expression analysis of *STI*
(A) 30 amplification cycles are not enough to detect endogenous *STI* transcript. The GFP:STI line used for the localisation studies showed increased *STI* transcript levels. The amounts of RNA are comparable. **(B)** Chip hybridisation experiments showed that *STI* and its homologue *STI-HOM* are expressed at comparable levels in most tissues analysed. Only cell-suspension culture cells showed a five-fold higher expression level than *STI-HOM*. This diagram was quoted and modified from the genevestigator website (Zimmermann et al. 2004). **(C-E)** GUS activity was detected ubiquitously in young leaves (C). Older developmental stages of leaves showed GUS activity only in trichomes (D+E).

5.4   GFP-STI is localised to the tip of emerging trichomes

A fusion protein between STI and GFP or another fluorescent protein, expressed by an ubiquitous expressing promoter like 35S, might give insights into the subcellular localization of STI. This localisation might narrow down possible functions during trichome development. For example a localisation of the fusion protein to the nucleus might hint to a function as a transcriptional regulator.

GFP was fused to the full length cDNA of *STI* under the control of the 35S promoter and transformed into *sti146* mutant plants (Bouyer 2004). These lines were analysed previously and

showed the signal of the fusion protein in different independent lines (D. Bouyer personal communication). After screening of several of these lines, only one showed a signal sufficient for a more detailed characterization. The subcellular localisation of the GFP:STI fusion protein was initially analysed by D. Bouyer and revealed a signal in the tip of emerging trichomes (Bouyer 2004). Nevertheless a temporal and spatial analysis of the fusion protein during the development of a trichome from a very young cell bulged out of the epidermis to a trichome with two to three branch points was not performed until now. Also the exact cellular localisation weather it is located to cell wall or to another structure was so far unclear.

To address the question of the localisation of the fusion protein throughout trichome development, the fusion protein was analysed by fluorescent microscopy and confocal imaging. Initial tests showed that the signal-intensity, in the line used, was only detectable after increasing the exposure time at the fluorescence microscope. The overall signal intensity of this line is close to the detection limit of the experimental setup, even though this line was selected because it showed the best signal. To illustrate this low signal intensity a comparison between GFP:STI, GL2::GFP-ER and GFP-mTalin was performed. GFP:STI was not visible at standard exposure conditions (Figure 26 B) like GFP-mTalin (Figure 26 I). By contrast GL2::GFP-ER was readily detectable and the signal was close to saturation. By increasing the exposure time to two seconds the signal of GFP:STI became weakly visible (arrows, Figure 26 B). GL2::GFP-ER was now oversaturated (Figure 26 G) and the overall signal intensity of GFP-mTalin (Figure 26 J) was high when compared to GFP:STI. Additionally the fusion protein is sensitive to bleaching by UV-light used to excite GFP. During observation with UV-light the fusions protein signal intensity was reduced within seconds and latest after one minute it was not detectable any more.

An overview of the fluorescent signal observed on an entire leaf is depicted in Figure 23A+B. The signal of the fusion protein showed the highest intensity in the youngest stages of trichomes which are unbranched. These stages and all other young trichome stages displayed the fusion protein in a round, cap-like structure located to the tip of the outgrowing branch. This signal was found even before a branch was morphological visible (Figure 23 A1+C+D). When the next branch was morphological visible two caps/domains of the fusion protein were observed at the tip of the branches, whereas the domain/cap of the first branch was decreasing in fluorescence (Figure 23E the upper right domain is older). Trichomes in e.g. L*er* wild type have mainly two branch points (equivalent to 3 branches), hence the fusion protein was visible in all tips of the trichome (Figure 23 A3).

Once a branch is growing out, the signal of the fusion protein was reduced. Fully expanded

trichomes showed no- or a signal that was close to the background noise (Figure 23B marked with arrowheads). The amount of the fusion protein was depended on the developmental stage, because a trichome with two branches (Figure 23 B1) that are almost identical in size showed a comparable amount of the fusion protein. The branches of trichomes are usually different in size as they develop successively. Therefore the strongest signal was visible in the tip of the youngest stages. As soon as the older branch was growing out, the signal strength was reduced (Figure 23 E). The signal in the tip of an emerging trichome was organised in a cap like structure. Nevertheless this cap had a speckled organisation, smaller amounts of the fusion protein stuck together to form small dots, that were visible in total as a cap like structure (Figure14E).
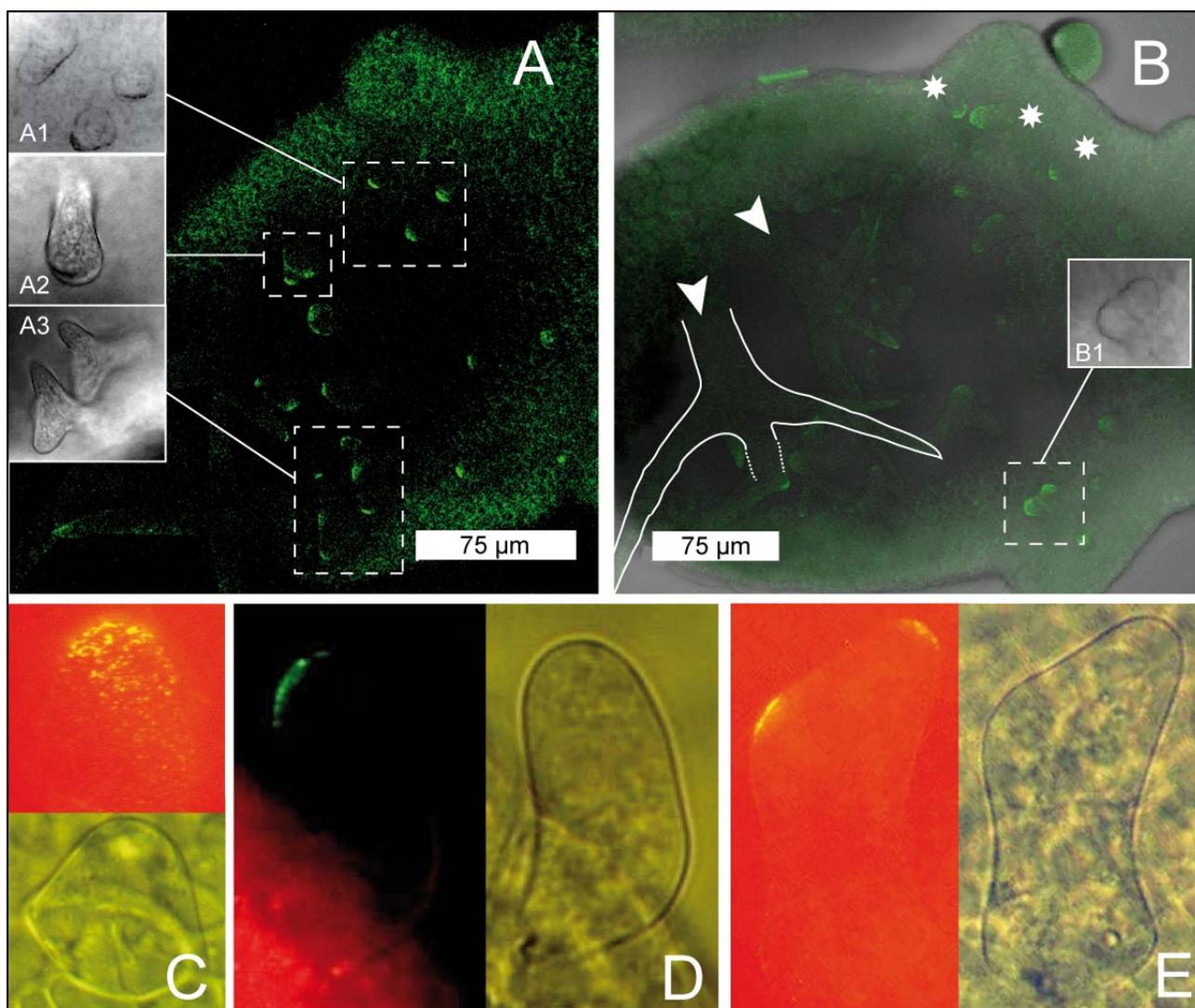
Figure 23: The localisation pattern of GFP-STI.
Parts (A+B) are showing the signal of the GFP-STI fusion protein on the complete leaf blade. **A1-A3** summarise a developmental series from a young unbranched trichome **(A1)** to an older trichome **(A3)** initiating the third branch. **C-E** are higher magnifications of individual trichomes from a very young, unbranched trichome that just grew out **(C and B** marked with stars)** to a slightly more enlarged cell **(D)** up to a young trichome with two branches **(E)**. Mature trichomes are almost devoid of any GFP:STI signal (B marked with arrowheads).

GFP:STI is localised to the plasma membrane

After these observations the approximate localisation of the GFP:STI fusion protein during trichome development was known, but it was still indefinite to which structure the fusion protein was localised. GFP:STI might be localised to the cell-wall or the plasma membrane. To identify the structure the fusion protein is localised to, plasmolysis studies were performed. Trichomes that that underwent an effective plasmolysis reduced the total volume of the cell plasma and vacuole by the efflux of likely water. Therefore these plasmolysed trichomes were easily detectable due to the changed cytoplasmic morphology (Figure 24). Younger trichomes underwent plasmolysis with a higher frequency than older trichomes since they are not fully developed and might be more susceptible to plasmolysis. In plasmolysed trichomes the signal of the fusion protein moved along with the shrinking plasma membrane, demonstrating that the fusion protein was localized to the plasma membrane and not to the cell wall.

In conclusion GFP:STI, which is able to rescue the *sti* mutant phenotype, is localised to the tip of future trichome branches. During outgrowth of these tips a reduction in signal intensity is observed. Adult trichome stages are almost devoid of GFP:STI. Plasmolysis studies indicate that GFP:STI is likely located to the plasma membrane.
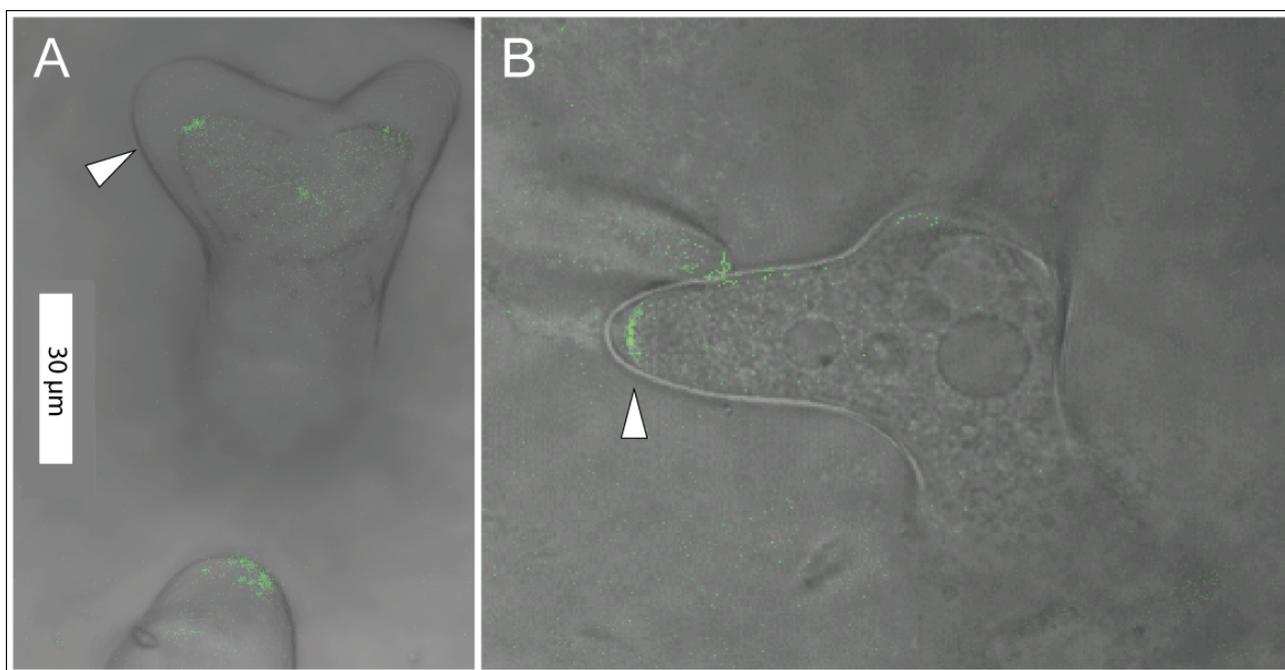
Figure 24 GFP-STI is located to the plasma membrane.
Plasmolysis experiments revealed that the fusion protein is localised to the plasma membrane and not to the cell wall. **(A)** A trichome with only one branch point is strongly plasmolysed (arrow-head). Beneath an unbranched trichome is not showing any effect of plasmolysis. **(B)** This trichome is in the process to form the third branch. The fluorescence is visible in the plasma membrane, but plasmolysis is not as severe as in A (arrowhead).
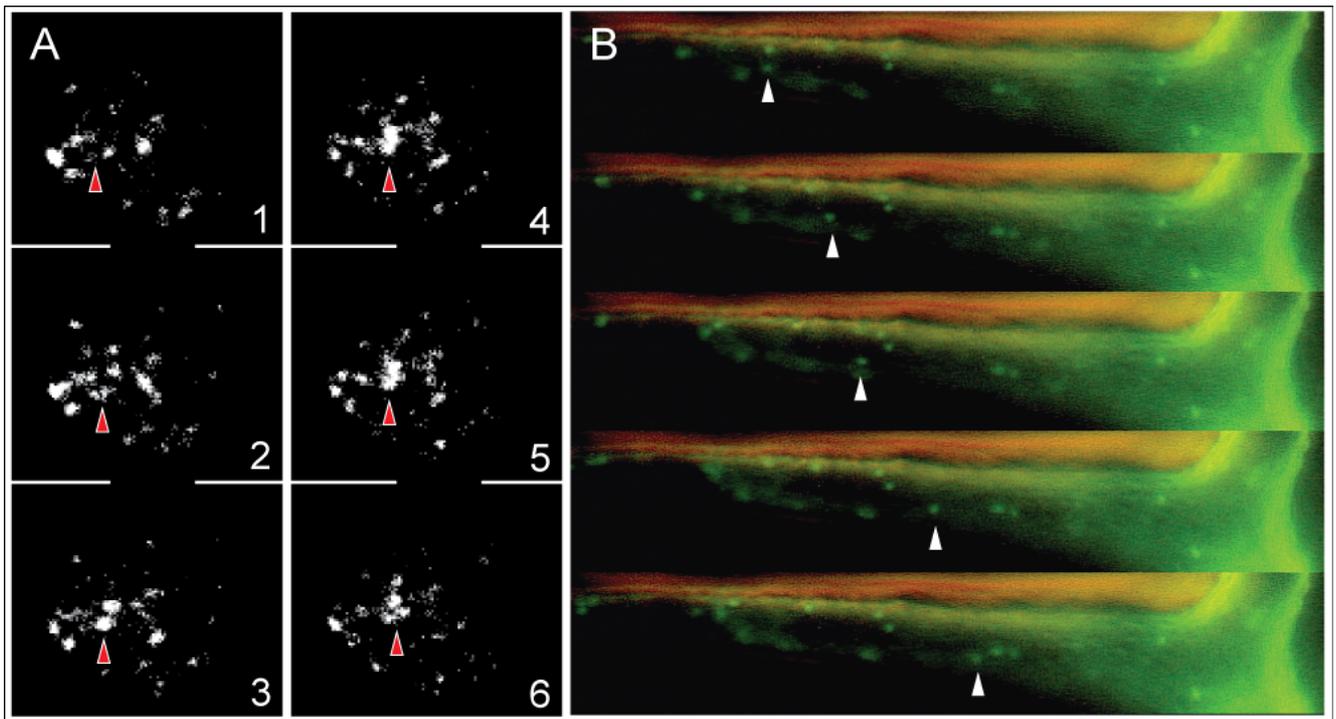
Figure 25: GFP:STI and YFP:S1/AS1 are moving in trichomes.
(A) This figure shows the fluorescent signal of GFP:STI over time. The trichome used for this series is very young and unbranched (comparable to Figure 23B marked with stars and C). The red arrow head marks exemplary a point appearing and increasing in size (1-3). In picture 4-6 the green arrow head marks a spot of proteins which is divided into several smaller spot. **(B)** Fragment S1/AS1 cannot rescue the mutant phenotype and does not show a cap like structure. But this protein fragment fused to YFP is strongly increased in fluorescence and is moving within adult trichomes (white arrow heads).
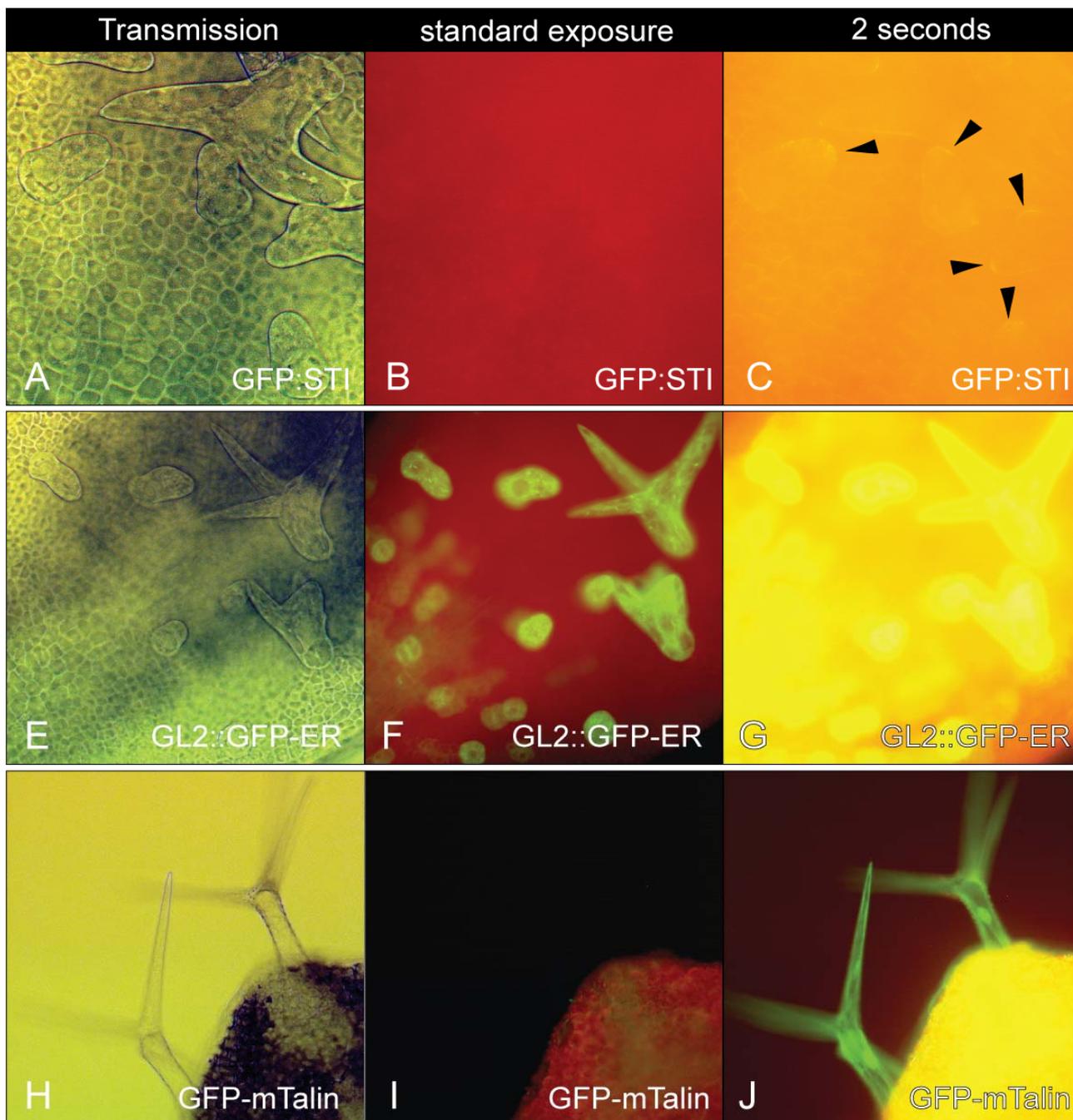
Figure 26: Intensity of GFP:STI compared to other trichome localised proteins.
(A-C) show GFP:STI expressed in trichomes. (A) transmission picture, (B) no protein is visible at standard exposure time. (C) a faint signal of GFP:STI is detected at different positions (arrows) if the exposure time is increased to two seconds. (E-F) show the signal of GL2::GFP-ER. Even at standard exposure conditions a strong signal is visible (F), after exposure of two seconds the signal intensity is oversaturated. (H-J) present the signal of GFP-mTalin which colocalises with the actin cytoskeleton (Kost et al. 1998). A red signal indicates background fluorescence from the chloroplast as a longpass filter was used which is not excluding these wavelengths.

5.5 The subcellular localization of STI is independent from the integrity of the cytoskeleton

The GFP:STI localisation observed tempted us to ask how STI is transported to the tip of developing trichomes. The cytoskeleton can serve as a track to deliver proteins to different regions within the cell (refer to chapter 1 and Figure 1).In order to investigate whether the STI localization is mediated by actin or microtubule dependent transport mechanisms, drug studies were performed.

The microtubule destabilising drug Oryzalin and the actin destabilising drug Latrunculin were examined for their effect on STI localization (Figure 27).

Treatment of whole plants with either Oryzalin or Latrunculin B did not affect the subcellular localisation of the protein when applied for one or three hours (Figure 27 A+B). GFP:STI was localised to the tips of young trichomes like without the treatment (refer to Figure 23). But these drugs affected indeed the cytoskeleton because trichomes grown during the period of drug-treatment showed a comparable phenotype as described by other researchers (Mathur et al. 1999; Mathur and Chua 2000). Trichomes of this control group showed a bloated deformed shape which is typical for an effective treatment (Figure 27 C+D).
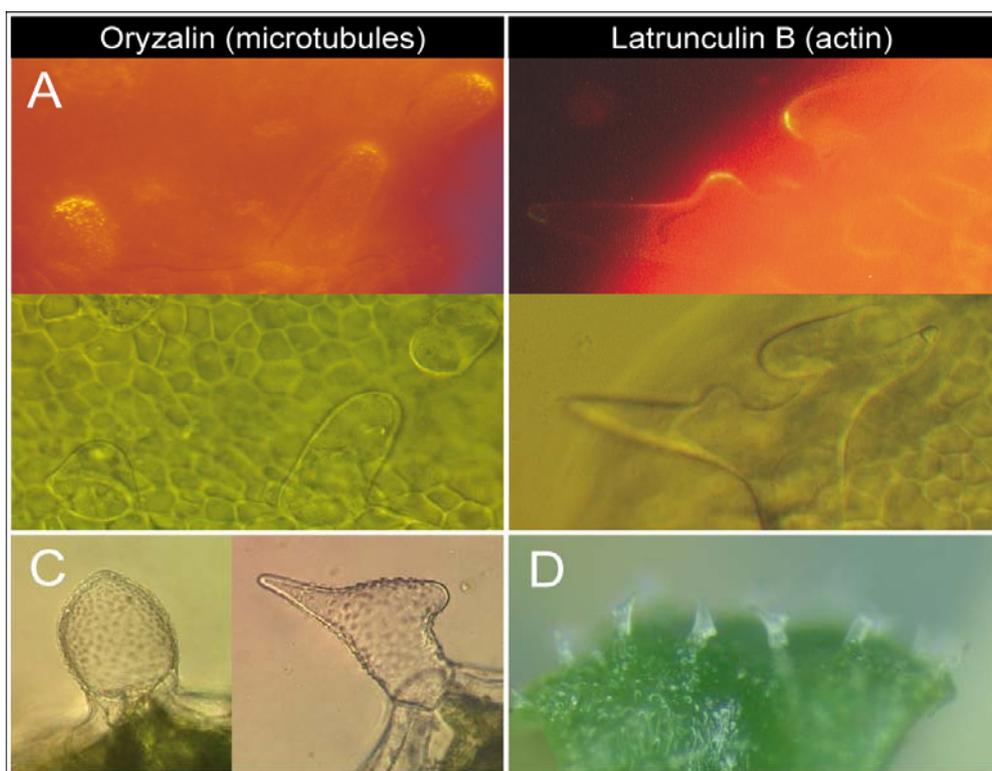
Figure 27: GFP-STI localisation after application of cytoskeleton destabilising drugs.
(A) Plants were treated with Oryzalin (microtubule destabilizing drug) and examined 1h after treatment. **(B)** Plants were treated with Latrunculin and analysed 3 h later. No difference concerning the localisation was observed after 1h (data not shown). **(C)** These plants represented the control-group that showed that the treatment with Oryzalin was indeed successful. The trichomes presented characteristic defects like ton-shaped trichomes. **(D)** These trichomes represented the control group for Latrunculin showing similar defects like in (C).

5.6 Crossings of GFP:STI

GFP-STI was crossed to different mutant backgrounds and examined for effects on its localisation. Other proteins known to be present in trichome development (summarised in (Hulskamp et al. 1998) might have an effect on the localisation of the GFP-STI fusion protein. The preselected GFP-STI used for the localisation analysis (Figure 23) was crossed to *triptychon* (*try*) (Schnittger et al. 1998), *furca* 1.1+1.3 (Luo and Oppenheimer 1999)*, angustifolia (an)* (Folkers et al. 2002a),

pGL2::CYCB1;1 (Schnittger et al. 2002) and *siamese* (*sim*) (Walker et al. 2000).

Only one line of the *sim* crossing with GFP:STI showed the expected signal in F2 generation (Figure 28 B+C). The fluorescence is additional to the mutant phenotype, trichome are clustered and branched but still showed the GFP-STI signal in the tip of the developing trichome. The overall signal intensity of GFP-STI is less bright in *sim* background than in *sti146* mutant background (*sti146* is the allele which was rescued by the GFP:STI construct, Figure 23). Possibly the presence of the signal, in only one line, is due to a homozygous *sti146* mutant background, as this certain plant showed a reduced overall size what is observed in *sti146* mutant plants too (data not shown).

To clarify whether an heterozygous *sti146* mutant situation can influence the GFP:STI signal a cross between GFP-STI and L*er* wildtype was analysed in F1 (Figure 28 A+B). GFP:STI was still detectable in the Ler background although the signal intensity was significantly decreased. Consequently one has to notice that GFP-STI is, like expected for a 35S construct, detectable in heterozygous state. The detection problem must have other so far unknown reasons.
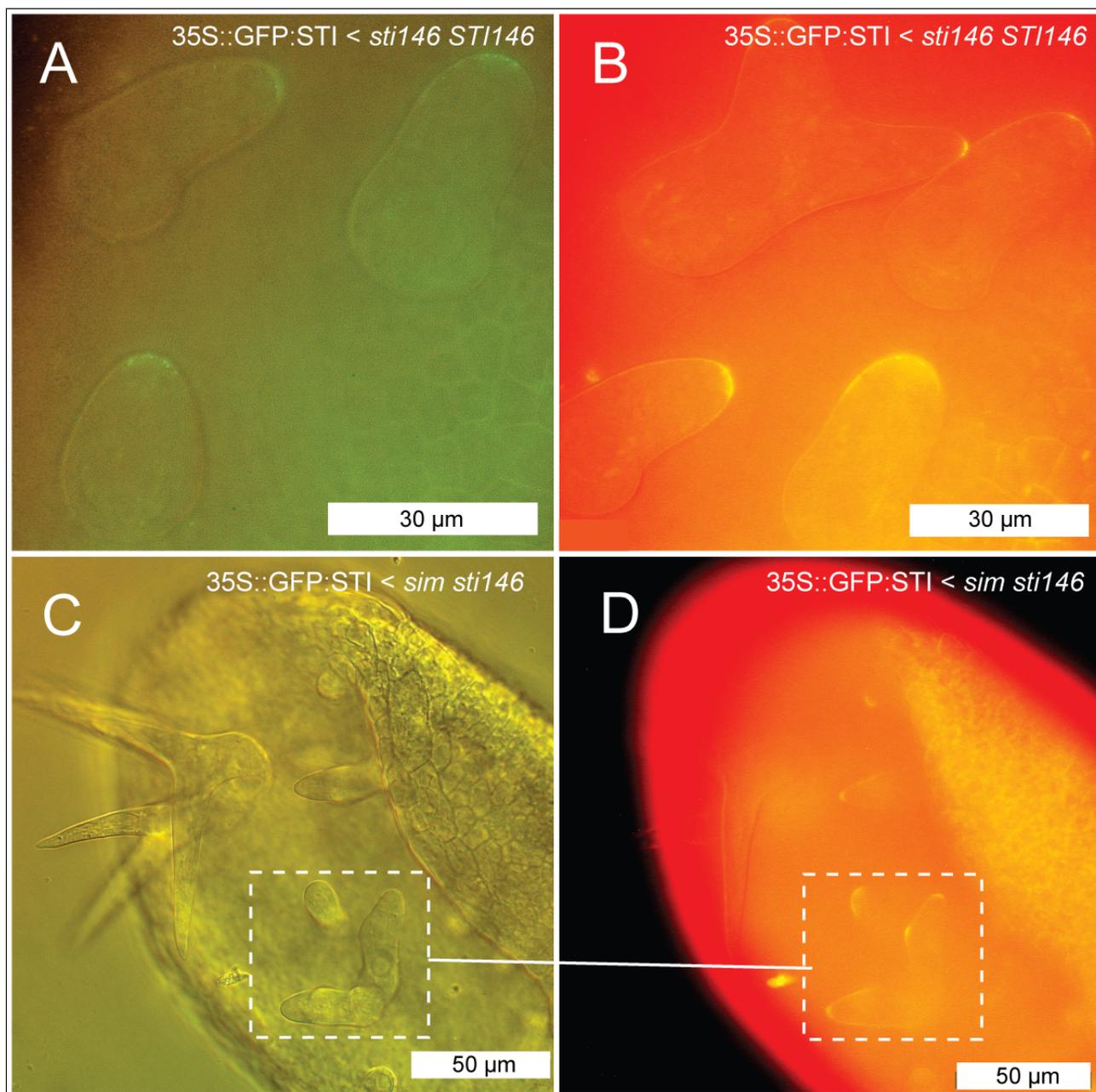
Figure 28: GFP:STI in different mutant backgrounds.
(A+B) A heterozygous 35S::GFP:STI construct generated by the crossing to L*er* wildtype and subsequent analysis of the F1 generation harbours only one copy of the *sti146* mutant allele. The signal is weaker but still detectable. **(C+D)** The F2 generation showed the signal of GFP-STI in s*iamese* (*sim*) (Walker et al. 2000) and *sti146* double mutant background. The signal intensity of GFP:STI is clearly weaker but still organized in a cap like structure.

5.7 Mapping of the domain responsible for the localisation

The specific localisation of the 35S::GFP:STI fusion protein to a cap like structure was unexpected and not observed in trichomes of *A. thaliana* until now. Therefore a mapping approach was used to clarify which domain of the STI protein targets it to the tip of young trichomes. An *in silico* analysis revealed that the STI protein consists of several domains and motifs, respectively (Figure 18). None of these are related to common signals or mechanisms involved in transport or localisation to the

plasma membrane. Small fragments of the cDNA were fused to a fluorescent protein and tested for their subcellular localization.

The full length cDNA was split into five overlapping fragments of approximately 1,2 kb. Additionally nine fragments of 400 bp were generated for fine-mapping (Figure 29). The expression level of a fusion construct can vary depending on the place of the fused protein (e.g. full length CLASP and YFP, refer to chapter 2.6) therefore YFP and CFP were fused N- or C-terminal (Table 7). Subsequently the five constructs harbouring the large fragments of the cDNA were transformed into *sti01* mutant background and into L*er* wild type.

As a proof of function the full length cDNA of STI was cloned into the same vector used for the fragments and was transferred into *sti01* mutant plants too. None of the transformed plants showed a rescue of the mutant phenotype in T1 generation, independent whether a fragment or the complete cDNA was used (data not shown Table 8). Regardless of this information the analysis for a fluorescent signal of the T2 was continued, as a rescue of the mutant phenotype was unlikely for a fragment fused to a fluorescent protein. Nevertheless, these five bigger fragments did neither show a fluorescence signal nor a rescue of the *sti* mutant phenotype in the T2 generation (data not shown).

At this time point of the analysis it was unclear why the fusion protein was not detectable (see discussion). After comparing the strategies for the generation of the original plant line used for the localisation analysis (Figure 23) and the strategy used to generate the fragment fusions, only one major difference was observed. The original localisation construct was transformed into *sti146* mutant background whereas the constructs including the fragments were transformed into *sti01* mutant background. Although it is not likely, that the mutant background (both alleles are likely knockouts) might interfere with the localisation and rescue of the fusion protein, all larger fragments constructs were transformed into *sti146* mutant background.

Again none of the lines generated showed a fluorescence signal comparable to the full-length fusion protein analysed in chapter 5.4 . Different to the lines analysed before (*sti01* background) some lines showed a fluorescent signal which was different than the cap like structure observed before. This signal was observed in two lines of fragment S2/AS4. But instead of a cap like structure, small dots with very low signal intensity seem to move within the trichome (data not shown). These dots appeared to be similar to fragment S1/AS1 which showed moving dots with very high signal intensity (Figure 25).
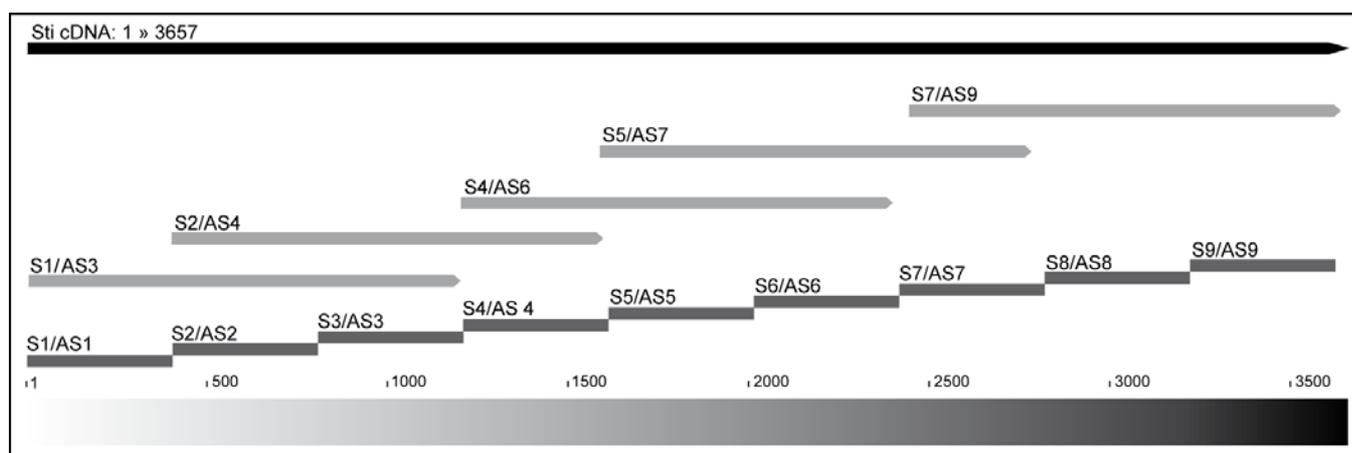
Figure 29: Fragments of Sti-cDNA used in this study and their distribution over the cDNA.
The total length of the STI cDNA is 3657bp. It was divided into five bigger overlapping fragments of approximately 1200bp and nine smaller fragments of around 400 bp.

Fragment	Size	CFP		YFP	
		N	**C**	**N**	**C**
S1/AS1	402	yes	yes	yes	yes
S2/AS2	399	yes	yes	yes	yes
S3/AS3	399	yes	yes	yes	yes
S4/AS4	399	yes	yes	yes	yes
S5/AS5	405	yes	yes	yes	yes
S6/AS6	399	yes	yes	yes	yes
S7/AS7	399	yes	yes	yes	yes
S8/AS8	399	nc	yes	yes	yes
S9/AS9	399	ok	x	yes	x
S1/AS3	1200	nc	nc	yes	nc
S2/AS4	1197	ok	ok	ok	ok
S4/AS6	1203			ok	
S5/AS7	1203	ok	nc	ok	ok
S7/AS9	1253	nc	nc	ok	nc

Table 7: List of Construct used for the mapping of the localisation domain.
The Fragment column refers to Figure 29 where the positions of the fragment within the cDNA are depicted. In column CFP or YFP all the constructs are listed that were generated for this project. N refers to the position of the fluorescent protein fusion and indicates that it (e.g. YFP) is located in front of the *STI* fragment in contrast to C that indicates that the YFP is located behind the fragment.

yes   indicates that the construct was finished.

nc   not constructed

x   combination not possible due to a Stop-codon in the cDNA

Table 8: Analysis of a fluorescence signal for the translational YFP/CFP fusions to larger STI-fragments.
All five bigger fragments were analysed for the presence of a fusion protein signal in a cap like structure like observed for the full-length cDNA (Figure 23). None of the constructs showed a comparable localisation pattern. One constructs presented moving dots instead of a cap like fluorescent signal.

Fragment	position	FZ[1]	background	N[3]
S1/AS3	1-1200	no fluorescence	*sti146*	10
S2/AS4	403-1600	moving dots	*sti146*	6
S4/AS6	1202-2402	no fluorescence	*sti146*	3
S5/AS7	1601-2803	no fluorescence	*sti146*	6
S7/AS9	2405-3657	no fluorescence	*sti146*	2[2]

[1] The fluorescence is compared to the signal observed with the full length construct (Figure 23).
[2] These independent lines did not show the *sti146* growth phenotype. [3] lines tested for fluorescence.

5.8   The rescue of *sti* mutants is dosage dependent

For the first rescue of the *sti* mutant, the full-length cDNA under control of the 35S promoter was used (Ilgenfritz et al. 2003). A successful rescue experiment should show a majority of rescued plants in T1 generation, if a ubiquitous expressing promoter like 35S is used.

The estimation of the rescue efficiency allows a first hint about the importance of the expression level of *STI*. If the missexpression with a different promoter cannot rescue the majority of mutant plants, it might be that the dosage of *STI* is important. To face such a possible situation the *STI* cDNA under the control of its putative promoter was analysed too. In addition the dosage of STI was reduced by crossing it to different unrelated mutant genes derived from the same ecotype. The subsequent analysis of the F1 generation presented controlled conditions with only one copy of both crossed genes. Two mutants are used for the crossing, *constitutive pathogen response 5 (cpr5)* (Kirik et al. 2001a) and *trichome birefringence 1 (tbr1)* (Potikha et al. 1995; Nita 2005). Both genes have a trichome phenotype which is likely not specific because additional phenotypes are observed. Furthermore a genetic interaction between STI and TBR1 or CPR5 is not expected. After crossing one of these mutants to another, leading to heterozygous situation for both alleles crossed, a wild type trichome phenotype is expected, if both mutations are recessive.

Analysis of the rescue efficiency from construct 35S::STI73 in *sti146* mutant background (generated by D. Bouyer), showed a clear variation concerning the rescue of the trichome phenotype among the T2 plants as only 55% of all lines presented wild-type phenotype (Table 9). Additional constructs with a similar structure were used to determine the rescue efficiency independently (the only difference was an N-terminal fused CFP or YFP). Both constructs used are not able to rescue the mutant phenotype, only 17-24% of the lines analysed rescued the mutant phenotype partially. In general all three constructs showed that the dosage of the *STI* transcript is likely to be important for the function of STI because all constructs expressed *STI* under a different promoter than the endogenous one. A further fusion of a fluorescent protein at the N-terminus impairs the function even more.

More than 5kb in front of the translational start of *STI* no gene is present (Figure 19). 2,39kb of the putative STI promoter were introduced into a vector driving the expression of the *STI* cDNA. This vector contained YFP in addition and was comparable to the vector used for the *at-clasp* rescue under endogenous promoter (Figure 11). The analysis of the T1 generation revealed 36 primary transformants in *sti146* mutant background. 53% of these lines did not show any rescue. 47% from the primary transformants showed a partial or complete rescue. Nevertheless the amount of partially

rescued lines was strongly increased (39%). Only 8% of the lines were rescued completely in T1 generation. In contrast to the 35S construct mentioned above, no trichome overbranching phenotype was observed. The next generation was not analysed due to a lack of time.

88% of the trichomes from the progeny that arose from the cross between *tbr1* and col wild-type displayed trichomes with two branch-points. 11% of these plants showed trichomes with three branch-points, whereas only 0,5% of the plants had trichomes with one branch-point. By contrast, in Col wild-type 90% of the trichomes on leaf three and four had two branch-points, whereas the remaining 10% had three branch-points (Table 1). These results are consistent with previous studies (Ilgenfritz 2000). Analysis of the F1 progeny from a cross between Col and *sticol* revealed a change in the branching frequency. 97% of the analysed trichomes had two branch-points (90% in Col wild-type), whereas the number of trichomes was simultaneously decreased to 0,4% (9,6% in Col wild-type). Moreover, an increase in the frequency of trichomes with a single branch-point was observed (0,7%) in Col wild-type. These experiments indicate that reduction of the STI dosage impairs trichome branching, resulting in a lower frequency of trichomes with more then two branch-points. As soon as a *sti* mutant allele is involved a reduction in branch-points is observed, if only one copy of *STI* is present. This hypothesis is substantiated through the additional crosses of *sticol* with *cpr5* or *tbr1*. The distribution of branched trichomes is almost identical when compared to the cross between Col and *sticol*. In summary these observations showed that the amount of STI is important, only one copy of it, as seen in different F1 generations cannot show a wild-type trichome branching pattern.

Table 9: Analysis of the rescue efficiency from different full-length constructs in *sti* mutant background.
The T2 generation was analysed for the rescue of the *sti* mutant trichome phenotype. The percentages shows the amount of independent lines (transformation events) belonging the rescue class.

construct	WT[4]	+-[4]	-[4]	not germ.[1+4]	not res.[2+4]	N
35S::CFP:STI<sti01	0 %	17 %	62 %	0 %	21 %	65
35S::YFP:STI<sti01	0 %	24 %	72 %	2 %	2 %	45
35S::STI73<sti146[3]	55 %	17 %	17 %	11 %	0 %	35

+ - trichomes have only 1 branch points; - plants show *sti* phenotype; N=total lines analysed
[1] no seeds germinated [2] no plants resistant to the selective marker [3] lines generated by D. Bouyer; [4] percentage of total lines

Table 10: The branching of crosses between *sti* and unrelated genes observed in F1 generation.

female x male	number of branch points			N
	1	2	3	
Col x *sticol*	2,6 %	97 %	0,4 %	572
Col x *tbr1*	0,5 %	88 %	11,5 %	606
cpr5 x *sticol*	2,8 %	96,8 %	0,4 %	525
tbr1 x *sticol*	2,1 %	97,4 %	2,1 %	581
Col	0,71 %	89,67 %	9,62 %	707

5.9   Overexpression of an N-terminal cDNA fragment phenocopies *sti*

STI showed a semi-dominant effect in the F1 generation of different genes crossed to it. This underbranching is likely not the effect of a genetic interaction as it occurs in the F1 of crossings with different genes and more important this semi-dominant effect was also visible when analysing the F1 from a crossing of *sti* with the corresponding wild type. It is likely that two copies of *STI* are necessary for STI function. Additional constructs expressing the full length cDNA under the 35S promoter have bad rescue efficiency (Table 9). The question arose what might be the reason for the bad rescue efficiency. Several constructs where used to test the rescue but all of them showed a great variation, or even failed to rescue at all (Table 9). Any major technical problem cannot be the cause for the bad efficiency to rescue the mutant phenotype, because rescue attempts with different constructs harbouring the full-length cDNA transformed into different backgrounds, led to similar results. Even the repetition of the rescue experiment with the original GFP-STI construct transformed into *sti146* (like it was done by D. Bouyer), yielded a low rescue rate for most transformants (data not shown). Possibly the semi-dominant effect, described before, is due to special properties of parts of the STI protein. This idea is supported by the observation, that fragment S1/AS3 showed a high percentage of plants with *sti* mutant phenotype in T1 generation after transformation into Columbia wild type plants.

Fragment S1/AS3 reverted 82 % of the total amount of T1-plants to *sti* mutant phenotype when transformed into wild type (Table 11). Fragment S1/AS1 and fragment S2/AS2 transformed into Col wild-type displayed only wild-type phenotype. Somehow fragment S3/AS3 triggered the reversion from wild-type to *sti* mutant phenotype. Subsequent analysis of the T2 progeny showed that plants without the resistance marker died after treatment with BASTA and presented the wild-type trichome phenotype. This observation excludes the possibility of cross contamination with *sti* mutant seeds. Furthermore both construct with the full-length cDNA of STI fused to YFP or CFP which where evaluated for their ability to rescue the *sti* mutant phenotype (Table 9), where analysed in T2 generation for the presence of a *sti* mutant phenotype. Indeed almost 57% of all lines (representing independent transformation events) showed a reduction in branching or even *sti* mutant phenotype even though the reduction was not as severe as observed with fragment S3/AS3.

Table 11: The effect of the overexpression of different *STI*-fragments.
Different fragments where analysed for their ability to (the position of the fragments is summarised in Figure 29). This table summarizes the number of plants showing wild-type or *sti* mutant phenotype after transformation into Col wild-type.

construct	Pos. (bp)	wild type [N]	*sti* [N]	% *sti*
S1/AS3	1-1200	30	168	82,15 %
S1/AS1	1-402	46	0	0 %
S2/AS2	403-801	15	0	0 %
S3/AS3	802-1200	42	73	63 %
35S::CFP:STI<Col	1-3657	12	16[a]	57 %
35S::YFP:STI<Col	1-3657	22	29[a]	57 %

[a] this number includes the lines that showed only underbranching
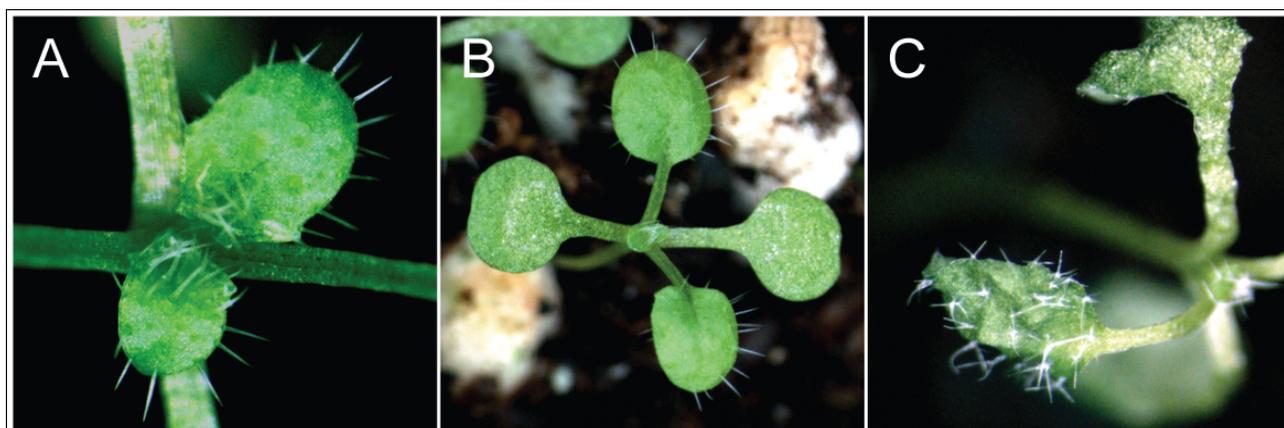
Figure 30: Dominant negative effect of fragment S1/AS3 after transformation in Col wild-type.
(A) Leave 3 and 4 of line 5 expressing construct S1/AS3 in Col showed a dominant negative effect. Leaves had a clear *sti* mutant trichome phenotype. **(B)** Line 7 exhibited an even stronger trichome phenotype. **(C)** All of the lines analysed were segregating populations in Columbia background and showed the common wild-type phenotype if no construct with the resistance marker was present. These results were obtained in segregating T2 lines.

5.10 Identification of interacting proteins

Two approaches have been chosen to find protein interacting with STI. In previous studies possible interactors of STI were identified with the yeast two hybrid system (Herrmann 2002; Kübbeler 2004). To test the relevance of some of the putative interactions, insertion lines within the identified genes were analysed for the presence of a trichome phenotype, wherever suitable insertions were available. Additionally one of the candidates (*GLUC2*) was overexpressed in Col and *sti* mutant background to test a possible interaction.

Different from the approach described before a biochemical method was used, in this study, to find new interactors. Plant crude extracts from the STI:GFP full length line and fragment S5/AS7 fused to YFP were generated and bound to GFP antibodies that are coupled to magnetic beads. With the use of a strong magnetic field the antibody coupled GFP:STI and the associated proteins were washed and later separated with a protein-gel under denaturating conditions. The bands received were cut out and analysed with PMF (Peptide Mass Fingerprinting) (Figure 31,Table 12).

To validate the putative interaction of GLUC2 (At5g55180) with STI the test system was changed from *S.cerevisiae* to *A. thaliana*. Because the cDNA found in the Two Hybrid screen did not contain the full-length coding region it was isolated from a Col cDNA library first. The cDNA was transferred into a plant transformation vector under the control of the GLABRA2 (GL2) promoter which is strongly expressed in trichomes (Rerie et al. 1994). The transformation into Col yielded 300 primary transformants and the transformation into *sti146* mutant background 240 transformants. No T1 plant in Col background showed an effect onto the trichome phenotype. Only 9 plants from the T1 transformed into *sti146* show up to 4 trichomes with two branch points.

Finally one can summarize that GLUC2 cannot change the trichome phenotype of the mutant or the wild type. Therefore it is likely that GLUC2 is not interacting with STI. Other candidates identified in a previous Two-Hybrid screen (Table 16) were analysed for a trichome specific phenotype. For the analysis T-DNA insertion lines were obtained for the following genes: At5g42100, At5g24650, At5g53320, At3g01340, At5g55180, At2g05790, At4g15930, At1g53310, At3g56880, At3g53180, At3g16400 and At1g25260. None of the different lines analysed for this genes showed a trichome phenotype.

Several new putative interactors were identified with the immuno precipitation method and PMF afterwards. Three candidates produced a high enough score to be significantly identified. Candidate A2 unfortunately is most likely a false positive interactor because its corresponding band appeared in the control too and it was identified in a previous study with an unrelated protein (Schrader 2006)

Both proteins, GFP:STI and fragment S5/AS7, used to identify its binding partners showed a related pattern of proteins on denaturing gels (Figure 31 A+B) but some differences were observed. Proteins with a size of approximately 54 kD (A3+A7) and 68 kD (A2+A6) appeared for both bait-proteins, but the amount of bound protein is increased for fragment S5/AS7 (A2) in contrast to A6. Candidate A1 (~88kD) was identified only for fragment S5/AS7. The other candidate, identified only for one bait-protein is A4 (~97 kD) and A5 (~75 kD). Both were identified for the bait protein containing the full-length cDNA.
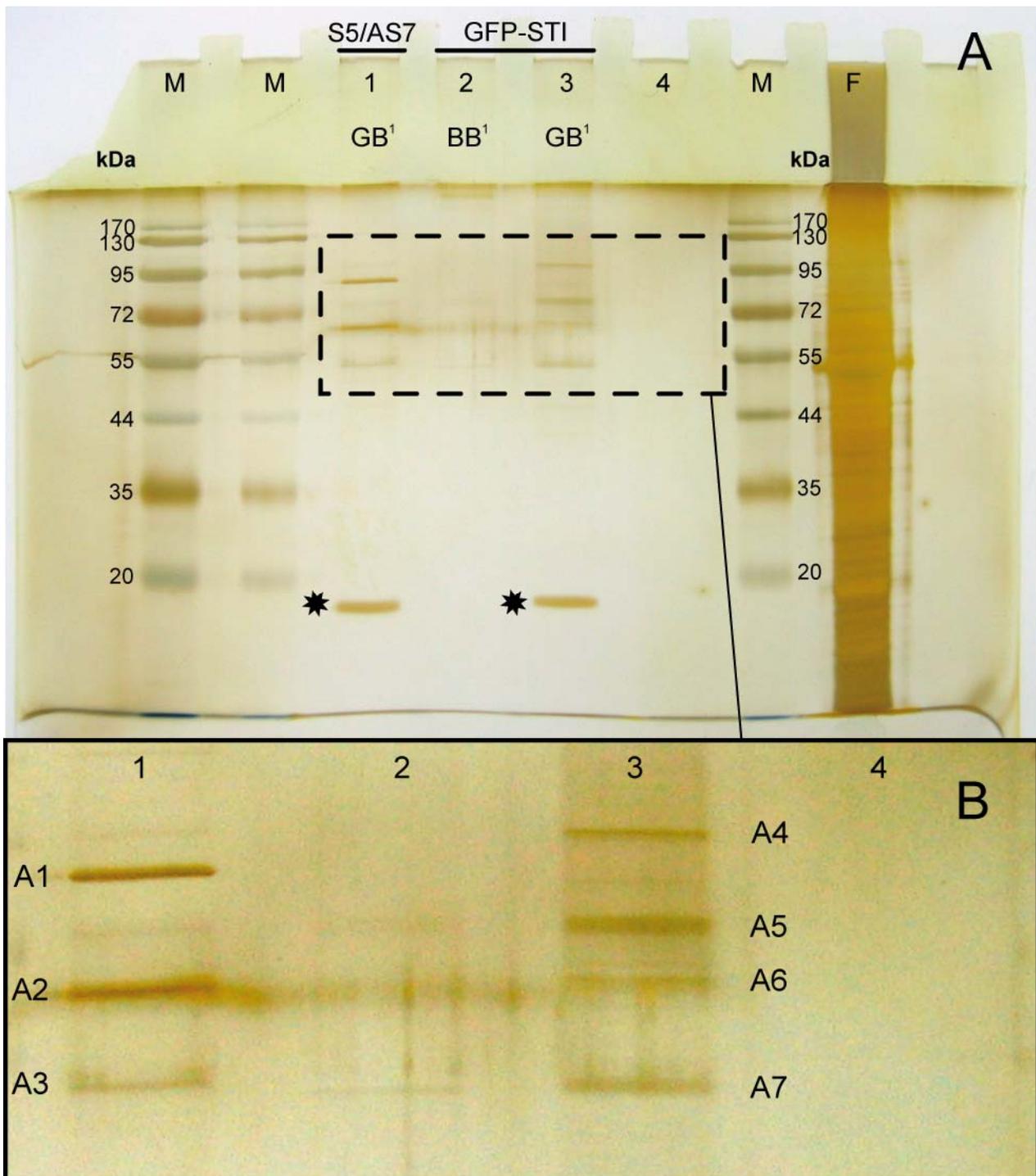
Figure 31: Different proteins precipitate with STI-GFP
(A) shows the complete gel with separating and stacking gel. Lanes marked with M contain a molecular mass marker with different protein sizes which are listed close to the marker. Lane 1 contains the proteins that precipitate with fragment S5/AS7 which were bound to GFP-beads. Lane 2 contains the proteins from GFP-STI full-length cDNA (the reference line use for the localisation studies) bound to basic beads without antibody. In lane 3 the proteins were visualised that precipitate with GFP-STI after they were bound to a GFP antibody connected through a strong magnetic field with the basic beads. Lane F contains the flow thru with all the proteins that cannot bind to STI or fragment S5/AS7.

The star indicates the position of the light chain of the antibody used to bind GFP.

Table 12: Candidates identified by PMF
All candidates were send for identification with PMF (Peptide Mass Fingerprinting) to the ZBA (http://www.zmmk-bioanalytik.de/). Only three proteins listed in Table 12 generated a significant score. Candidate A2 also named PYK10 (Nitz et al. 2001) was identified in a different study with similar technical setup (Schrader 2006). Because of the different nature of the studied protein (Schrader 2006) this candidate is most likely false positive. Additionally a smear is observed in the negative control in the range of protein candidate A2.

Nr.	AGI	putative function	Score
A1	At3g15730	Phospholipase Dα1	184
A2	At3g09260	β-Gluconidase PYK10	109
A3	At1g31140	transcription factor MADS-box	86

5.11 STI and STI-HOM share 72,5% identical nucleotides

STI has a homologous gene that possibly arose from a segmental duplication event (http://mips.gsf.de/proj/thal/db/gv/rv/SegDupATA-ATB-2_1.html). This gene is like STI a gene without known function. It is located on chromosome one and has the locus ID At1g14460. To simplify the name of this gene it is named *STI-HOM* in this study. The STI-HOM gene structure is predicted to be similar to STI. It contains six exons and five introns but the intron located in the 5' UTR is not present in STI-HOM (Figure 32). Alignments of STI and STI-HOM show that 72,5% of the nucleotides are identical. Both proteins share 62,6% identical aa. For a detailed analysis about possible homologs or orthologs please refer to the introduction and Figure 16.

A complete cDNA for this gene was not present in common stock centres but ESTs confirmed that STI-HOM is expressed. For this study the full-length cDNA was isolated from a Col leave cDNA bank. Sequencing of the acquired cDNA revealed that the exon-intron structure is likely true for the tissue the RNA was isolated from. STI-HOM is expressed at lower levels than STI, which was tested by RT-PCR on a leave cDNA bank (data not shown). Data from whole genome chips showed, that STI-HOM is expressed at comparable levels in all tissues analysed (Figure 22 C). The methods described above reflect only the situation at a given time-point. To analyse the expression level over time new constructs were generated that included 1,5kb of the putative promoter of STI-HOM fused to GUS. Figure 33 shows the expression of this promoter fragment in Col (B+C) and sti146 (A). The expression in both genetic backgrounds is not distinguishable. Young leaves are stained completely until they reach adult size. Trichomes, epidermis, stomata and the vascular tissue are stained. Later stages of leaves still show strong staining in stomata and the vascular tissue although the staining in the vasculature is incomplete (Figure 33 A+B).
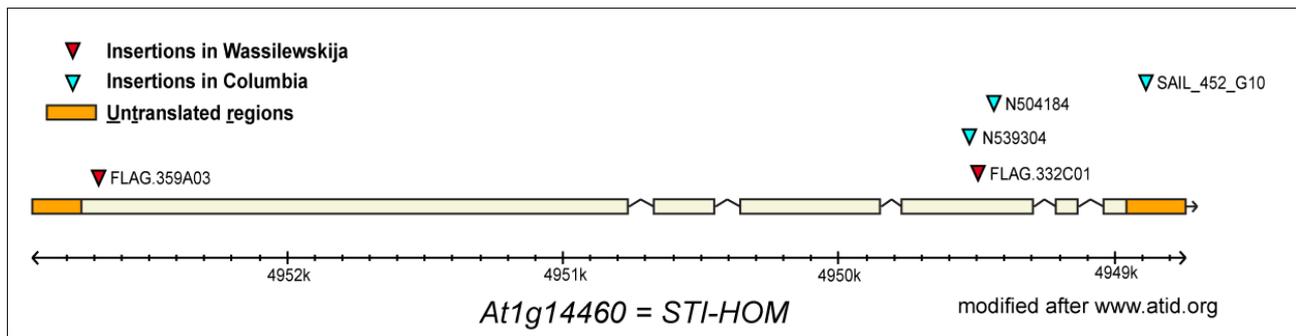
Figure 32: Genomic structure of *STI-HOM* (At1g14460).
Like STI STI-HOM consists of five exons. Most available insertion lines are located at the end o the gene and are no good candidate for a complete knock out. Only line FLAG.359A03 has an insertion at the beginning of exon one.
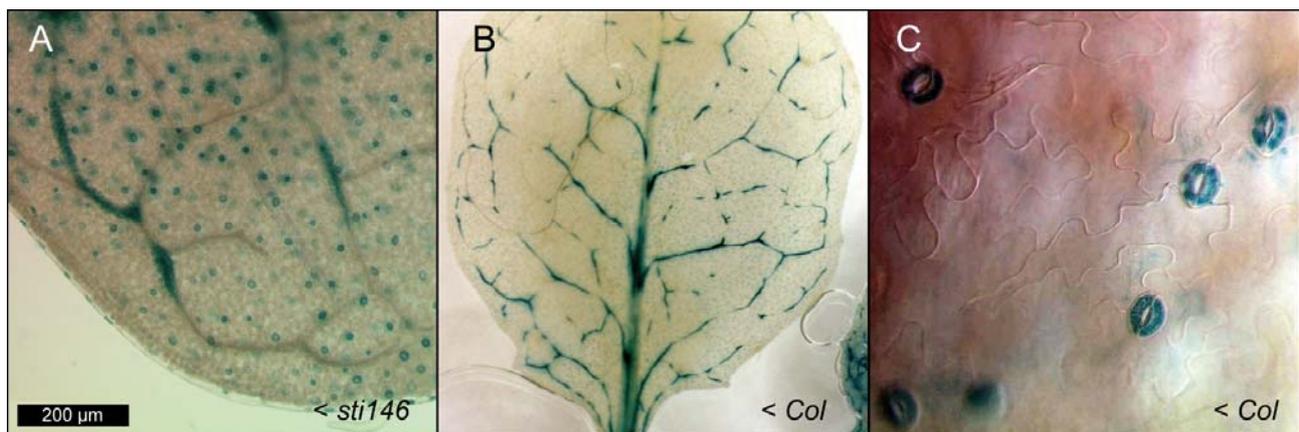
Figure 33: Gus activity of the putative STI-HOM promoter.
(A) shows the expression of the GUS reporter gene under the control of the putative STI-HOM promoter in sti146 mutant background. **(B)** shows the expression of the same construct in Col wild-type. **(C)** is a magnification of the epidermis showing strong staining in stomata.

The localisation of YFP:STI-HOM under the control of the 35S promoter was analysed in Col wild-type and *sti146* mutant background. None of the lines analysed (10) showed a signal in trichomes during analysis of the T1 generation transformed into wild-type. The result was identical for the primary transformants in *sti146* (three lines analysed). Additional none of these lines was able to rescue the *sti* mutant phenotype. The lines transformed into Col show no deviation from the wild-type trichome phenotype.

To further evaluate the importance of STI-HOM for STI function, a mutant and double mutant analysis was performed. The following T-DNA insertion lines were analysed for trichome phenotypes: N504184, N539304, FLAG.332C01 and FLAG.359A03 (Figure 32). None of these lines displayed a trichome phenotype, they are indistinguishable from wild-type. Due to the high similarity on nucleotide level a redundant function of both proteins is conceivable. A double mutant analysis between FLAG.359A03 (*sti-hom*) and FLAG.019E04 *(sti)* might clarify this issue. However the analysis of the F2 generation concerning a change in trichome morphology revealed no deviation from the expected situation. One out of 16 plants should be homozygous for both

insertion lines but only wild-type and *sti* mutant trichomes were observed.

To determine a possible connection between STI and STI-HOM the construct with 1,5kb of the putative promoter from STI-Hom, used for the GUS reporter assay above, was used again. STI under the control of the 1,5kb promoter fragment cannot rescue the *sti146* mutant phenotype (13 lines analysed). In contrast to that STI under the control of its own putative promoter can rescue its own mutant phenotype only to a certain extent (5.8). But STI-HOM under the control of the putative STI promoter cannot rescue the *sti146* mutant phenotype (42 lines analysed). Additional STI-HOM under the control of the 35S promoter cannot rescue the *sti146* mutant phenotype either (see localisation).

6   Discussion

Cell morphogenesis is a key process in establishing a complex structure like a trichome of *A. thaliana*. As these trichomes consist of a single cell this model-system seems to be simplified enough do analyse the underlying processes. Several mutant screens identified mutants with defects in various stages of trichome development (Marks and Esch 1992; Hulskamp et al. 1994; Luo and Oppenheimer 1999). These studies showed that a variety of different protein classes shows defects in trichome related developmental processes. Many of the proteins are members of transcription factor families (e.g. GL1, GL3, TRY), others are related to the microtubule cytoskeleton (e.g. ZWI, TFC-A) or the actin cytoskeleton (e.g. DIS1, KLK). Not all proteins identified can be assigned to a putative function, like described before. These genes are for example *STI* (Ilgenfritz et al. 2003) and *AN* (Folkers et al. 2002b; Kim et al. 2002). STI plays an important role in branching as amorph alleles of *sti* do not branch any more. Two studies analysed the function of this gene with unknown function before (Ilgenfritz 2000; Bouyer 2004).

The most prominent domain which was predicted in the STI protein shows similarity to the γ-subunit of DNA-Polymerase III. Polymerases of type III are responsible for the replication of genomic DNA (Knippers et al. 1990). However no general defect in plant development was observed as one has to postulate for a protein with an important function in DNA replication. However the model system *A. thaliana* exhibits a high degree of redundancy. During the development of *A. thaliana* chromosomal regions were duplicated which led therefore to the duplication of former single copy genes too (AGI 2000). These duplicated genes might acquire different functions during evolution. Therefore a specialized function for STI in trichomes is conceivable. The process mostly related to replication in trichomes is endoreduplikation. During the maturation trichomes increase their DNA content from 2C to 32C (Koornneef et al. 1982; Hulskamp et al. 1994). Nevertheless *sti* mutant trichomes do not show any deviation from the wild-type DNA content (Ilgenfritz et al. 2003). As trichomes do not undergo cytokinesis, it is not likely that another process despite of endoreduplikation is associated to the putative function of this conserved domain so that the function of *STI* is probably not related to a replication process. The function of DNA-Polymerase III from *E. Coli* is dependent on ATP (Knippers and Knippers 1990). *In silico* studies showed that the ATP-binding conserved aa termed "p-loop" are conserved in STI. Possibly the process STI is involved in requires energy or the shape of the protein is changed upon binding of ATP. This possibility is truly speculative since the binding of ATP is not proven.

Independently of the conserved γ-subunit identified by *in silico* analysis, other smaller motifs were identified. A nuclear-localisation-signal (NLS) was detected by these methods. According to the

information provided by the website, used for the analysis (see chapter 5.1), more than 200 proteins with a similar NLS are located to the nucleus and have the capability to bind DNA. According to the analysis of fragments and the full-length cDNA fused to a fluorescent protein no case was detected where the fusion-protein was visible in the nucleus. If this signal is indeed functional it might be possible that the protein is not localized to the nucleus in this special cell type, but can be found in the nucleus of other cell-types. Additionally different localisation patterns are conceivable. Upon certain cues (Lee et al. 2006) or by a temporal pattern (Mas 2005) the localisation of the protein could be adapted. Another possibility for not detecting the protein until now in the nucleus might be a strict control of the amount of transcript or protein like it is observed for PEST sequence containing proteins (Adachi et al. 2006). Two putative PEST-motifs are located within the protein. PEST sequences are proline (P), glutamic acid (E), serine (S) and threonine (T) enriched sequences that target proteins for rapid degradation (Rogers et al. 1986; Rechsteiner and Rogers 1996). According to these publications a score above five (arbitrary units) characterises a candidate with a good probability to be a target for rapid degradation. Both PEST-sequences found in STI exhibit a score of around nine. Until now functional examination of these motifs was performed but several lines of evidence indicate that STI abundance might be strictly regulated, as the overexpression of one putative PEST sequence of STI can induce the *sti* mutant trichome phenotype in Col wild-type background. These new observations will be discussed later together with the rescue efficiency.

The structure of the STI transcript

The sequence for the STI cDNA was described for two *A. thaliana* ecotypes, L*er* (Ilgenfritz 2000) and Col (M.D. Marks, NCBI accession AF264023). Despite off the known polymorphisms between both ecotypes, differential splicing was observed in the last exon leading to a deletion of nine nucleotides (Ilgenfritz 2000). Recently a new putative Col cDNA was isolated by the RIKEN Institute that showed an open-reading-frame of only 1900bp instead of 3756bp for the complete transcript. Nevertheless the RIKEN cDNA was still comparable to the previously published once, concerning the total size. This new truncated open-reading-frame is caused by a 88bp deletion within the transcript. Due to the fact that the rest of the expected transcript is still there and this truncation is not close enough at a splicing border, it is likely that the RIKEN cDNA is inaccurate. Most likely a polymerase error or a defective RNA-template was causative for this deletion. During the analysis of the transcripts of the Col cDNA an intron within the 5' untranslated region was detected. About 72% of the genes with available EST data contain introns (Chung et al. 2006) whereas introns in the 5' UTR are more frequent (19,9%) than in the 3' UTR (5,6%) (Chung et al. 2006). The function of such an intron is not understood but they might increase the level of RNA (Callis et al. 1987). As all rescue- or localisation construct did not contain this intron it is

conceivable that the expression of STI might be increased upon presence of this intron if the hypothesis of Callis and co-workers is true. However only further experiments can investigate the importance of this intron.

Expression of the STI transcript

Previous studies reported that *STI* is expressed in all tissues analyzed (Ilgenfritz 2000; Ilgenfritz et al. 2003). Nevertheless the possibility of cross-hybridization with the close homolog of *STI* termed *STI-HOM* (At1g14460) could not be excluded. The availability of expression profiles via the use of *A. thaliana* whole genome chips allowed comparative studies of both genes in different tissues (Figure 22B). The expression levels of *STI* and its homolog are comparable high in seedlings, inflorescence and rosette leaves. Just the expression of *STI* in suspension culture is increased by the order of magnitude four. *STI* expression in roots and callus is also increased but to a minor extent. Causes for the upregulation of *STI* transcription in callus and suspension culture are ambiguous. One hypothesis might be that *STI* is upregulated in contrast to STI-HOM, prior or at the same time of differentiation. Both cell types mentioned are undifferentiated (callus) or at least barely differentiated (cell-culture) as they do not contain all cell types of an adult plant. Another explanation could be that gene expression is changed for many genes due to the artificial nature of e.g. cell-culture. More evidence for a high expression at early time-points came from STI::GUS fusion constructs (Figure 22 D-F). The putative promoter is active in young trichomes and trichomes that are completely branched on growing leaves. Older leaves with adult leave size do not express *STI* any more (data not shown). Interestingly *STI* expression is stronger and ubiquitous in very young stages of leaves. *STI* is not restricted to trichomes. In contrast to the putative *STI* promoter the putative promoter of *STI-HOM* is not or hardly active in trichomes. According to the current model of trichome development and the mutant phenotypes observed it is not likely that STI function is needed in early stages of leave development, before trichomes are selected out of the epidermal cell-layer and more important STI is likely not needed after the completion of trichome branching. Possibly *STI* is expressed in preparation of the later branching processes but a protein is not made or not active at early stages. From the localization studies with *GFP:STI* it is known that the protein is visible in a cap like structure directly after a trichome cell becomes morphological visible. Possible explanations for an expression not limited to a trichome cell are diverse. STI could have a so fare unknown function in other cell types. The protein could be translated upon the decision to trichome fate was made but the RNA is made in most cell-types.The activitiy of the *STI* promoter in e.g. young trichomes anticipates that the protein is made too.But the regulation of *STI* might take place on protein level (two PEST sequences are predicted) which is not detected by a promoter GUS fusion construct. In addition the localization of *GFP:STI* under the control of the

35S promoter in a cap like structure and not everywhere in the trichome is a another hint for a regulation at protein level. Furthermore it is still conceivable that the putative promoter used for the visualization of the transcript does not resemble the endogenous transcription levels completely as the rescue in T1 generation was only partially (see chapter 5.8).

6.1   GFP-STI is localised to the emerging tip of trichomes

Upon outgrowth from the epidermal cell layer, GFP:STI is visible in a cap-like structure. Before a new branch is visible due to a changed morphology, the fluorescent protein will mark this position. During progression thru trichome development every new branch is marked (Figure 23 A+B). It is possible to observe the signal of the fusion protein for all three branches, but the signal for the youngest branch is still the brightest. During the observation of GFP:STI it turned out that the signal is weak and subject to rapid photo-bleaching. This rapid bleaching might be due to the low amount of protein which is only visible if concentrated at a certain place like the tip of trichomes. The sensitivity to bleaching could be explained by the low amount of protein as it was not found in other tissues. Additionally a short lifetime of the protein or a strict control of the protein activity can explain the observed situation. Nevertheless it cannot be excluded that the fusion of STI to GFP might be causative for a short lifetime of the fusion protein (for example YFP fusions to the At-CLASP cDNA yielded different signal-intensities depended on place of the YFP fusion, see chapter 2.6). However a structural problem of the fusion protein, like low stability seems not very likely as the mutant phenotype is rescued by this construct. Until now it is unclear how the fusion protein is transported to the tip of trichomes. Mainly two alternatives are imaginable; the protein is transported along microtubules or actin filaments. A simple diffusion approach appears to be unlikely as the localisation is specific and exclusive to tips. To access the question of transport drugs studies were performed (Figure 27). After the application and a certain incubation delay the signal of the fusion protein was still visible albeit the signal intensity was insignificantly reduced. The drugs applied were proven to be affective as later trichomes displayed morphological defects which are usually observed after treatment with these drugs (Mathur and Chua 2000). Several possibilities might explain the result observed. The fusion protein is not transported via both filaments or it is stable enough to be detected after the incubation interval at its previous position. The tracks STI uses to be transported to the tip, if it is not diffusion, cannot be clarified by this experiment. It is conceivable that the incubation interval was not long enough to affect the localisation of the fusion protein. However a prolonged incubation time leads to severe cell- and cytoskeleton-defects which in turn could affect the localisation of STI and as a result it might not be possible tto recognise a specific effect onto the localisation of the fusion protein. To exclude the

possibility of movement along actin or microtubules colocalisation studies of GFP:STI with differently labelled filaments might solve this problem in future experiments.

Recent experiments showed that the GFP:STI fusion protein is able to move (Figure 25). These new pictures show that the cap like structure of GFP:STI consists of single spots with a certain dynamic. The spots can increase or decrease the total intensity and new spots appear in an angle expected for a protein transported along filaments. Even if the drug experiments suggest no involvement of any filaments tested, it might still be that this transport was not observed due to the reasons mentioned above. Surprisingly one of the fragments of STI fused to YFP (S1/AS1, Figure 25B) showed a strong signal even when observed under the binocular. The total signal intensity of this fusion protein is strongly enhanced but a cap-like structure which is observed by with the complete cDNA was never detected. Additionally this fragment is able to move quite fast.

GFP:STI is localised to the plasma membrane

Before this study the cellular localisation of GFP:STI was only mapped to the tip of trichomes. The compartment it is localized to was still unclear but two major possibilities were conceivable, the plasma membrane or the cell-wall. To clarify its subcellular localisation plasmolysis studies were performed. These experiments showed that the fusion protein moves together with the shrinking cell-plasma (Figure 24). It is likely that the fusion protein is located to the plasma membrane. Unfortunately it is not clear how GFP:STI can bind to the membrane. Former *in silico* analysis for the existence of transmembrane helices didn't reveal any result. Maybe the structure needed for binding to the plasmamembrane is not detected by the programs used due to a not conventional composition of amino acids. Alternatively it is conceivable that the protein is modified by prenylation or a GPI-lipid anchor to associate it to membranes (Brown et al. 1992). *In silico* analysis showed that no common motif is present needed by the enzymes to attach any modification. To summarise, there is no proof that STI can bind membranes directly, the localisation itself cannot support a direct binding as an indirect binding cannot be excluded by this observation too. The current information available suggests that the binding to other proteins might be causative for the localisation. Nevertheless future investigations are essential to check this hypothesis.

Several mutant backgrounds do not interfere with the localisation of GFP:STI

Crosses between a new mutant and other mutants with similar phenotype might reveal possible genetic interactions. *sti* mutants were crossed to almost all mutants involved in the development of trichomes (Marks and Esch 1992; Hulskamp et al. 1994; Folkers et al. 1997; Luo and Oppenheimer 1999). Mutations in the *sti* locus are often epistatic since double mutants show only *sti* mutant

phenotype (*sti try, sti gl3*). The differentiation between an additive or epistatic situation is not always clear, if both phenotypes show only a marginal difference. A truly additive phenotype was observed between *nok122* and *sti-EMU* because the double mutant is not showing the single phenotype of either of the mutants and is therefore less branched than *nok*. The outcome of the studies mentioned above can be found in the introduction (4). As many genetic interactions are known up to now it should be determined whether or not a different mutant combination can effect the localisation of the protein. The first event utilized direct transformation of the original construct into the respective mutant background. Many different lines were generated but none of them showed a fluorescent signal at all (data not shown). Reasons for this are numerous. Most important seems to be the presence of the endogenous amount of STI. It might be that the amount of protein is strictly regulated and both STI proteins, the endogenous and the newly introduced fusion protein, compete for binding to a third protein. As a result of this competition the overall fusion protein available for detection might be below the detection limit. Furthermore the position of the T-DNA within the genome could be important for a suitable level of transcription. Something similar was observed for the initial transformation event where GFP:STI was screened among other lines. Not all lines showed fluorescence but one (used for this study) gave a bright enough signal to be utilized for the further analysis mentioned above. Additionally this line was subject to southern blot analysis which showed that the T-DNA in this special line might be integrated in inverted repeats (data not shown). Combining these information leads to the assumption that the position and the amount of protein is possibly important for STI function.

The second approach to localise GFP:STI in different mutant backgrounds used consequently crosses between the selected GFP:STI line and the mutants of interest. The cross between GFP:STI and *sim* showed an additive phenotype. Trichomes show the characteristic *sim* phenotype of multicellular trichomes and in addition the fluorescence of the fusion protein (Figure 28C+D). The intensity of the GFP:STI signal is reduced compared to the wild-type situation. Furthermore the identification of this allele was time consuming. Most lines derived from the crossing didn't show any signal possibly due to a residual wild-type copy of STI. Plants carrying one wild-type copy are not easy to identify as the GFP:STI is expressed ubiquitously and rescues the mutant *sti* mutant phenotype. None of plants derived from different crossings showed a fluorescent signal although the genetic background was like expected judged by morphological criteria and basta selection. To access the question why the signal of the fusion protein cannot be detected in most cases, heterozygous lines of the GFP:STI fusion protein were established thru crossing to the corresponding wild-type. The F1 progeny of this crossing shows the GFP:STI signal similar to the homozygous line but slightly reduced in intensity. Via this experiment it can be concluded that one

wild-type copy of STI is only causative for a reduction of the signal intensity but not for the complete loss. Additional possibilities for the absence of any detectable signal might be the overall weak signal intensity of the original line. Furthermore the sti146 allele, which is the genetic background for the GFP:STI construct, might effect the signal intensity of the fusion protein. This allele has a strong root defect which is likely caused by a second site mutation (unpublished observation). Maybe the general slower growth of this allele is affection the signal intensity.

Is the localisation of GFP:STI controlled by a domain of the protein itself?

The presence of the cap like structure in plants transformed with the GFP:STI construct raises the question, which part of the STI protein is necessary to resemble the original localisation. To detect this part the complete cDNA of *STI* was splitted with a PCR based technique into five bigger and nine smaller fragments (Figure 29). Subsequent fusion to YFP or CFP and transformation into wild-type and *sti* mutant background allowed the visualisation of the fusion protein *in planta*. As a functional control the full-length cDNA was transformed into *sti01* too. Unexpectedly none of the lines was able to rescue the mutant phenotype in T2 generation (Table 9). The reason for this result is still unclear. A technical reason can be excluded as the fusion frame was sequenced and the presence of the T-DNA was proven. The only major difference between the original line used for the localisation studies and the new similar control line was the mutant background of the *sti* allele. The new construct used *sti01* as transformation background instead of *sti146,* which was used for the original localisation construct. Nonetheless the localisation for all five bigger fragments fused to YFP was analysed in T2 generation but no fluorescence was detected. To exclude the possibility of an interference with the mutant background, all bigger constructs were transformed into *sti146* mutant background. Again a fluorescent signal like observed for the reference line was not detected. In contrast to the constructs transformed in *sti01* mutant background a faint signal, like observed for the movement of GFP:STI and the fragment S1/AS1, was visible in some of the plants (Table 8). Regardless of this observation a cap like structure was observed in no case. Different possibilities are conceivable to explain the results. A much bigger part of the cDNA might be needed to show the originally observed signal (lines produced by D. Bouyer). Therefore no construct carried all the information needed. Additionally the expression level of the construct might be important too, as GFP:STI under 35S promoter showed a high variation in trichome rescue (Table 9). The possible importance of the expression of the STI transcript is discussed in chapter 6.2. Furthermore the mutant background, in this case *sti146*, seems to increase the signal observed as faint moving dots are observed. To conclude, a localisation domain per se possibly does not exist. Instead the complete protein could be essential for the proper localisation pattern. Furthermore it might be that a fragment with the same localisation domain observed for the complete protein could not be

visualised due to a signal intensity below the detection threshold because the reference signal itself was already close to the detection limit. A fragment with the sequence sufficient to resemble the localisation pattern might miss any sequence to stabilize itself and could be even worse detectable. Further experiments are required to discriminate between the scenarios described above.

6.2   The *sti* mutant rescue depends on several factors

Previous studies showed that a ubiquitous expressed *STI* full-length cDNA under the control of the 35S promoter can rescue the *sti146* mutant phenotype (Ilgenfritz et al. 2003). Nevertheless the rescue efficiency was varying from underbranched to strongly overbranched trichomes compared to wild-type. Analysis of expression levels revealed that the expression levels of over- and underbranched plants were indistinguishable (Ilgenfritz et al. 2003). However the expression level of endogenous *STI* was not analysed. A similar rescue efficiency was observed in lines overexpressing *CFP:STI* or *YFP:STI* (Table 9). None of the lines can completely rescue the *sti* mutant phenotype. The reason for the absence of completely rescued plant remains to be clarified. But the decrease of rescued versus partially rescued plants, when comparing lines with or without GFP, suggest that the fusion to GFP reduces the rescue efficiency. The modified N-terminus might alter the stability of the protein or impairs binding to other proteins. Nevertheless, the decreased rescue rate cannot solely be explained by a fused GFP, as the high variability of the rescue efficiency is also observed in plants expressing an untagged version of STI under the control of the 35S promoter. It is feasible that the position of the T-DNA in the genome might influence the rescue efficiency (Peach et al. 1991; Day et al. 2000). Integration in proximity to a regulatory element could decrease or increase the expression level of the transgene. In contrast to this hypothesis the expression levels of the lines mentioned above are not different but the phenotypes differ very well. Recently a publication on the importance of positional effects versus silencing through exceeding a certain transcript threshold became available (Schubert et al. 2004). The authors claim that positional effects do not effect the transcriptional levels of any transgene analysed. More copies of the same transgene will increase the expression almost proportional until a certain gene specific transcript-threshold is reached. After this threshold is exceeded gene silencing will occur. These observations made by Schubert et al. could explain the appearance of different phenotypes, although transcript levels were constant.. It is possible that the 35S promoter used for the constructs in this study is not the optimal choice to rescue the *sti* mutant phenotype. If the hypothesis is applicable it might be that the 35S promoter used is exceeding the endogenous transcript-threshold of *STI* and gene silencing is taking place. In turn the 35S promoter might not be

the optimal choice for the rescue of the *sti* mutant phenotype.

To clarify the importance of the expression level a construct with the putative *STI* promoter was used to rescue the mutant phenotype. Analysis of the heterozygous T1 progeny showed that 53% of the lines analysed are not rescued and only 8% showed a good rescue (refer to chapter 5.8). A reasonable explanation for the moderate rescue efficiency might be an incomplete promoter. Certain elements that enhance the STI transcript-level might be located further upstream/downstream or in intronic regions, which were not covered by the construct. Alternatively it is conceivable that one copy of *STI* in the genome is not sufficient for STI function and the rescued plants are due to multiple integration events. At this point a final conclusion about this observation is not possible. The analysis of the T2 progeny will allow to judge about this hypothesis but due to time constraints this experiment was not performed.

Further experiments indicated that the amount of STI is critical for its function. Heterozygous *sti* lines are not able to rescue the mutant phenotype as expected for a recessive mutation. Therefore *sti* is semidominant in the F1 generation. This effect is specific to *sti*, since crosses with unrelated genes showed a comparable result (Table 10). These unrelated mutants crossed to Col wild-type did not affect trichome branch number. This observation strongly argues for the idea that STI function is dosage dependent. Moreover it suggests that the amount of transcript likely limits the rescue of the trichome phenotype. Probably the amount of the STI protein generated from the reduced level of RNA is not sufficient to promote wild-type trichome fate. Interestingly the reduction in branch number is much less than 50% because only a slight reduction in trichome branch numbers was observed (Table 10).

All results discussed in this paragraph indicate that the amount of *STI* transcript is an important factor for STI function. But so far the regulatory mechanisms that affect the transcript or the protein itself were not investigated. This notion is supported by the finding that different constructs never rescued the mutant phenotype (refer to Table 9). To analyse whether regulatory signals are present in the transcript respectively the protein, the constructs used for the mapping of the localisation domain were analysed in wild-type background. Indeed, 82% of the plants harbouring fragment (S1/AS3) showed a conversion to the *sti* mutant trichome phenotype when transformed into Col wild-type (Table 11). This fragment is covered by three smaller fragments of approximately 400bp size (S1/AS1; S2/AS2; S3/AS3 summarized in Figure 29). Only fragment S3/AS3 displayed a conversion to the *sti* mutant trichome phenotype in the T1 generation, whereas both other fragments had wild-type trichomes. The conversion to the *sti* mutant trichome phenotype is therefore correlated to fragment S3/AS3. An *in silico* analysis of the STI protein sequence revealed that a

putative PEST sequence is located within fragment S3/AS3 (Figure 18). PEST sequences are often present in proteins which are rapidly degraded (Rogers et al. 1986; Rechsteiner and Rogers 1996). The importance of this sequence could not be verified due to time restrictions but some observations argue for an involvement of the PEST sequence in STI function. Overexpression of the cDNA from the STI homolog (STI-HOM) can neither rescue the mutant phenotype nor induce the STI mutant trichome phenotype when transformed into wild-type (see chapter 6.4). In contrast to this observation the full-length cDNA of *STI* under the control of the 35S promoter was able to transform wild-type trichomes into underbranched trichomes (refer to Table 11). However the amount of plants with underbranched trichomes was reduced in comparison to fragment S3/AS3. Interestingly the alignment of the cDNA from *STI* and its putative homolog showed a deletion of 21 bp within the putative PEST sequence (Figure 34).

This deletion could explain the failure of STI-HOM to convert wild-type into *sti* mutant trichomes, although both proteins are 72,5% identical. If this PEST sequence is functional *in planta* a regulation on protein level is conceivable. Alternatively the gene product of fragment S3/AS3 might represent a domain responsible for binding to other proteins. Consequently, increased amounts of the putative binding domain might interfere with binding of wild-type STI proteins to target proteins resulting in a conversion to *sti* mutant phenotype. Nevertheless future studies are needed to understand the reason for the conversion to *sti* mutant trichome phenotype.
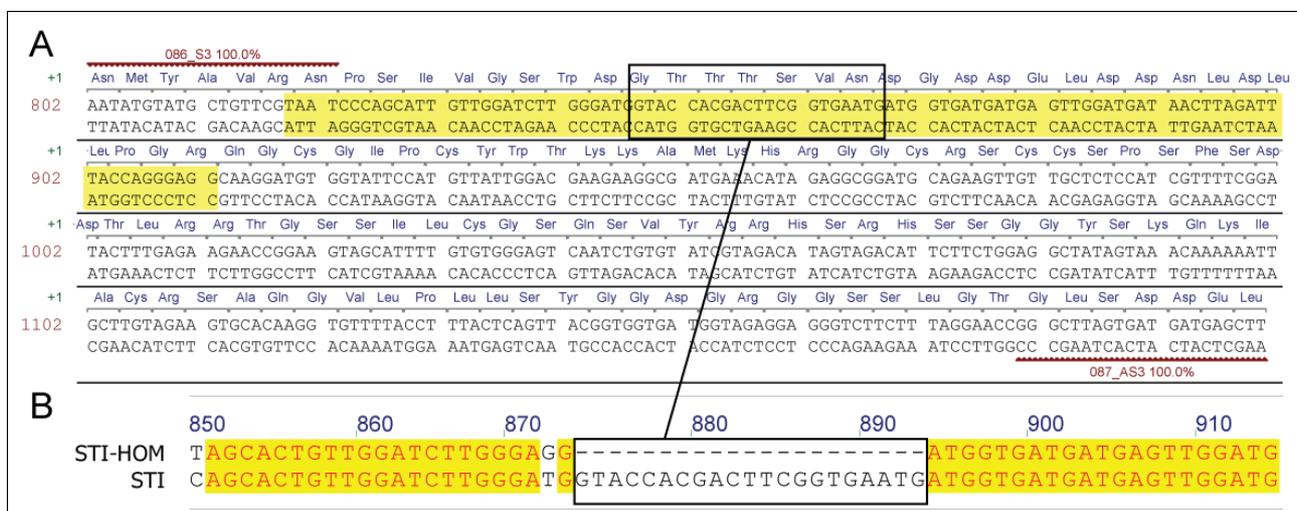
Figure 34: Fragment S3/AS3 in comparison to the putative homolog.
(A) The sequence of fragment S3/AS3 is depicted which was generated by primers 86 and 87. Labelled in yellow is the predicted PEST sequence. **(B)** This alignment compares STI and STI-HOM within this region. The black rectangle marks the position in the STI-HOM cDNA which is missing 21bp in the putative PEST sequence. The rectangle in (A) shows the position of the deletion in fragment S3/AS3. Yellow labelled characters are identical between both cDNAs.

6.3 STI might interact with Phospholipase ζ1

The detection of interactions between proteins can facilitate the understanding of the function of an unknown protein. Different Two-Hybrid screens were performed to identify putative interacting proteins for STI (Herrmann 2002; Kübbeler 2004). The significance of the candidates found in *S. cerevisiae* remains to be verified as all of them are found in another organism and an artificial test setup. One candidate (Gluc2) was chosen and constitutively expressed in *sti146* mutant background and wild-type (refer to chapter 5.10). Unfortunately no effect concerning trichome development was observed. It is likely that this candidate is not interacting with STI. Otherwise it might be that a phenotype was overlooked due to a marginal phenotypical change or redundancy which is observed often in *A. thaliana*. Nevertheless the last possibility seems to be more unlikely. Anymore a number of T-DNA insertion in candidates identified in the same screen were analysed for trichome phenotypes but none of them showed a visible change in trichome morphology (5.10). Different possibilities might explain this result. The Two-Hybrid screen itself was not suitable to screen for possible interactors. The verification of some interactors was not successful as none of them showed interaction in a direct Two-Hybrid (Cho-Chun Huang personal communication). Additionally the position of the T-DNA insertion was not optimal to yield a knock-out of the targeted gene and therefore a possible phenotype was not observed. Furthermore a possible interactor might be a regulator of STI and due to redundancy or a weak phenotype it wasn't detected. Finally one has to say that no real candidate for interaction with STI was identified and the screening procedure might be not suitable.

Therefore a new method was used which appears to be closer to the in vivo interaction situation. This method admits the use of plant extracts. Binding partners for two bait-proteins were identified, GFP:STI full-length which was used for the localisation also and fragment S5/AS7. Three proteins were identified by this method (Figure 31). Candidate A2 was identified as At3g09260 (β-Gluconidase PYK10). This gene was analysed by Nitz 2001 and is a root and seed specific expressed gene (Nitz et al. 2001). By identification of this candidate with a similar technical setup but a totally unrelated protein, it is likely that this candidate is a false positive interactor (Schrader 2006). Additionally a signal of similar size than PYK10 was detected in the negative control too. About the other candidate, A3 with similarity to AGAMOUS-LIKE 63 transcription factor, no publication is available so far. A possible connection between STI and this candidate is truly speculative, further studies are essential. However candidate A1 (Phospholipase Dα1) appeared in the patterning field before. Ohashi and coworkers showed that Phospholipase (PLD) ζ1 is a direct target of GL2 in root hair patterning (Ohashi et al. 2003). As many genes play a dual role in trichome and root patterning, e.g. CPC, GL2 and GL3 (Guimil et al. 2006; Schellmann et al. 2007),

it is conceivable that PLDs might be involved in trichome patterning. Nevertheless a closer investigation of this hypothesis is essential. The Phospholipase D family consists of 12 members in *A. thaliana* (Qin et al. 2002). The candidate identified as a putative binding partner for STI (PLDα1) was described by Zhang and coworkers before (Zhang et al. 2004). According to their results PLDα1 is stimulated by abscisic acid (ABA) and produces in turn phosphatidic acid (PA). PA is bound to the ABI1 a Protein Phosphatase 2C, which is tethered to the plasma-membrane. Thru this membrane relocation of ABI1 the response to ABA can take place. Whether PLDα1 plays a role in combination to STI is a matter of investigation for the future.

6.4   The putative STI homolog (STI-HOM) is functionally distinct

The *A. thaliana* genome contains one gene that shares 72% identical nucleotides compared to *STI*. Different approaches were utilized to determine whether this gene is important for STI function and STI-HOM is functionally redundant. Furthermore it is also conceivable that STI-HOM evolved a different function. The comparison of the gene- and transcript- structure revealed no major differences. Only the small intron located in the 5'UTR of the *STI* transcript is not found in *STI-HOM*. If this intron has a function like elevating the overall expression level (Callis et al. 1987) the expression levels for STI-HOM are expected to be decreased. RT-PCR showed that leaves contain lower amounts of STI-HOM than STI, but the data from whole genome-chips does not support this finding completely (Figure 22 C). Concerning to the expression data generated by these chips rosette leaves contain more transcript. Generally the RNA which is hybridized to the chips is generated from leaves of different age. If the expression is changing during maturation of the leave, the total expression level would reflect a mixture of the different expression levels observed in diverse leave stages. To elucidate this possibility further, plants expressing GUS under the control of the putative STI-HOM promoter were analyzed (Figure 33). And indeed the expression in leaves changed from an expression in the entire epidermis to expression restricted to the vasculature and stomata. Interestingly the expression of this construct was undistinguishable in wild-type and *sti146* mutant background. This is a first hint for a STI independent function.

To clarify a possible STI independent function the rescue efficiency of STI-HOM under the control of the putative STI promoter was analyzed. None of the lines could rescue the *sti* mutant phenotype. Furthermore the expression of STI-HOM under 35S promoter yielded no rescue again. Also the analysis of T-DNA insertion lines revealed no trichome phenotype. To exclude the possibility that a new phenotype is only visible in a double-mutant situation, a double-mutant situation was created too. However no trichome phenotype different from the *sti* single mutant was observed. In summary

it is possible that STI and STI-HOM have a different function in *A. thaliana*. However one has to mention that a functional relation between both proteins cannot be completely excluded. *Sti* mutants are epistatic to most other genes involved in trichome development. It is conceivable that STI-HOM is active downstream of STI and a trichome phenotype was therefore not observed. However a redundant function of STI-HOM is not likely.

6.5 Outlook

Until now the functional characterization of STI is still incomplete. The identification of a region leading to a dominant-negative effect after overexpression suggests that endogenous binding partners of STI cannot bind anymore. Nevertheless the fragment, showing this negative effect, still has a size of around 400bp. Further deletion analysis of this fragment and the subsequent overexpression might narrow down the fragment sufficient to show the same effect. Likely the negative effect is due to a competition for binding to endogenous STI or the fragment. However the effect observed might be a consequence of reduced STI RNA levels. This hypothesis should be tested by semi-quantitative RT-PCR.

If competition for binding partners is the more probable scenario an interactor search with Two-Hybrid or co-immuno precipitation might help. The co-immuno precipitation tests with full-length STI or fragment 2.6 fused to a fluorescent protein revealed already several promising candidates. Nevertheless further improvements for the experimental setup are needed to increase the amount of putative interacting protein and verify the results described in this work. The repetition of these experiments with the other available fragments might show changes of putative interacting proteins and might hint to different binding properties of regions from the STI protein.

The movement of the GFP-STI protein and one fragment again raises the question of the tracks used for the transportation to the target region. As drug studies did not allow a final decision whether they might by utilized for the transport, other experiments should be performed. GFP-STI should be crossed to microtubule and actin labelling lines and the simultaneous excitation of both proteins might show whether they serve as tracks for the transport of STI or not.

The analysis of the STI homolog protein STI-HOM showed no importance for STI function. It might be interesting to test which function this STI similar protein acquired during evolution. A closer look at different cell-types not analysed in this study might reveal other phenotypes not observed until now. In addition the analysis of the YFP tagged lines generated in this study in tissues and time-point not analysed might help too. In addition the confirmation of a *sti-hom* knock-out line might be analysed by chip-hybridisation experiments for changes in the expression pattern of different genes in the *A. thaliana* transcriptom. The identification of genes with altered expression can hint to the process this protein might be involved in if no visible phenotype is determined.

❖ Materials and Methods

6.6 Materials

6.6.1 Chemicals

Chemicals used during this thesis were purchased from Sigma (http://www.sigmaaldrich.com/), Roth (http://www.carl-roth.de/) and Merck (http://www2.merck-chemicals.com).

6.6.2 Kits

Preparations of small plasmid-DNA amounts were performed with the "peqGOLD Plasmid Miniprep Kit I" from Peqlab (http://www.peqlab.de/). If larger amounts of plasmid-DNA were needed bigger culture volumes were purified by the "QIAGEN Plasmid Midi Kit" from Qiagen (www.qiagen.de). Gel fragments were purified by the "MinElute Gel Extraction Kit" from Qiagen. The clean-up of PCR-reactions was done with the "High Pure PCR Product Purification Kit" from Roche (https://www.roche-applied-science.com).

6.6.3 Enzymes

Restriction endonucleases and DNA modifying enzymes were purchased from Fermentas (http://www.fermentas.com/). Different thermo stable DNA-polymerases were used during this work: Phusion™ polymerase (http://www.finnzymes.fi/), TaKaRa ExTaq™, Prime STAR™ (http://www.takarabioeurope.com/) and different PFU or TAQ from Fermentas.

6.6.4 Oligos

Oligos were synthesised by Invitrogen (http://www.invitrogen.com/), Sigma (http://www.proligo.com/), Biomers (http://www.biomers.net/) and Eurogentec (http://www.eurogentec.com/). The oligos used for the construction of any constructs in this study are listed in the appendix (6.9).

6.6.5 Plasmids

Different plasmids were used for general cloning purposes like subcloning of PCR-products (Table 13). These are pBluescript SK+ and pGEM-T easy. To generate gateway compatible entry-clones conventional restriction/ligation procedures were used with vectors pENTR1A and pENTR4. For the directional cloning of PCR-products vectors pDONR201 and pDONR207 were utilized. The overexpression of YFP or CFP tagged protein *in planta* was done with vectors pENSG/pEXSG or the pEarleyGate series.

Table 13: Plasmids used for molecular cloning purposes

Name	purpose	Gateway	source
pGEM™-T easy	cloning	no	Promega
pBluescript™ SK+	cloning	no	Stratagene
pENTR4	generation of gateway entry-clones	yes	Invitrogen
pENTR1A	generation of gateway entry-clones	yes	Invitrogen
pDONR201	generation of gateway entry-clones	yes	Invitrogen
pDONR207	generation of gateway entry-clones	yes	Invitrogen
pENSG-YFP/CFP	N-terminal YFP/CFP Tag, plant transformation	yes	lab of Jane Parker
pEXSG-YFP/CFP	C-terminal YFP/CFP Tag, plant transformation	yes	lab of Jane Parker
pEarleyGate 100	overexpression, plant transformation	yes	(Earley et al. 2006)
pEarleyGate 101	C-terminal YFP/CFP Tag, plant transformation	yes	(Earley et al. 2006)
pEarleyGate 104	N-terminal YFP/CFP Tag, plant transformation	yes	(Earley et al. 2006)
pEarleyGate 201	N-terminal HA-Tag, plant transformation	yes	(Earley et al. 2006)

6.6.6 Bacterial strains

Two different E. coli strains were used for the generation of plasmid DNA, DH5α and DB3.1. Strain DB3.1 is needed for the maintenance of Gateway plasmids harbouring the toxic ccdB gene.

DH5α: *sup*E44 Δ*lac*U169 (φ80*lacZ*ΔM15) *hsd*R17 *rec*A1 *end*A1 *gyr*A96 *thi*-1 *rel*A1

DB3.1: F$^-$ *gyr*A462 *end*A1 Δ(sr1-*recA*) *mcr*B *mrr hsd*S20(r$_B$-, m$_B$-) *sup*E44 *ara*-14 *gal*K2 *lac*Y1 *pro*A2 *rps*L20(Sm^R) *xyl*-5 λ- l*eu mtl*1

6.6.7 Yeast strains

One yeast strain (AH109) was used to perform the direct interaction assays.

AH109: *MATa, trp1-901, leu2-3, 112, ura3-52, his3-200, gal4Δ, gal80Δ, LYS2 : : GAL1$_{UAS}$-GAL1$_{TATA}$-HIS3, MEL1 GAL2$_{UAS}$-GAL2$_{TATA}$-ADE2, URA3::MEL1$_{UAS}$-MEL1$_{TATA}$-lacZ*

6.6.8 Plant lines

Several wild-types were used for crossings and transformation events: L*er*, Col and Ws. Different *sti* mutant alleles in several phenotypes were used too and not listed in this chapter any more. For a list of *sti* T-DNA mutants please refer to Table 6.

Table 14: T-DNA insertion lines used
SALK lines were generated at the Salk Institute (Alonso et al. 2003). Flag lines were generated at the INRA in Versailles (Brunaud et al. 2002). SAIL lines were established by Syngenta (Sessions et al. 2002). WiscDSLox lines were generated at the University of Wisconsin (http://www.hort.wisc.edu/krysan/2010/default.htm).

No.	Name	ecotype	purpose	source
1	*clasp034 =N583034*	Col	phenotypical characterisation of *at-clasp*	SALK
2	*clasp061=N620061*	Col	phenotypical characterisation of *at-clasp*	SALK
3	*clasp782=N549782*	Col	phenotypical characterisation of *at-clasp*	SALK
4	*FLAG_359A03*	Ws4	phenotypical characterisation of *sti-hom*	FLAG DB
5	*FLAG_332C01*	Ws4	phenotypical characterisation of *sti-hom*	FLAG DB
6	*N504184*	Col	phenotypical characterisation of *sti-hom*	SALK
7	*N539304*	Col	phenotypical characterisation of *sti-hom*	SALK
8	*N519116*	Col	characterisation of *the putative Sti interactor At5g42100*	SALK
9	*N805651*	Col	characterisation of *the putative Sti interactor At5g42100*	SAIL
10	*N509199*	Col	characterisation of *the putative Sti interactor At5g24650*	SALK
11	*N509251*	Col	characterisation of *the putative Sti interactor At5g24650*	SALK
12	*N628780*	Col	characterisation of *the putative Sti interactor At5g53320*	SALK
13	*N584853*	Col	characterisation of *the putative Sti interactor At5g53320*	SALK
14	*N545825*	Col	characterisation of *the putative Sti interactor At3g01340*	SALK
15	*N606213*	Col	characterisation of *the putative Sti interactor At3g01340*	SALK
16	*N833677*	Col	characterisation of *the putative Sti interactor At3g01340*	SAIL
17	*N834479*	Col	characterisation of *the putative Sti interactor At5g55180*	SAIL
18	*N843836*	Col	characterisation of *the putative Sti interactor At5g55180*	SAIL
19	*N622510*	Col	characterisation of *the putative Sti interactor At4g15930*	SALK
20	*WiscDsLox338A04*	Col	characterisation of *the putative Sti interactor At4g15930*	WiscDsLox
21	*N588836*	Col	characterisation of *the putative Sti interactor At1g53310*	SALK
22	*N565162*	Col	characterisation of *the putative Sti interactor At1g53310*	SALK
23	*N570605*	Col	characterisation of *the putative Sti interactor At1g53310*	SALK
24	*N572307*	Col	characterisation of *the putative Sti interactor At3g56880*	SALK
25	*N651487*	Col	characterisation of *the putative Sti interactor At3g56880*	SALK
26	*N541405*	Col	characterisation of *the putative Sti interactor At3g53180*	SALK
27	*N516332*	Col	characterisation of *the putative Sti interactor At3g53180*	SALK
28	*N572600*	Col	characterisation of *the putative Sti interactor At3g16400*	SALK
29	*N521165*	Col	characterisation of *the putative Sti interactor At1g25260*	SALK

6.6.9 Software

The in silico manipulation of DNA or Proteins and the preparation of diverse cloning steps was assisted by the "Vector NTI Suite 10" from Invitrogen (www.invitrogen.com). Picture manipulation was performed with "Photoshop" from Adobe (www.adobe.com), "GIMP" (www.gimp.org/) and "Irfanview" (www.irfanview.de/). The manipulation of confocal stacks was done with "LCS-Lite" from Leica (http://www.confocal-microscopy.com/) or "ImageJ" (http://rsb.info.nih.gov/ij/). Most figures were assembled with the vector-graphic program "Illustrator" from Adobe.

6.6.10 Microscopy

The analysis of fluorescent protein fusion was done with the DMRE fluorescent microscope from Leica (http://www.leica-microsystems.com/) attached to the KY-F70-3CCD from JVC (http://www.jvcpro.de/) controlled by the DISKUS software (http://www.hilgers.com/). The acquisition of optical section of fluorescent protein fusions was done by the TCS SP2 AOBS from Leica.

6.7 Methods

6.7.1 Molecular biology related methods

All standard molecular biology methods were performed according to two reference method compilations (Ausubel 1987; Sambrook et al. 2001). Only not very common methods or changed protocols are listed.

6.7.2 Plant related methods

Plant growth and maintenance:

Seeds were sawn onto wet soil and additional spraying with water allowed optimal germination results. These pots covered with a lid were put for at least three days into a 4°C cold room without light to break dormancy. Generally these pots were transferred to climate chambers with 24°C and 16 hours illumination. If slower plant growth was needed, for example for at-clasp mutant lines, pots were transferred to a growth chamber with 16°C.

Seed sterilisation:

For selection purposes or the later observation under the fluorescence microscope, seeds were sterilised and plated onto agar plates under sterile conditions.

Plant transformation:

Plant transformation were performed after the modified protocol from Clough and co-workers (Clough et al. 1998). Plants were grown until the first flowers are visible. At the same time 20 ml YEP medium are inoculated with the *A. tumefaciens* strain. After 2-3 days 5 ml of this preculture are transferred to a new 200 ml culture. After one day the cells are harvested by centrifugation for 30 min at 3000 rpm. The pellet is resuspended in 300 ml 10 % sucrose solution. After addition of 150 µl Silvet® the plants are dipped into this solution for 15-20 seconds. These plants are covered to preserve humidity and shifted to a room without direct sunlight for one day.

6.7.3 Biochemical related methods

All basic related methods are described in the following compilations (Coligan 1996; Sambrook and Russell 2001).

Protein extraction under denaturing conditions:

Whole plants or few leaves were ground in cracking puffer. After heating at 99°C for 10 minutes a centrifugation step removed most cell debris. Up to 15µl of these crude extract was loaded onto an SDS-page.

Cracking buffer: 60mM Tris/HCl pH8, 1% Mercaptoethanol, 10% Glycerol, 1% SDS, 0,01% Bromphenol blue

Immunoprecipitation:

Prior to the immunopreciptiation assay whole protein extracts were generated under native conditions. Plant material (0,3-1g) was ground in Lysis-buffer at 4°C which was complemented with 100µl "Complete protease inhibitor" and 17,5µl 1M DTT.

For the immunoprecipitation assay 1ml of the native extract was incubated with 120µl anti-GFP MicroBeads (Milteny Biotec) according to the supplied instructions. Different from this protocol the column was washed five times with 200µl Wash Buffer2. The elution was performed with 60µl Elution buffer preheated to 95°C at RT.

Lysis buffer: 50 mM TrisHCl (pH 8.0), 150 mM NaCl, 1% Triton X-100

Silverstaining

To allow the detection of precipitated proteins by mass spectrometry a compatible protocol was adopted (Blum et al. 1987). The gel was fixed in 50% MeOH/5% HAc for 20 min and subsequently washed 10min in 50% MeOH. After overnight washing in distilled water the gel was sensitized 1min with 0,02% sodium thiosulfate and washed two times 1min in water. The staining procedure was started by incubation the gel 20min in 0,15% silver nitrate/0,4% formalin. Afterwards the gel was washed two times one minute in distilled water and developed in 2% sodium carbonate/0,07% formalin until the staining showed sufficient contrast. The reaction was stopped by the application of 5% HAc. Bands were cut out and analysed by the Peptide Mass Fingerprint (PMF) method at the "Zentrale Bioanalytik (ZBA)" (http://www.zmmk-bioanalytik.de/).

6.8 Special Methods

6.8.1 Vector construction

Mapping of the putative localisation domain in STI

All fragments used for the detection of the localisation domain or the dominant negative fragment were generated by a PCR based approach. For a list of fragments used, refer to Table 7. Primers were designed to amplify 400bp or 1200bp of the *STI* cDNA. All primers incorporate attB1 respectively attB2 recombinase recognition sequences into the PCR-product for subsequent transfer to donor vectors. This recombination event was performed by LR- or BP-Clonase™ from Invitrogen according to the manufacturers instructions. After transfer of the PCR-product into

pDONR201 the fragment was sequenced. Correct constructs were transferred to pENSG-YFP/CFP or pEXSG-YFP/CFP with LR-clonase.

Table 15: The primer combinations used for the generation of STI fragments fused to YFP/CFP.

fragment	primers	size
S1/AS1	82 + 83	402
S2/AS2	84 + 85	399
S3/AS3	86 + 87	399
S4/AS4	90 + 89	399
S5/AS5	91 +92	405
S6/AS6	93 + 94	399
S7/AS7	95 + 96	399
S8/AS8	97 + 98	399
S9/AS9	99 + 100	399
S1/AS3	82 + 87	1200
S2/AS4	84 + 89	1197
S4/AS6	90 + 94	1203
S5/AS7	91 + 96	1203
S7/AS9	95 + 100	1253

STI under control of its endogenous promoter

The putative promoter was amplified with primers 367 and 368 incorporating recognition-sequences for AscI and ClaI. This 2,39 kb big construct was ligated, after phosphorylation, into the pBlueSk+ vector. Vector pENSG-YFP was cleaved with AscI and ClaI to release the original 35S promoter. After ligation of the putative STI promoter into the same sites the final vector with STI promoter is ready. As it is compatible to the Gateway™ system any entry-clone can be transferred into this vector. To analyse the expression of the putative *STI* promoter the GUS reporter-gene was transferred by a LR-reaction into this vector. The STI cDNA was transferred by LR-reaction too for the subsequent analysis of the rescue efficiency in *sti* mutant background.

STI-HOM under its endogenous promoter

The putative promoter of *STI-HOM* was handled in similar fashion. Due to the short distance of to the next upstream gene of *STI-HOM* only 1,5 kb of the 5'-prime region were amplified with primers 369 and 370. The following procedure was identical to the construction of the *STI* promoter containing vector.

At-CLASP under its endogenous promoter

The putative endogenous *At-CLASP* promoter was amplified with primers 365 and 366 incorporating AscI and XhoI recognition sequences. The following procedure was comparable to the *STI* and *STI-HOM* promoter. In contrast to these promoters the *pENSG-YFP* vector was digested with AscI and XhoI.

Production of the At-CLASP localisation- and rescue-constructs

Different constructs were generated to rescue the *at-clasp* mutant phenotype and to investigate the

localisation pattern. The production of the rescue construct with the putative *At-CLASP* promoter is described above. In addition rescue constructs with the full-length *At-CLASP* cDNA under control of the 35S promoter were constructed (Figure 12). Construct *35S::YFP:AT-CLASP* was generated by LR-reaction with the *At-CLASP* cDNA in pDONR207 and pEarleyGate 104 (Earley et al. 2006). Construct *35S::YFP:At-CLASP* was generated by LR-reaction with the *At-CLASP* cDNA without stop codon an *pEarleyGate 101*.

Construct *35S::YFP:Cortex* was generated by amplification of the C-terminal region of *At-CLASP* with primers 291 and 263. The PCR product was transferred into *pDONR207* by BP-reaction. A following LR-reaction with this donor vector and *pEarleyGate 104* yielded the final construct.

Construct *35S::YFP:A+B* was generated by amplification of the N-terminal region of *At-CLASP* with primers 276 and 299. The PCR product of 3,5kb size was transferred by BP-reaction into vector *pDONR207*. Via LR-reaction with the donor vector and *pEarleyGate 104* the final construct was generated.

❖ **Appendix**

Table 16: STI interactors identified in a Two-Hybrid screen (Herrmann 2002).

candidate	AGI	putative function or similarity	frame
250_37	At1g09760	U2 small nuclear ribonucleoprotein A	3
250_21	At1g19380	unknown protein	2
250_5	At1g25260	acidic ribosomal protein P0-related	3
250_44	At1g53310	PHOSPHOENOLPYRUVATE CARBOXYLASE 1	1
250_68	At1g74060	60S ribosomal protein L6 (RPL6B)	1
250_53	At3g01340	transport protein SEC13 family protein / WD40	3
250_45	At3g16400	MYROSINASE-BINDING PROTEIN-LIKE / PROTEIN-470	1
250_52	At3g44310	NITRILASE 1(NIT1)	1
250_84	At3g53180	glutamate-ammonia ligase	1
250_69	At3g56880	VQ motif-containing protein	2
250_92	At4g15930	dynein light chain, putative	1
250_29	At4g27450	unknown protein	1
250_77	At5g01790	unknown protein	3
250_13	At5g24650	mitochondrial import inner membrane translocase subunit	2
250_76	At5g42100	putative β-1,3,-Glucanase	3
250_60	At5g53320	leucine-rich repeat transmembrane protein	2
250_36	At5g62030	diphthamide synthesis DPH2 family protein	1

6.9 Primer list

All primers in Table 17 were used during this thesis. The purpose of every primer is listed too. Experiments and conditions of many primer pairs are listed at the place of description or in chapter 6.8.1 .

Table 17: Primers used during this thesis.

name	sequence	purpose
001_Gus-AS	TTGTTTGCCTCCCTGCTGCG	detection of GUS
002_Gus-S	CGTCCTGTAGAAACCCCAACC	detection of GUS
003_35S-AS	CCTCTCCAAATGAAATGAAC	detection of 35S promoter
004_35S-S	CGTACCCCTACTCCAAAAAT	detection of 35S promoter
005_bar_AS	AAACCCACGTCATGCCAG	detection of basta resistance gene
006_bar_S	CTGCACCATCGTCAACCACTAC	detection of basta resistance gene
007_T3	ATTAACCCTCACTAAAG	T3 promoter
008_rfa-S	CCCTTATACACAGCCAGTCT	detection of gateway cassettes
009_rfa-AS	GGAAGCATAAAGTGTAAAGC	detection of gateway cassettes
010_Sti-Seq4 anti	CTCTGTCCAATCAATTCCTC	sequencing of STI
011_Sti-Seq4	GAGTGTCATTTGCTGCCATC	sequencing of STI
012_Sti-Seq3 anti	GAGACATCAAGACTATTGGG	sequencing of STI
013_Sti-Seq3	GAAGAAGGAAGTACACCGGA	sequencing of STI
014_Sti-Seq6	TAGGAGGACTTCACTTTAGTA	sequencing of STI
015_Sti-seq2 anti	TTTCGCTTCATGGGAATGAT	sequencing of STI
016_Sti-anti	AAAAATCCTTGCGGTTGATG	sequencing of STI
017_Sti	GGAAGAAGAAAAAATGTCAGGTTC	sequencing of STI
018_Sti-Rek-anti	TCACCATAGGTCGAGAGA	generation of STI Entry-clone
019_Sti-Rek	ATGTCAGGTTCGAGAGTT	generation of STI Entry-clone
020_duc2 anti	TGCGTCAATGTAGCTGATAG	detection of duc gene
021_duc2	CCAACAGGAAGTGGAAAGAC	detection of duc gene
022_duc-AS	ACTTCCTGTTGGAGAGTTAA	detection of duc gene
023_GFP-sense	AATCTGCCCTTTCCAAAGAT	detection of GFP
024_TH-T anti	GGAGATTAAGAGGAGAAG	detection of TH gene
028_Gl3-Seq	GGTGGAAGAAATCATCGT	sequencing of GL3
029_Gl3	GTACCACAGAACATATTACGG	sequencing of GL3
030_Try-T anti	GGTATGTTTGTGGGAAGA	detection of TRY

031_duc2 Rek.anti	CTATGCTTCTGATCTCGG	generation of duc Entry-clone
032_CPC-T anti	TCTCTTCGTCTGTTGGCA	detection of CPC
035_Sti-Seq1 anti	GGGACAACGAGTAACTCGGT	sequencing of STI
036_duc2 Rek.	ATGGGCATATCTTCACTA	generation of duc Entry-clone
038_T1-T anti	TCGAACAGATTTGGAACC	detection of T1
039_Gl3-Rek.anti	TCAACAGATCCATGCAAC	generation of GL3 Entry-clone
040_an-Seq	TCTTACTTGACATTACAA	sequencing of AN
041_Gl3-anti	GTGAGTCCAACATTAACTTC	sequencing of GL3
042_Gl3-Rek	ATGGCTACCGGACAAAAC	generation of GL3 Entry-clone
043_duc2 Ext anti	AGGGATCATCACAGGAGAACTATG	sequencing of DUC
044_an-Seq 2 anti	TATCCATCTTTCAGTAGC	sequencing of AN
047_an-Seq3 anti	ATCCATTCTTCGAGCAGC	sequencing of AN
049_Gl3-Seq anti	ACTAAGCTCGTCGTCCAT	sequencing of GL3
051_an-Rek anti	TAATCGATCCAACGTGTG	generation of AN Entry-clone
052_an-Rek	ATGAGCAAGATCCGTTCG	generation of AN Entry-clone
053_duc Ext	AGGTTGAAGAAGGCATTGGAGAAC	sequencing of DUC
054_Sti-seq5 anti	AGCAACAACTTCTGCATCCG	sequencing of STI
055_Sti-Seq7	TGAAATGGTACTAAGGCGAA	sequencing of STI
056_Sti-Seq5	AGCAGAGACTGTTAAGCGAG	sequencing of STI
057_Sti-Seq2	TGTGGTATTCCATGTTATTG	sequencing of STI
059_gl1-T anti	CCATAAAGCGTTATTGCC	detection of GL1
060_STI_Prom rek anti	TTTTTCTTCTTCCTAAATTT	amplification of STI 5' region
061_duc_Prom rek anti	GTTCTCCAATGCCTTCTTCA	amplification of DUC 5' region
062_STI_Prom rek	TCAGGATTAATACTTCTAAT	amplification of STI 5' region
063_duc_prom rek	GGTGTCTTAAACCCGAGAG	amplification of DUC 5' region
068_an-Seq2	GTGAGGAAGTATGGATGG	sequencing of AN
069_T1_Rek-25_anti	GGTATCGAACAGATTTGG	generation of T1 Entry-clone truncated
070_T1-Rek.anti	TCAAAGGCAATACCCATT	generation of T1 Entry-clone truncated
071_TTG	GTCTCTTGAAAAATCCGACTGAC	sequencing of TTG1
073_TTG-anti	ACATCGGATCAATCCCATTG	sequencing of TTG1
074_CFP/YFP/GFP c-terminal SacI sense	ATGGTGAGCAAGGGCGAGGA	amplification of GFP, vector generation
075_CFP/YFP/GFP c-terminal EcoRI antisense	TTACTTGTACAGCTCGTCCA	amplification of GFP, vector generation
076_sti-AS	TCCAGGAGGAAGTAGTACCT	sequencing of STI
077_pHcRed1-C1 amino Hind3 sense	ATGGTGAGCGGCCTGCTGAAGGAGAGTATG	amplification of RFP, vector generation
078_pHcRed1-C1 Xba1 amino antisense	GTTGGCCTTCTCGGGCAGGT	amplification of RFP, vector generation
079_pEYFP-C1 c-terminal EcoRI Stop antisense	TTACTTGTACAGCTCGTCCATGC	amplification of YFP, vector generation
080_pHcRed1-C1 c-terminal Sac1 sense	ATGGTGAGCGGCCTGCTGAAGGAGAGTATG	amplification of RFP, vector generation
081_pHcRed1-C1 c-terminal EcoRI Stop antisense		amplification of RFP, vector generation
082_S1	ATGTCAGGTTCGAGAGTTTCG	generation of STI cDNA fragments
083_AS1	ATCACCACCATTCCTCGCATC	generation of STI cDNA fragments
084_S2	TCGTATCGTAGAGAAATACAA	generation of STI cDNA fragments
085_AS2	GTACGAACTAGTGGATAAAGC	generation of STI cDNA fragments
086_S3	AATATGTATGCTGTTCGTAAT	generation of STI cDNA fragments
087_AS3	AAGCTCATCATCACTAAGCCC	generation of STI cDNA fragments
089_AS4	TTCATGTCTGGGAAAAGTAAG	generation of STI cDNA fragments
090_S4	TCTACCAATTATGGAGAGCTT	generation of STI cDNA fragments
091_S5	GATTTTTGGGAACTTGATGGA	generation of STI cDNA fragments
092_AS5	CGAGATGCTGAAACTATGTTG	generation of STI cDNA fragments
093_S6	GAGCAGCTGAGTTTGCTGGGA	generation of STI cDNA fragments
094_AS6	ACTTTGCTTCAGCTGGGATCA	generation of STI cDNA fragments
095_S7	ATGCCTTCTCCTGGCACCACA	generation of STI cDNA fragments
096_AS7	CTGAGGCAGCTGCTCTATACT	generation of STI cDNA fragments
097_S8	CATGGGAAACTTATATCTATC	generation of STI cDNA fragments
098_AS8	AAAGACACACCTGGATCGATA	generation of STI cDNA fragments
099_S9	ATACGGGTAAAACCCGAAAGG	generation of STI cDNA fragments
100_AS9	GAAGGTAACATTAGAAGATGA	generation of STI cDNA fragments
101_Sti Prom 1,5 S	TCGATAAAAATATATTATGGC	amplification of STI 5' region
102_Sti Prom AS	ACTCAGATCCGAAACTCT	amplification of STI 5' region
103_STI Prom 2 S	CATAAACATTTATTTTCAC	amplification of STI 5' region
104_STI Prom 0,5kb	GGCTTTGACGAGACCCGA	amplification of STI 5' region
105_prey	GAAAGCAACCTGACCTACAGGAAAGAG	sequencing of prey constructs
106_ S004184_LP	TTGCTTCAATCCTTTTCATTGGA	detection of SALK_004184
107_ S004184_RP	CGAAAAATACAGCGAAGCCTTTC	detection of SALK_004184
108_ SALK_004775_LP	CCCTAAAACTTTTTAATACCCT	detection of SALK_004775
109_ SALK_004775_RP	TGGTTACGAAGATGCTCACCGA	detection of SALK_004775
110_G008A06_RP	TGGTGCTCAAGAGACATTTCACC	detection of GABI_008A06
111_G008A06_LP	TCTCTGTGTTACCACATTTTCATTG	detection of GABI_008A06
112_G320E08_LP	TTGGTAGAATGAACGAACACGTGAG	detection of GABI_320E08
113_G320E08_RP	TGTTGGAACCAGTTTCCCATTTG	detection of GABI_320E08
114_LBb1_SALK	GCGTGGACCGCTTGCTGCAACT	recovery of SALK LB sequences
115_o3144_Gabi	GTGGATTGATGTGATATCTCC	recovery of GABI T-DNA sequences

116_o8418_Gabi	GCAATGAGTATGATGGTCAATATG	recovery of GABI T-DNA sequences
117_o2588_Gabi	CGCCAGGGTTTCCCAGTCACGACG	recovery of GABI T-DNA sequences
118_o3269_Gabi	GAAGGCGGGAAACGACAATCTG	recovery of GABI T-DNA sequences
119 o10706_Gabi	GAACCCTAATTCCCTTATCTGGG	recovery of GABI T-DNA sequences
120 o10706AS_Gabi	CCCAGATAAGGGAATTAGGGTTC	recovery of GABI T-DNA sequences
121 o8409_Gabi	ATATTGACCATCATACTCATTGC	recovery of GABI T-DNA sequences
122 09525_Gabi	CCACACGTGGATCGATCCGTCG	recovery of GABI T-DNA sequences
123 LB AS_Gabi	TCTACATGGATCAGCAATGA	recovery of GABI T-DNA sequences
124 o8760_Gabi	GGGCTACACTGAATTGGTAGCTC	recovery of GABI T-DNA sequences
125 LBa1_SALK	TGGTTCACGTAGTGGGCCATCG	recovery of SALK T-DNA LB
126_CFP/YFP/GFP amino Xbal antisense	CTTGTACAGCTCGTCCATGC	tagging of CFP/YFP/GFP
129_EntrySeq2 anti	CTGGATGGCAAATAATGA	sequencing of entry-clones
131_EntrySeq	CTCGGGCCCCAAATAATGAT	sequencing of entry-clones
134_021165_LP	CGTCGGAGTTGGAAGTATCGC	detection of SALK_021165
135_021165_RP	TGGAGTTGGTCGCTGACTTTG	detection of SALK_021165
136_088836_LP	GTGTGGCGGTCAGATTCTTGC	detection of SALK_088836
137_088836_RP	TCTTGGATGGGTGGTGATCGT	detection of SALK_088836
138_070605_LP	GCAAAAGGGTCAAATCCAAAA	detection of SALK_070605
139_070605_RP	CAAAATTACGGAAGAATGCATGTTG	detection of SALK_070605
140_065162_LP	TTTTCACCTGCTTCGCTCTGAA	detection of SALK_065162
141_065162_RP	TCAACTTCCGTGCATTGACACA	detection of SALK_065162
142_045825_LP	ACCCGCCACACTGGTGTTTT	detection of SALK_045825
143_045825_RP	TGCTCATGGTTGTGTTCCCTG	detection of SALK_045825
144_106213_LP	CCAACAGGGTGTGCTTGGTCT	detection of SALK_106213
145_106213_RP	TCGCCTCTTTCGCTTTGTCTC	detection of SALK_106213
146_072600_LP	TCGTCCCGTTTATCTACTGCTGG	detection of SALK_072600
147_072600_RP	TGATTTAGTGATTTTGCGGTGG	detection of SALK_072600
148_041405_LP	TGGATGCCGGTTTAATTTGGA	detection of SALK_041405
149_041405_RP	CGATGTTCCTCAACCGCTTCT	detection of SALK_041405
150_016332_LP	CTTCGGTCACGCTTGTTCCAG	detection of SALK_016332
151_016332_RP	AAAGCTTAGAAACAGGATTGGA	detection of SALK_016332
152_072307_LP	TGAGATTAGTGTGTTGTAGTGGG	detection of SALK_072307
153_072307_RP	TTCGGTGGAAGTGGAGATGGA	detection of SALK_072307
154_151487_LP	TGCTGACGCGTGTCTTCTCCT	detection of SALK_151487
155_151487_RP	GGTCGGAGCTCCCAAATCTGT	detection of SALK_151487
156_122510_LP	TCTTTTAATTTTTACTTCCTGCGCT	detection of SALK_122510
157_122510_RP	CATGTGTATTGGTCATTTGGTTG	detection of SALK_122510
158_046196_LP	GCTCGTGGGCTTGGCCTAATA	detection of SALK_046196
159_046196_RP	AGGGATCTGATGGAGGGGTGA	detection of SALK_046196
160_141285_LP	TGCCGGACTGTTGAGTTCCTC	detection of SALK_141285
161_141285_RP	GAGTTTAAGTGGCTATATGACAATG	detection of SALK_141285
162_009251_LP	AATCCTCGACACACCAACCGA	detection of SALK_009251
163_009251_RP	AAAGCTCCCTGAACACCACCC	detection of SALK_009251
164_009199_LP	ATCGGAGAAAGTGAGCGGTCC	detection of SALK_009199
165_009199_RP	GCAATAAATGGCTGAAAGTGACA	detection of SALK_009199
166_019116_LP	CGCACTCAGGTCGTATAGGCG	detection of SALK_019116
167_019116_RP	TCTCATCGTCTCCTCCATCGG	detection of SALK_019116
168_128780_LP	ATGCAGCCATATCCTTTCCCG	detection of SALK_128780
169_128780_RP	TCCTGATCTCCATATTCCAGGTTTG	detection of SALK_128780
170_084853_LP	TATATCCCCGCGTAGACCCGT	detection of SALK_084853
171_084853_RP	TATCATCCACATGCCGGAACC	detection of SALK_084853
172_WisLox_p745=LB	AACGTCCGCAATGTGTTATTAAGTTGTC	detection of WisLox T-DNA LB
173_Sti_RT_S	ATTCTCGTTGCTTATATCGC	RT-PCR of STI
174_Sti_RT_AS	AGTTTTGATCTGCTTTCCAC	RT-PCR of STI
175_At1g14460_RT_S	GAAGAAGAGTAAGGAATTGG	RT-PCR of STI-HOM
176_At1g14460_RT_AS	TTTAGTGGGGAAATTCTCAG	RT-PCR of STI-HOM
177_At4g24790_RT_S	GGCAATAGCTGAGTTAGAA	RT-PCR of STI similar At4g24790
178_At4g24790_RT_AS	TGGAGTACACATAGCAGAAG	RT-PCR of STI similar At4g24790
179_At4g18820_RT_S	GTGAAAGACAAAAGCCTGCC	RT-PCR of STI similar At4g18820
180_At4g18820_RT_AS	GCTAACGCAGAGGAACCA	RT-PCR of STI similar At4g18820
181_At5g45720_RT_S	AGGAAAGGCGAAGCTGGT	RT-PCR of STI similar At5g45720
182_At5g45720_RT_AS	ACCGAGTATTTTTACGGCTAC	RT-PCR of STI similar At5g45720
183_CFP/YFP/GFP amino Hind3 Sense	ATGGTGAGCAAGGGCGAGGA	tagging of CFP/GFP/YFP
184_Gluc1_S_Rek	ATGGCTTCTTCTTCTCTG	generation of GLUC1 entry-clone
185_Gluc1_AS_Rek	CTAAATGTCTACGAAAAT	generation of GLUC1 entry-clone
186_Gluc1_AS_kein_Stop_Rek	AATGTCTACGAAAATTGT	generation of GLUC1 entry-clone
187_Gluc1_Seq1_S	GTGGGAGCTACAAAAGTCAA	sequencing of GLUC1
188_Gluc1_Seq2_S	CATCTTGGACTTCCACGTCA	sequencing of GLUC1
189_Gluc1_Seq3_S	TCTTTAACGAGAACATGAAG	sequencing of GLUC1
190_Gluc2_S_Rek	ATGGCGGTCTTCGTTTTA	generation of GLUC2 entry-clone
191_Gluc2_AS_Rek	TCAATGCCCTGTTGGAAA	generation of GLUC2 entry-clone

192_Gluc2_AS_kein_Stop_Rek	ATGCCCTGTTGGAAACTC	generation of GLUC2 entry-clone
193_Gluc2_Seq1_S	CCGAGACAACTGTACTAACC	sequencing of GLUC2
194_Gluc2_Seq2_S	CGTCGCATCTTATGGTGAAT	sequencing of GLUC2
195_Gluc2_Seq3_S	TGAGAGAAACTACGGGTTGT	sequencing of GLUC2
196_Gluc3_S_Rek	ATGGATCCCTCACACCA	generation of GLUC3 entry-clone
197_Gluc3_AS_Rek	TTAATATCCTGTCGGAAA	generation of GLUC3 entry-clone
198_Gluc3_AS_kein_Stop_Rek	ATATCCTGTCGGAAACTC	generation of GLUC3 entry-clone
199_Gluc3_Seq1_S	GTTCTCAAAGCATTATCCGG	sequencing of GLUC3
200_Gluc3_Seq2_S	TGATCAATGTCTATCCTTTC	sequencing of GLUC3
201_Gluc3_Seq3_S	GTCTCTTCTTCCCTGATGAG	sequencing of GLUC3
202_Sail_LB	TTCATAACCAATCTCGATACAC	recovery of SAIL LB-sequence
203_CFP_pEX_AS_Seq	TGAACTTCAGGGTCAGCTTG	tagging of CFP/GFP/YFP
204_Sti_Seq9_AS	GTCAGCGGTTTGTAACCA	sequencing of STI
205_Sti_gen._AS1	CAATTATTATGGATGAAGTA	generation of genomic STI enty-clone
206_Sti_gen._AS1_Rek	CAATTATTATGGATGAAGTA	generation of genomic STI enty-clone
207_Sti_Prom_Seq1	GGTTCGATGAAACATTAGTA	sequencing of STI 5' region
208_Sti_Prom_Seq2	AAACAAGAAGGATATTTCTAGT	sequencing of STI 5' region
209_Sti_Prom_Seq3	CCATTATAAAATTTCGCGAG	sequencing of STI 5' region
210_Sti_Prom_Seq4	GGTGATTACCATTAAAAGCA	sequencing of STI 5' region
211_Sti_Prom_Seq5	CGTTATAGGTAATGTCGTCT	sequencing of STI 5' region
212_Sti_Prom_Seq6	CAACATTTACCTCAGTGATT	sequencing of STI 5' region
213_Sti_Prom_Seq7	CAGGACAAAGATTCGGCCTT	sequencing of STI 5' region
214_Sti_Prom_Seq8	GAGAATTTTATCGATGATGG	sequencing of STI 5' region
215_Sti_Prom_Seq9	ATGTCACTAAATATTATTCAATG	sequencing of STI 5' region
216_Sti_Prom_Seq10	GTTCATTTCCATACCAAACT	sequencing of STI 5' region
217_Sti_Prom_Seq11	TCTGTTTAATGGATGTGCTA	sequencing of STI 5' region
218_Sti_Prom_Seq12	TTGTTAAACTCTTTTCAAGTC	sequencing of STI 5' region
219_Sti_Prom_Seq13	GAGATCAAACTGTCTCAGATTT	sequencing of STI 5' region
220_Sti_Prom_Seq14	CAAATGTAGGTGATTCTTTC	sequencing of STI 5' region
221_Sti_Prom_Seq15	GCTTCATGTTATTTATGCCACAACA	sequencing of STI 5' region
222_Sti_Prom_Seq16	CGTATTTCCAATTCCTCATC	sequencing of STI 5' region
223_Sti_Prom_Seq17	CCAGTTCCACCATCACCAGG	sequencing of STI 5' region
224_Sti_Prom_Seq18	CTCCAATTTGAATTTGATCG	sequencing of STI 5' region
225_Sti_Prom_Seq19	GTTCTCACTGAGAACTCTCG	sequencing of STI 5' region
226_Sti_Prom_Seq20	AGGGTTTTTCTGTCGAGAGT	sequencing of STI 5' region
227_Sti_Prom_Seq21	GCTCTATCCAATAACAACCG	sequencing of STI 5' region
228_Sti_Prom3-S	AGGATGTGTGTTTGGGCATG	sequencing of STI 5' region
229_Sti_Prom4-S	GTCTTGCTTAGTACGCATAG	sequencing of STI 5' region
230_Sti_Prom5-AS	AAACTCTCGAACCTGACATT	sequencing of STI 5' region
231_Sti_Prom6-AS	TCTTCTAATGTTACCTTCTG	sequencing of STI 5' region
232_Sti_Prom7-AS	CGATGGTGGAACTGGATGAG	sequencing of STI 5' region
233_At5g42100 anti	CTAAATGTCTACGAAAATTG	amplification of GLUC1
234_At5g42100 S	ATGGCTTCTTCTTCTCTGCA	amplification of GLUC1
235_At2g05790 AS	TTAATATCCTGTCGGAAACT	amplification of GLUC3
236_At2g05790 S	ATGGATCTCCTCACACCACT	amplification of GLUC3
237_uni51-S	CTGTTGGTGTGTCTATTAAATCG	sequencing of pUNI51
238_uni51-AS	TGGCTGGCAACTAGAAGGCAC	sequencing of pUNI51
239_Sim_S_Rek	ATGGATCTTGATTTAATA	generation of SIM entry-clone
240_Sim_AS_Rek	TCATCTTCGTGAACAAGA	generation of SIM entry-clone
241_Sim_S_EcoRI	ATGGATCTTGATTTAATACA	generation of SIM tagged cDNA
242_Sim_AS_PstI	TCATCTTCGTGAACAAGAAC	generation of SIM tagged cDNA
243_Gluc2_RT_S	TCTACTCATACTCTCTTCCTTC	RT-PCR of GLUC2
244_Gluc2_RT_AS	AACAGAGCGAACAGATAAAC	RT-PCR of GLUC2
245_Gluc3_RT_S	CTCATCTTCCTCCTCCTCCT	RT-PCR of GLUC3
246_Gluc3_RT_AS	GTCAATAAGTTCTGGTCGGA	RT-PCR of GLUC3
247_At1g14460_RT_S2	AGGATGGAGAAAGAGAAGAA	RT-PCR of STI-HOM
248_At1g14460_RT_AS2	AACAACACCAACAAGCTCAT	RT-PCR of STI-HOM
249_At4g18820_RT_S2	TGAGGTTGTTGTTGGTGATA	RT-PCR of At4g18820
250_At4g18820_RT_AS2	TTTGTGTTTTTTCTCCCCTG	RT-PCR of At4g18820
251_At2g02480_RT_S2	CGTGGGAAAGAGAAGAAGGTGT	RT-PCR of STI
252_At2g02480_RT_AS2	CTCCTCTACCATCACCACCG	RT-PCR of STI
253_At1g14460_AS	TCAATCTCTTTGTTGTTACC	amplification of STI-HOM cDNA
254_At1g14460_S	CTTTGATTCCTCCTTGGGTA	amplification of STI-HOM cDNA
255_At1g14460_S_Rek	ATGTCGGGTTTAAGGATT	generation of STI-HOM entry-clone
256_At1g14460_AS_Rek	TTACTTCCTTGGCCTAGC	generation of STI-HOM entry-clone
257_At1g14460_AS_ohne-Stop_Rek	CTTCCTTGGCCTAGCACA	generation of STI-HOM entry-clone
258_At1g14460_S	AGTTAGAGAAACAACAATGGA	amplification of STI-HOM cDNA
259_At5g45720_AS	TTGGATGATGGAAATGTTTG	detection of STI similar At5g45720
260_MK_prey_AS_innen5	AAGAATTTTCGTTTTAAAACCTAAGAGTC	sequencing of prey vectors M.Kübbler
261_MK_prey_S_innen4	TAACTATCTATTCGATGATGAAGATACCCC	sequencing of prey vectors M.Kübbler
262_MK_ad_5n_prey_S2	GGATGTTTAATACCACTACAATGGATGATG	sequencing of prey vectors M.Kübbler

263_Clasp_Rek_AS	TCAGGTGTCTGCGTCGAT	generation of At-CLASP entry-clone
264_Clasp_Rek_AS_ohne-Stop	GGTGTCTGCGTCGATAGG	generation of At-CLASP entry-clone
265_Clasp_Seq1_S	CTTGTTTGGATCTCCTTAAG	sequencing of At-CLASP cDNA
266_Clasp_Seq2_S	AAAGAGCAGTCCCAGGGCAA	sequencing of At-CLASP cDNA
267_Clasp_Seq3_S	AGAAATTCAACGATCAGTTG	sequencing of At-CLASP cDNA
268_Clasp_Seq4_S	GCTGAATCAACACATAGTATCAACA	sequencing of At-CLASP cDNA
269_Clasp_Seq5_S	TGATCCTCACCACAAGGTCG	sequencing of At-CLASP cDNA
270_Clasp_Seq6_S	ATTGGGACATCATCTGAGGA	sequencing of At-CLASP cDNA
271_Clasp_Seq7_S	GGACCAAGTACTTCAATCAAAT	sequencing of At-CLASP cDNA
272_Clasp_Seq8_S	GAGCCAAAGCGCGGATGTCC	sequencing of At-CLASP cDNA
273_Clasp_Seq9_AS	GGAGATCCAAACAAGAATCA	sequencing of At-CLASP cDNA
274_Clasp_Catma_S	ATGCTTGGGAAAGCATTTTTGC	RT-PCR of At-CLASP (CATMA)
275_Clasp_Catma_AS	ACTGAACCATAAGTACAAGCGGCTC	RT-PCR of At-CLASP (CATMA)
276_Clasp_Rek_S	ATGGAGGAAGCTTTAGAAATGGC	generation of At-CLASP entry-clone
277_duc2_Rek_AS_ohne-Stop	TGCTTCTGATCTCGGTTT	generation of DUC entry-clone
278_Cpr5_300_Rek.S	ATGATGATGAAGAAGAAG	generation of CPR5 entry-clone
279_Cpr5_300_Rek.AS	TTCTAATTCGGTTTTTGAA	generation of CPR5 entry-clone
280_Cpr5_340_Rek.AS	ATCCTCGATTCTCTTTAT	generation of CPR5 entry-clone
281_Cpr5-Seq1-AS	TTCGTCGAGCCATACCTAAC	sequencing of CPR5
282_Cpr5-Seq2-S	AACTCAAGGGAAAGAAGAAA	sequencing of CPR5
283_Cpr5-Seq3-S	ACAACTCTCTTGTGTCCCTC	sequencing of CPR5
284_Cpr5-Tag-AS	AACTTCTAGGAGGGACACAA	sequencing of CPR5
285_RAFL7-11_Vorne_AS	TGATCCATAACTTCGTATAA	identification of RAFL7-11 clones
286_RAFL7-11_Hinten_S	TCCGGCCATAAGGGCCTGATC	identification of RAFL7-11 clones
287_At1g14460_5'UTR_AS	AACAGTAAATATCTCATAGT	amplification of STI-HOM with UTRs
288_At1g14460_3'UTR_S	TATGTAAGATTTGTTTTCTG	amplification of STI-HOM with UTRs
289_Stichel_5'UTR_S	GAAATCGAAGGAAGCTGATT	amplification of STI with UTRs
290_Stichel_3'UTR_AS	GATGATAAATTAGAGCTTGAG	amplification of STI with UTRs
291_Clasp_Cortex_S	GGTCTAAATCTGACAAGCGTTG	generation of At-CLASP cortex frag.
292_EF1_S	ATGCCCCAGGACATCGTGATTTCAT	detection of EF1
293_EF1_AS	TTGGCGGCACCCTTAGCTGGATCA	detection of EF1
294_duc2neu_Rek_S	ATGGATTCGGTTGTTCCA	generation of DUC entry-clone
295_duc_Atg_S	ATGGATTCGGTTGTTCCATGG	gener. of DUC entry-clone new ATG
296_AttL1_AS	CAAGCCTGCTTTTTTGTACAAACTTG	detection of attL1 sites
297_duc2_AS	AGGCTAAATCACGTGTTGGCA	sequencing of DUC2
298_T7	AATACGACTCACTATAG	sequencing from T7 promoter
299_Clasp_+Stop_Rek_AS	AACGCTTGTCAGATTTAGACC	generation of At-CLASP entry-clone
300_SNP1_S_Sti01	GAACTGGTCACGTTCTTCGTCA	SNP for detection *sti01*
301_SNP1_AS_Sti01	TGGTACCATCCCAAGATCCAGCA	SNP for detection *sti01*
305_SNP2_S_Sti01	GGATGTGGTATTCCGTGTTACTG	SNP for detection *sti01*
306_SNP2_AS_Sti01	CCCACACAAAATGCTACTTCCG	SNP for detection *sti01*
307_STI_AS_Vorne	CTTTCCCACGACGATTAGTA	sequencing of STI
308_35s_S_peG201	ACAATCCCACTATCCTTCGC	sequencing of 35S
309_Sti.Rek-ohne Stop AS	TCTTCTAATGTTACCTTC	generation of STI entry-clone
310_Sti-fehlt S	TCCTCAATGTACAAGGTTTT	completion of STI-Col cDNA
311_Sti fehlt AS	TCATCGTCAGTTGCTCTAGA	completion of STI-Col cDNA
312_Sti-Riken-V2-Del_AS	ACATAGTTTCGCATCTCGAAGT	completion of STI-Col cDNA
313_Spiral1_Rek_S	ATGGGTCGTGGAAACAGC	generation of SPR1 entry-clone
314_Spiral1_Rek_AS	TTACTTGCCACCAGTGAAGAGATA	generation of SPR1 entry-clone
315_Invitrogen Eseq2 anti	GTAACATCAGAGATTTTGAGACAC	sequencing of entry-clones
316_Eb1A_Rek_S	ATGGCGACGAACATCGGA	generation of EB1A entry-clone
317_EB1A_Rek_AS	TTAGGCTTGAGTCTTTTC	generation of EB1A entry-clone
318_Eb1B_Rek_S	ATGGCGACGAACATTGGGATGATGG	generation of EB1B entry-clone
319_Eb1B_Rek_AS	TTAAGTTTGGGTCTCTGC	generation of EB1B entry-clone
320_Eb1C_Rek_S	ATGGCTACGAACATTGGG	generation of EB1C entry-clone
321_Eb1C_Rek_AS	TCAGCAGGTCAAGAGAGG	generation of EB1C entry-clone
322_Eb1C_Seq1	AGTTTATGCAGTGGATGAAA	sequencing of EB1
323_Eb1_AS_vorne	TCAAAGTTAACCTTGTGCAT	sequencing of EB1
324_Eb1B_Seq1_S	AAGGCCGACCACTAGACAAT	sequencing of EB1
325_Eb1A_Seq1_S	TTAACAGGCTTGTCAAAGGC	sequencing of EB1
326_Tua4_Rek_S	ATGAGAGAGTGCATTTCG	generation of TUA4 entry-clone
327_Tua4_Rek_AS	TTAGTATTCCTCTCCTTC	generation of TUA4 entry-clone
328_Tua4_Rek_AS_ohne Stop	GTATTCCTCTCCTTCATC	generation of TUA4 entry-clone
329_Tua4_Seq1	AGACTGTTGGTGGAGGTGAC	sequencing of TUA4
330_Tua4_Seq2	AGACTGTTGGTGGAGGTGAC	sequencing of TUA4
331_Tua4_Seq3	CATGATGGCTAAGTGTGACC	sequencing of TUA4
332_CFP_AscI_S_Carboxy	ATGGTTAGCAAAGGAGAAGA	tagging of CFP < vector contruction
333_CFP/GFP_SacI_AS_Carboxy	TTATTTGTATAGTTCATCCA	tagging of CFP < vector contruction
334_RFP_AscI_S_Carboxy	ATGGCCTCCTCCGAGGACGT	tagging of RFP < vector contruction
335_RFP_SacI_AS_Carboxy	TTAGGCGCCGGTGGAGTGGC	tagging of RFP < vector contruction
336_CFP_KpnI_S_Amino	ATGGTTAGCAAAGGAGAAGA	tagging of CFP < vector contruction

337_CFP/GFP_AscI_AS_Amino	TTTGTATAGTTCATCCATGC	tagging of CFP < vector contruction
338_RFP_KpnI_S_Amino	ATGGCCTCCTCCGAGGACGT	tagging of RFP < vector contruction
339_RFP_AscI_AS_Amino	GGCGCCGGTGGAGTGGCGGC	tagging of RFP < vector contruction
340_GFP_AscI_S_Carboxy	ATGGGTAAAGGAGAAGAACT	tagging of GFP < vector contruction
342_GFP_KpnI_S_Amino	ATGGGTAAAGGAGAAGAACT	tagging of GFP < vector contruction
343_pENS_Cerulean_S	ATGGTTAGCAAAGGAGAAGA	tagging for FP vector exchange
344_pENS-Cerulean_AS	TTTGTATAGTTCATCCATGC	tagging for FP vector exchange
345_pENS_RFP-Q66_S	ATGGCCTCCTCCGAGGACGT	tagging for FP vector exchange
346_pENS_RFP-Q66_AS	GGCGCCGGTGGAGTGGCGGC	tagging for FP vector exchange
347_pEX_Cerulean_S	ATGGTTAGCAAAGGAGAAGA	tagging for FP vector exchange
348_pEX_Cerulean_AS	TTATTTGTATAGTTCATCCA	tagging for FP vector exchange
349_pEX_RFP-Q66_S	ATGGCCTCCTCCGAGGACGT	tagging for FP vector exchange
350_pEX_RFP-Q66_AS	TTAGGCGCCGGTGGAGTGGC	tagging for FP vector exchange
351_Sti_Seq_hinten_Raus	ATGATACTAACTTCGGAAAC	sequencing of STI
352_At1g14460_Seq1_S	CAAAGTCAGAGATGGTGACA	sequencing of STI-HOM
353_At1g14460_Seq2_S	TGGGAGTCAATCTGTGTATC	sequencing of STI-HOM
354_At1g14460_Seq3_S	GGATATGAATCAGAATCAGG	sequencing of STI-HOM
355_At1g14460_Seq1_AS	GCGGCTCAACGACGAATCTC	sequencing of STI-HOM
356_Cerulean_Seq_S	ACCTGTCCACACAATCTGCC	sequencing out of cerulean
357_Cerulean_Seq_AS	GTATGTTGCATCACCTTCAC	sequencing out of cerulean
358_Clasp_cTerm_S_BamHI	TACTGGATCCAAGGATTCTGATTACACATTTG	At-CLASP pull-down constructs
359_Clasp_cTerm_AS_SalI	TCAGTCGACTCAGGTGTCTGCGTCGATAG	At-CLASP pull-down constructs
360_Clasp_Eb1-gro達S_BamHI	TACGGATCCGACTGGTCAATGCGTATTTC	At-CLASP pull-down constructs
361_Clasp_Eb1-gro達AS_XhoI	TACCTCGAGTCAAATTTCAGGGTTACCAGCGT	At-CLASP pull-down constructs
362_Clasp_Eb1-klein_S_BamHI	TCAGTCGACTCAGGTGTCTGCGTCGATAG	At-CLASP pull-down constructs
363_Clasp_Eb1-klein_AS_XhoI	TACCTCGAGTCATGAGTTCAGTCCGTCGTTAAGGGC	At-CLASP pull-down constructs
364_GST_S_Seq1	AGCAAGTATATAGCATGGCC	sequencing of GST
365_Clasp_5'_AscI_S	TAAGGCGCGCCATATTTCAAAGTAGAAATCACA	tagging of At-CLASP 5' UTR
366_Clasp_5'_XhoI_AS	GATCTCGAGACCAAACCACCGACGGACGA	tagging of At-CLASP 5' UTR
367_Sti-Prom-AscI-S	TATGGCGCGCCTGGTATTATAGTATTGATCACATTA	tagging of STI 5' UTR
368_Sti_Prom_ClaI_AS	TAGATCGATTTTTTCTTCTTCCTAAATTT	tagging of STI 5' UTR
369_Hom_Prom_AscI_S	TATGGCGCGCCGAATCGAAAATGAGCCGCGTGTAGT	tagging of STI-HOM 5' UTR
370_Hom_Prom_ClaI_AS	TAGATCGATTTTTCTTTCTTTCTCTCCAGAA	tagging of STI-HOM 5' UTR
371_Sti_N_pGex_BamHI_S	TATGGATCCATGTCAGGTTCGAGAGTTTC	STI pull-down constructs
372_Sti_N_pGex_XhoI_AS	TAACTCGAGTCACGAAACGATGGAGAGCAACAACT	STI pull-down constructs
373_Sti_C_pGex_BamHI_S	TATGGATCCGAGAGCGAAGGTTCCATTGC	STI pull-down constructs
374_Sti_C_pGex_XhoI_AS	TAACTCGAGTCATCATCTTCTAATGTTACCTTC	STI pull-down constructs
375_Sti_Seq10_S	TGAGGAAGAGTAATGTTGGT	sequencing of STI
376_Sti_Seq11_S	AATAGACATTCTTCTGGAGG	sequencing of STI
377_Sti_Seq12_S	AACATGGTTCACAGCGACTT	sequencing of STI
378_Flag_LB_LB4	CGTGTGCCAGGTGCCCACGGAATAGT	amplification of the FLAG T-DNA
379_FLAG_RB_RB4	TCACGGGTTGGGGTTTCTACAGGAC	amplification of the FLAG T-DNA
380_pJawohl_Intron_S	ACTTTTAGAGTCAACTCTCG	testing of pJawohl constructs
381_pJawohl_Intron_AS	AACACAGATTATCATCACTAAT	testing of pJawohl constructs
382_Gus_AS_Vorne_Raus	GCCCTGATGCTCCATCACTT	amplification out of GUS
383_Gus_S_Hinten_Raus	GGCTGGATATGTATCACCGC	amplification out of GUS
384_Hom_Prom_Seq1_S	CTCGGGATTCTCCTTCTTCT	sequencing of STI-HOM 5'
385_Hom_Prom_Seq2_S	AAACGTTGTCTCCATGTTAT	sequencing of STI-HOM 5'
386_Clasp_Prom_Seq1	AGACCATAACATAATAGTGG	sequencing of At-CLASP 5'
387_Sul_S_BcuI	AAAAATGGCTTCTATGATAT	tagging of *SUL* gene
388_SulI_AS_SacI	CTAGGCATGATCTAACCCTC	tagging of *SUL* gene
389_pENS-YFP_S_BcuI_Sul_del.	ACTAGTGGTAGATCCCCCTCGATCGA	introducing new sites into pENS
390_pENS-YFP_AS_SacI_Sul_del.	GAGCTCTGACCCCTAGAGTCAAGCAG	introducing new sites into pENS
391_Hyg_S_BcuI	ATGAAAAAGCCTGAACTCACCGCGA	tagging of *HYG* gene
392_Hyg_AS_SacI	CTATTTCTTTGCCCTCGGAC	tagging of *HYG* gene
393_SpeI+AgeI in XbaI_S Linker	CTAGCACTAGTACTACCGGTG	linker SpeI+AgeI in XbaI
394_SpeI+AgeI in XbaI_AS Linker	CTAGCACCGGTAGTACTAGG	linker SpeI+AgeI in XbaI
395_Sti_Seq_12_S	TGAAGCCTTGTGGGTACTGT	sequencing of STI
396_Sti_Prom_Seq-raus_AS_1	ACCTAACTGATGCCATAATA	sequencing of STI 5'
397_Hom_Prom_Seq-raus_AS_1	GCCTTAACGAGCTTATCATG	sequencing of STI-HOM 5'
398_Clasp_Ver_034	CCATAAACCGCCTCACCTCT	sequencing of At-CLASP
399_Agri_SeqL-B	GTAACATCAGAGATTTTGAGACAC	sequencing of AGRI clones
400_Sti_Prom_AS1	GTCAGCTCCTTCTTCAGATGC	sequencing of STI 5'
401_Sti_Prom_AS2	TAGAGAAAGATTAGTGAAT	sequencing of STI 5'
402_Sti_Prom_AS3	GGTTAAATGAGTTGATTCCTGA	sequencing of STI 5'
403_Sti_Prom_AS4	TGCATCATCTGATCATCAGTGAA	sequencing of STI 5'
404_Sti_Prom_AS5	CATCGATAAAATTCTCTCTTGTTGT	sequencing of STI 5'
405_Sti_Prom_AS6	CGACGAAATGTATAACATCACATG	sequencing of STI 5'
406_Sti_Prom_AS7	TTGGAGACTCGATCTCTTATTCTTA	sequencing of STI 5'
408_Sti_Prom_AS9	TTAGCCTTTGCATGTTGAGAA	sequencing of STI 5'
409_Sti_Prom_AS10	GTCTCAACATGGTAAGATAATCGAT	sequencing of STI 5'

410_TBR1_HPA2 CAPS-F_HpaII	ATACGGTTTAGTTTCGGTTCA	*tbr1* CAPS marker
411_TBR1_HPA2 CAPS-R_HpaII	CCAATTTTAGCCCGATATTT	*tbr1* CAPS marker
412_Agri 51	CAACCACGTCTTCAAAGCAA	sequencing of AGRI clones
413_Agri 56	TGGGGTACCGAATTCCTC	sequencing of AGRI clones
414_Agri 64	CTTGCGCTGCAGTTATCATC	sequencing of AGRI clones
415_Agri 69	AGGCGTCTCGCATATCTCAT	sequencing of AGRI clones
419_Clasp_S_RT1	ATGGAGGAAGCTTTAGAAATGG	At-CLASP RT-PCR primer
420_Clasp_AS_RT1	TAAGTACAAGCGGCTCGTCA	At-CLASP RT-PCR primer
421_Clasp_S_RT2	AAATGAGGTCTCCCGCGA	At-CLASP RT-PCR primer
422_Clasp_AS_RT2	TCCTGCAACAAGTCCTTCAA	At-CLASP RT-PCR primer
423_TFC-A_EAL-S	CAATGGCAACGATAAGGAAC	TFC-A detection
424_TFC-A_EAL-AS	GATTTAACACTCATCGCTG	TFC-A detection
425_TFC-A_Mutant_S1	CGTAATGCGAGCACACAAGTGA	TFC-A detection
426_TFC-A_Mutant_S2	CCATCATTGTATACTTGAC	TFC-A detection
427_Salk_RB-1	TTCGCCCAATAGCAGCCAGTC	detection of SALK tNDA RB
428_Salk_RB-2	CCAGTCATAGCCGAATAGCCTCTCC	detection of SALK tNDA RB
429_Kan_S	ATGATTGAACAAGATGGATTGCACG	detection of KAN
430_Kan_As	TCAGAAGAACTCGTCAAGAAGGCG	detection of KAN
431_Sti_RT-fl-S	GTGGCAGTTCGAGTCAGTTT	STI RT-PCR primer almost full-length
432_Sti_RT-fl-AS	GGAGTTCCCTTGACCTGTTT	STI RT-PCR primer almost full-length
433_Clasp_RT-fl-S	GAGCGGCTTGGTGATAGTAA	CLASP RT-PCR primer almost f.l.
434_Clasp_RT-fl-AS	CCTACCCACAAGCTTCGTTA	CLASP RT-PCR primer almost f.l.
435_Hom_RT-fl-AS	CGTCTCTCTCGACTTCTTCG	STI-HOM RT-PCR primer almost f.l.
436_Hom_RT-fl-S	TCTCATCCTTTCGCTCTCAC	STI-HOM RT-PCR primer almost f.l.
437_Sti_S_cNDA	GCGAAGCTGAGAGAGGAGAA	sequencing of STI
438_Sti-AS_cDNA	TCCAACAAATGCAACACAAAA	sequencing of STI
439_Sti-S-gen_60?	TCGGATGGTGGGATTGTTAT	sequencing of STI
440_Sti-AS-gen_60?	TTTATTCTCCGCGACAAACC	sequencing of STI
455_TFC-WT-Ident-S	ATCATCGCCTGGTTCGTTTC	TFC-A detection
456_TFC-WT-Ident-AS	GCAAGTGTGCCATTTCAAAGA	TFC-A detection

❖ List of literature

Adachi, S., et al. (2006). "Expression of B2-type cyclin-dependent kinase is controlled by protein degradation in Arabidopsis thaliana." Plant Cell Physiol **47**(12): 1683-6.

AGI, T. A. G. I. (2000). "Analysis of the genome sequence of the flowering plant Arabidopsis thaliana." Nature **408**(6814): 796-815.

Akhmanova, A., et al. (2001). "Clasps are CLIP-115 and -170 associating proteins involved in the regional regulation of microtubule dynamics in motile fibroblasts." Cell **104**(6): 923-35.

Alonso, J. M., et al. (2003). "Genome-wide insertional mutagenesis of Arabidopsis thaliana." Science **301**(5633): 653-7.

Altschul, S. F., et al. (1990). "Basic local alignment search tool." J Mol Biol **215**(3): 403-10.

Andrade, M. A. and P. Bork (1995). "HEAT repeats in the Huntington's disease protein." Nat Genet **11**(2): 115-6.

Andrade, M. A., et al. (2001). "Comparison of ARM and HEAT protein repeats." J Mol Biol **309**(1): 1-18.

Ausubel, F. M. (1987). Current protocols in molecular biology. Brooklyn, N. Y.

Media, Pa., Greene Publishing Associates ;

J. Wiley, order fulfillment.

Bergmann, D. C. and F. D. Sack (2007). "Stomatal Development." Annu Rev Plant Biol.

Blum, H., et al. (1987). "Improved silver staining of plant proteins, RNA and DNA in polyacrylamide gels." Electrophoresis **8**(2): 93-99.

Bouquin, T., et al. (2003). "The Arabidopsis lue1 mutant defines a katanin p60 ortholog involved in hormonal control of microtubule orientation during cell growth." J Cell Sci **116**(Pt 5): 791-801.

Bouyer, D. (2004). "Analysis of trichome differentiation in Arabidopsis thaliana: From cell fate initiation to cell death."

Brininstool, G. M. (2003). A ROLE FOR CONSTITUTIVE PATHOGEN RESISTANCE5 IN PROMOTING CELL EXPANSION IN ARABIDOPSIS THALIANA. Agricultural and Mechanical College, Louisiana State University.

Brown, D. and G. L. Waneck (1992). "Glycosyl-phosphatidylinositol-anchored membrane proteins." J Am Soc Nephrol **3**(4): 895-906.

Brunaud, V., et al. (2002). "T-DNA integration into the Arabidopsis genome depends on sequences of pre-insertion sites." EMBO Rep **3**(12): 1152-7.

Buchanan, B. B., et al. (2000). Biochemistry & molecular biology of plants. Rockville, Md., American Society of Plant Physiologists.

Bulinski, J. C. and G. G. Gundersen (1991). "Stabilization of post-translational modification of microtubules during cellular morphogenesis." Bioessays **13**(6): 285-93.

Burk, D. H., et al. (2001). "A katanin-like protein regulates normal cell wall biosynthesis and cell elongation." Plant Cell **13**(4): 807-27.

Callis, J., et al. (1987). "Introns increase gene expression in cultured maize cells." Genes Dev **1**(10): 1183-200.

Camilleri, C., et al. (2002). "The Arabidopsis TONNEAU2 gene encodes a putative novel protein phosphatase 2A regulatory subunit essential for the control of the cortical cytoskeleton." Plant Cell **14**(4): 833-45.

Chung, B. Y., et al. (2006). "Effect of 5'UTR introns on gene expression in Arabidopsis thaliana." BMC Genomics **7**: 120.

Churchman, M. L., et al. (2006). "SIAMESE, a plant-specific cell cycle regulator, controls endoreplication onset in Arabidopsis thaliana." Plant Cell **18**(11): 3145-57.

Clough, S. J. and A. F. Bent (1998). "Floral dip: a simplified method for Agrobacterium-mediated transformation of Arabidopsis thaliana." Plant J **16**(6): 735-43.

Coligan, J. E. (1996). Current protocols in protein science. Brooklyn, N.Y., Wiley.

Corda, D., et al. (2006). "The multiple activities of CtBP/BARS proteins: the Golgi view." Trends Cell Biol **16**(3): 167-73.

Cowan, N. J. and S. A. Lewis (1999). "A chaperone with a hydrophilic surface." Nat Struct Biol **6**(11): 990-1.

Day, C. D., et al. (2000). "Transgene integration into the same chromosome location can produce alleles that express at a predictable level, or alleles that are differentially silenced." Genes Dev **14**(22): 2869-80.

Deavours, B. E., et al. (1998). "Ca2+/calmodulin regulation of the Arabidopsis kinesin-like calmodulin-binding protein." Cell Motility and the Cytoskeleton **40**(4): 408-416.

Deeks, M. J. and P. J. Hussey (2003). "Arp2/3 and 'the shape of things to come'." Curr Opin Plant Biol **6**(6): 561-7.

Dhonukshe, P., et al. (2006). "Arabidopsis tubulin folding cofactor B interacts with alpha-tubulin in vivo." Plant Cell Physiol **47**(10): 1406-11.

Dhonukshe, P. and T. W. Gadella, Jr. (2003). "Alteration of microtubule dynamic instability during preprophase band formation revealed by yellow fluorescent protein-CLIP170 microtubule plus-end labeling." Plant Cell **15**(3): 597-611.

Di Cristina, M., et al. (1996). "The Arabidopsis Athb-10 (GLABRA2) is an HD-Zip protein required for regulation of root hair development." Plant J **10**(3): 393-402.

Drabek, K., et al. (2006). "Role of CLASP2 in microtubule stabilization and the regulation of persistent motility." Curr Biol **16**(22): 2259-64.

Dujardin, D., et al. (1998). "Evidence for a role of CLIP-170 in the establishment of metaphase chromosome alignment." J Cell Biol **141**(4): 849-62.

Dujardin, D. L. and R. B. Vallee (2002). "Dynein at the cortex." Curr Opin Cell Biol **14**(1): 44-9.

Earley, K. W., et al. (2006). "Gateway-compatible vectors for plant functional genomics and proteomics." Plant J **45**(4): 616-29.

Edgar, B. A. and T. L. Orr-Weaver (2001). "Endoreplication cell cycles: more for less." Cell **105**(3): 297-306.

El Refy, A., et al. (2003). "The Arabidopsis KAKTUS gene encodes a HECT protein and controls the number of endoreduplication cycles." Mol Genet Genomics **270**(5): 403-14.

Esch, J. J., et al. (2003). "A contradictory GLABRA3 allele helps define gene interactions controlling trichome development in Arabidopsis." Development **130**(24): 5885-94.

Folkers, U., et al. (1997). "Cell morphogenesis of trichomes in Arabidopsis: differential control of primary and secondary branching by branch initiation regulators and cell growth." Development **124**(19): 3779-86.

Folkers, U., et al. (2002a). "The cell morphogenesis gene ANGUSTIFOLIA encodes a CtBP/BARS-like protein and is involved in the control of the microtubule cytoskeleton." Embo J **21**(6): 1280-8.

Folkers, U., et al. (2002b). "The cell morphogenesis gene ANGUSTIFOLIA encodes a CtBP/BARS-like protein and is involved in the control of the microtubule cytoskeleton." Embo J **21**(6): 1280-8.

Fyvie, M. J., et al. (2000). "Mosaic analysis of GL2 gene expression and cell layer autonomy during the specification of Arabidopsis leaf trichomes." Genesis **28**(2): 68-74.

Galjart, N. (2005). "CLIPs and CLASPs and cellular dynamics." Nat Rev Mol Cell Biol **6**(6): 487-98.

Gard, D. L., et al. (2004). "MAPping the eukaryotic tree of life: structure, function, and evolution of the MAP215/Dis1 family of microtubule-associated proteins." Int Rev Cytol **239**: 179-272.

Gönczy, P., et al. (2000). Functional genomic analysis of cell division in C. elegans using RNAi of genes on chromosome III. **408:** 331-336.

Grennan, A. K. (2005). "Putative Arabidopsis arp2/3 complex controls leaf cell morphogenesis." Plant Physiol **139**(4): 1574-5.

Guimil, S. and C. Dunand (2006). "Patterning of Arabidopsis epidermal cells: epigenetic factors regulate the complex epidermal cell fate pathway." Trends Plant Sci **11**(12): 601-9.

Hamada, T., et al. (2004). "Characterization of a 200 kDa microtubule-associated protein of tobacco BY-2 cells, a member of the XMAP215/MOR1 family." Plant Cell Physiol **45**(9): 1233-42.

Herrmann, U. (2002). Identifikation neuer Interaktionspartner von Trichom-Entwicklungsgenen mit dem Hefe-Zwei-Hybrid-System.

Hong, R. L., et al. (2003). "Regulatory elements of the floral homeotic gene AGAMOUS identified by phylogenetic footprinting and shadowing." Plant Cell **15**(6): 1296-309.

Hulskamp, M. (2004). "Plant trichomes: a model for cell differentiation." Nat Rev Mol Cell Biol **5**(6): 471-80.

Hulskamp, M., et al. (1998). "Cell morphogenesis in Arabidopsis." Bioessays **20**(1): 20-9.

Hulskamp, M., et al. (1994). "Genetic dissection of trichome cell development in Arabidopsis." Cell **76**(3): 555-66.

Hussey, P. J., et al. (2002). "The plant cytoskeleton: recent advances in the study of the plant microtubule-associated proteins MAP-65, MAP-190 and the Xenopus MAP215-like protein, MOR1." Plant Mol Biol **50**(6): 915-24.

Ilgenfritz, H. (2000). Molekulare und genetische Charakterisierung von STICHEL.

Ilgenfritz, H., et al. (2003). "The Arabidopsis STICHEL gene is a regulator of trichome branch number and encodes a novel protein." Plant Physiol **131**(2): 643-55.

Inoue, Y. H., et al. (2000). "Orbit, a novel microtubule-associated protein essential for mitosis in Drosophila melanogaster." J Cell Biol **149**(1): 153-66.

Jefferson, R. A. (1989). "The GUS reporter gene system." Nature **342**(6251): 837-8.

Johnson, H. B. (1975). "Plant pubescence: an ecological perspective." Bot. Rev. **41**: 233-258.

Kandasamy, M. K., et al. (2002). "Functional nonequivalency of actin isovariants in Arabidopsis." Mol Biol Cell **13**(1): 251-61.

Kim, G. T., et al. (2002). "The ANGUSTIFOLIA gene of Arabidopsis, a plant CtBP gene, regulates leaf-cell expansion, the arrangement of cortical microtubules in leaf cells and expression of a gene involved in cell-wall formation." EmBO Journal **26**(6): 1267-1279.

Kirik, V., et al. (2001a). "CPR5 is involved in cell proliferation and cell death control and encodes a novel transmembrane protein." Curr Biol **11**(23): 1891-5.

Kirik, V., et al. (2002a). "The Arabidopsis TUBULIN-FOLDING COFACTOR A gene is involved in the control of the alpha/beta-tubulin monomer balance." Plant Cell **14**(9): 2265-76.

Kirik, V., et al. (2005). "Functional diversification of MYB23 and GL1 genes in trichome morphogenesis and initiation." Development **132**(7): 1477-85.

Kirik, V., et al. (2002b). "Functional analysis of the tubulin-folding cofactor C in Arabidopsis thaliana." Curr Biol **12**(17): 1519-23.

Kirik, V., et al. (2001b). "Ectopic expression of the Arabidopsis AtMYB23 gene induces differentiation of trichome cells." Dev Biol **235**(2): 366-77.

Kirik, V., et al. (2004a). "The ENHANCER OF TRY AND CPC1 gene acts redundantly with TRIPTYCHON and CAPRICE in trichome and root hair cell patterning in Arabidopsis." Dev Biol **268**(2): 506-13.

Kirik, V., et al. (2004b). "ENHANCER of TRY and CPC 2 (ETC2) reveals redundancy in the region-specific control of trichome development of Arabidopsis." Plant Mol Biol **55**(3): 389-98.

Knippers, R. and R. Knippers (1990). Molekulare Genetik. Stuttgart ; New York, G. Thieme.

Koornneef, M. (1981). "The complex syndrome of *ttg* mutants." Arabidopsis Information Service **18**: 45-51.

Koornneef, M., et al. (1982). "EMS-and radiation-induced mutation frequencies at individual loci in *Arabidopsis thaliana* (L.) Heynh." Mutation Research **93**: 109-123.

Kopczak, S. D., et al. (1992). "The small genome of Arabidopsis contains at least six expressed alpha-tubulin genes." Plant Cell **4**(5): 539-47.

Kost, B., et al. (1998). "A GFP-mouse talin fusion protein labels plant actin filaments in vivo and visualizes the actin cytoskeleton in growing pollen tubes." Plant J **16**(3): 393-401.

Kübbeler, M. (2004). "Untersuchung der Protein-Protein-Interaktionen von ANGUSTIFOLIA und STICHEL mit Hilfe des Hefe-Zwei-Hybrid-Systems."

Kurata, T., et al. (2005). "Cell-to-cell movement of the CAPRICE protein in Arabidopsis root epidermal cell differentiation." Development **132**(24): 5387-98.

Lansbergen, G. and A. Akhmanova (2006). "Microtubule plus end: a hub of cellular activities." Traffic **7**(5): 499-507.

Lansbergen, G., et al. (2004). "Conformational changes in CLIP-170 regulate its binding to microtubules and dynactin localization." J Cell Biol **166**(7): 1003-14.

Lee, S. B., et al. (2006). "BnNHL18A shows a localization change by stress-inducing chemical treatments." Biochem Biophys Res Commun **339**(1): 399-406.

Lemos, C. L., et al. (2000). "Mast, a conserved microtubule-associated protein required for bipolar mitotic spindle organization." Embo J **19**(14): 3668-82.

Luo, D. and D. G. Oppenheimer (1999). "Genetic control of trichome branch number in Arabidopsis: the roles of the FURCA loci." Development **126**(24): 5547-57.

Maiato, H., et al. (2005). "Drosophila CLASP is required for the incorporation of microtubule subunits into fluxing kinetochore fibres." Nat Cell Biol **7**(1): 42-7.

Marks, M. D. (1997). "Molecular genetic analysis of trichome development in *Arabidopsis*." Annual Review of Plant Physiology and Plant Molecular Biology **48**: 137-163.

Marks, M. D. and J. J. Esch (1992). "Trichome formation in *Arabidopsis* as a genetic model for studying cell expansion." Current Topics in Plant Biochemistry and Physiology **11**: 131-142.

Mas, P. (2005). "Circadian clock signaling in Arabidopsis thaliana: from gene expression to physiology and development." Int J Dev Biol **49**(5-6): 491-500.

Mathur, J. (2005). "The ARP2/3 complex: giving plant cells a leading edge." Bioessays **27**(4): 377-87.

Mathur, J. (2006). "Local interactions shape plant cells." Curr Opin Cell Biol **18**(1): 40-6.

Mathur, J. and N. H. Chua (2000). "Microtubule stabilization leads to growth reorientation in Arabidopsis trichomes." Plant Cell **12**(4): 465-77.

Mathur, J., et al. (2003a). "Mutations in actin-related proteins 2 and 3 affect cell shape development in Arabidopsis." Plant Cell **15**(7): 1632-45.

Mathur, J., et al. (2003b). "A novel localization pattern for an EB1-like protein links microtubule dynamics to endomembrane organization." Curr Biol **13**(22): 1991-7.

Mathur, J., et al. (2003c). "Arabidopsis CROOKED encodes for the smallest subunit of the ARP2/3 complex and controls cell shape by region specific fine F-actin formation." Development **130**(14): 3137-46.

Mathur, J., et al. (1999). "The actin cytoskeleton is required to elaborate and maintain spatial patterning during trichome cell morphogenesis in Arabidopsis thaliana." Development **126**(24): 5559-68.

Mauricio, R. and M. D. Rausher (1997). "Experimental Manipulation of Putative Selective Agents Provides Evidence for the Role of Natural Enemies in the Evolution of Plant Defense." Evolution **51**(5): 1435-1444.

Meinhardt, H. (1982). Models of biological pattern formation. London, New York, Paris, Academic Press.

Meinhardt, H. (1994). "Biological pattern formation: New observations provide support for theoretical predictions." BioEssay **16**(9): 627-632.

Mimori-Kiyosue, Y., et al. (2005). "CLASP1 and CLASP2 bind to EB1 and regulate microtubule plus-end dynamics at the cell cortex." J Cell Biol **168**(1): 141-53.

Mimori-Kiyosue, Y., et al. (2006). "Mammalian CLASPs are required for mitotic spindle organization and kinetochore alignment." Genes Cells **11**(8): 845-57.

Mineyuki, Y. (1999). "THE PREPROPHASE BAND OF MICROTUBULES: ITS FUNCTION AS A CYTOKINETIC APPARATUS IN HIGHER PLANTS." International review of cytology **187**: 1-49.

Mineyuki, Y. and B. A. Palevitz (1990). "Relationship between preprophase band organization, F-actin and the division site in Allium Fluorescence and morphometric studies on cytochalasin-treated cells." Journal of Cell Science **97**(2): 283-295.

Neer, E. J., et al. (1994). "The ancient regulatory-protein family of WD-repeat proteins." Nature **371**: 297-300.

Nita, A.-S. (2005). GENETIC MAPPING AND MOLECULAR CHARACTERIZATION OF tbr1 MUTANT IN ARABIDOPSIS THALIANA.

Nitz, I., et al. (2001). "Pyk10, a seedling and root specific gene and promoter from Arabidopsis thaliana." Plant Sci **161**(2): 337-346.

Ohashi, Y., et al. (2003). "Modulation of phospholipid signaling by GLABRA2 in root-hair pattern formation." Science **300**(5624): 1427-30.

Oppenheimer, D. G., et al. (1997). "Essential role of a kinesin-like protein in Arabidopsis trichome morphogenesis." Proc Natl Acad Sci U S A **94**(12): 6261-6.

Pasqualone, D. and T. C. Huffaker (1994). "STU1, a suppressor of a beta-tubulin mutation, encodes a novel and essential component of the yeast mitotic spindle." J Cell Biol **127**(6 Pt 2): 1973-84.

Payne, C. T., et al. (2000). "GL3 encodes a bHLH protein that regulates trichome development in arabidopsis through interaction with GL1 and TTG1." Genetics **156**(3): 1349-62.

Peach, C. and J. Velten (1991). "Transgene expression variability (position effect) of CAT and GUS reporter genes driven by linked divergent T-DNA promoters." Plant Mol Biol **17**(1): 49-60.

Pereira, A. L., et al. (2006). "Mammalian CLASP1 and CLASP2 cooperate to ensure mitotic fidelity by regulating spindle and kinetochore function." Mol Biol Cell **17**(10): 4526-42.

Perez, F., et al. (1999). "CLIP-170 highlights growing microtubule ends in vivo." Cell **96**(4): 517-27.

Pierre, P., et al. (1992). "CLIP-170 links endocytic vesicles to microtubules." Cell **70**(6): 887-900.

Pollard, T. D. and C. C. Beltzner (2002). "Structure and function of the Arp2/3 complex." Curr Opin Struct Biol **12**(6): 768-74.

Potikha, T. and D. P. Delmer (1995). "A mutant of Arabidopsis thaliana displaying altered patterns of cellulose deposition." Plant Journal **7**(3): 453-460.

Qin, C. and X. Wang (2002). "The Arabidopsis phospholipase D family. Characterization of a calcium-independent and phosphatidylcholine-selective PLD zeta 1 with distinct regulatory domains." Plant Physiol **128**(3): 1057-68.

Rechsteiner, M. and S. W. Rogers (1996). "PEST sequences and regulation by proteolysis." Trends Biochem Sci **21**(7): 267-71.

Rerie, W. G., et al. (1994). "The GLABRA2 gene encodes a homeo domain protein required for normal trichome development in Arabidopsis." Genes Dev **8**(12): 1388-99.

Rizzo, M. A., et al. (2004). "An improved cyan fluorescent protein variant useful for FRET." Nat Biotechnol **22**(4): 445-9.

Rogers, S., et al. (1986). "Amino acid sequences common to rapidly degraded proteins: the PEST hypothesis." Science **234**(4774): 364-8.

Sambrook, J. and D. W. Russell (2001). Molecular cloning : a laboratory manual. Cold Spring Harbor, N.Y., Cold Spring Harbor Laboratory Press.

Saraste, M., et al. (1990). "The P-loop--a common motif in ATP- and GTP-binding proteins." Trends Biochem Sci **15**(11): 430-4.

Schellmann, S. and M. Hulskamp (2005). "Epidermal differentiation: trichomes in Arabidopsis as a model system." Int J Dev Biol **49**(5-6): 579-84.

Schellmann, S., et al. (2007). "Epidermal pattern formation in the root and shoot of Arabidopsis." Biochem Soc Trans **35**(Pt 1): 146-8.

Schellmann, S., et al. (2002). "TRIPTYCHON and CAPRICE mediate lateral inhibition during trichome and root hair patterning in Arabidopsis." Embo J **21**(19): 5036-46.

Schnittger, A., et al. (1998). "Tissue layer and organ specificity of trichome formation are regulated by GLABRA1 and TRIPTYCHON in Arabidopsis." Development **125**(12): 2283-9.

Schnittger, A., et al. (2002). "Ectopic B-type cyclin expression induces mitotic cycles in endoreduplicating Arabidopsis trichomes." Curr Biol **12**(5): 415-20.

Schnittger, A., et al. (2003). "Misexpression of the cyclin-dependent kinase inhibitor ICK1/KRP1 in single-celled Arabidopsis trichomes reduces endoreduplication and cell size and induces cell death." Plant Cell **15**(2): 303-15.

Schrader, A. (2006). Charakterisierung von MIDGET mit Schwerpunkt auf Protein-Protein-Interaktionen.

Schubert, D., et al. (2004). "Silencing in Arabidopsis T-DNA transformants: the predominant role of a gene-specific RNA sensing mechanism versus position effects." Plant Cell **16**(10): 2561-72.

Sedbrook, J. C., et al. (2004). "The Arabidopsis sku6/spiral1 gene encodes a plus end-localized microtubule-interacting protein involved in directional cell expansion." Plant Cell **16**(6): 1506-20.

Seki, M., et al. (1998). "High-efficiency cloning of Arabidopsis full-length cDNA by biotinylated CAP trapper." Plant J **15**(5): 707-20.

Seki, M., et al. (2002). "Functional annotation of a full-length Arabidopsis cDNA collection." Science **296**(5565): 141-5.

Sessions, A., et al. (2002). "A high-throughput Arabidopsis reverse genetics system." Plant Cell **14**(12): 2985-94.

Sitte, P., et al. (1998). "Strasburger-Lehrbuch der Botanik. 34." Auflage, Gustav Fischer-Verlag, Stuttgart.

Small, J. V., et al. (2002). "How do microtubules guide migrating cells?" Nat Rev Mol Cell Biol **3**(12): 957-64.

Smith, T. F., et al. (1999). "The WD repeat: a common architecture for diverse functions." Trends Biochem Sci **24**(5): 181-5.

Snustad, D. P., et al. (1992). "The small genome of Arabidopsis contains at least nine expressed beta-tubulin genes." Plant Cell **4**(5): 549-56.

Szymanski, D. B., et al. (1998). "Control of GL2 expression in Arabidopsis leaves and trichomes." Development **125**(7): 1161-71.

Szymanski, D. B., et al. (1999). "Organized F-actin is essential for normal trichome morphogenesis in Arabidopsis." Plant Cell **11**(12): 2331-47.

Toledo-Ortiz, G., et al. (2003). "The Arabidopsis basic/helix-loop-helix transcription factor family." Plant Cell **15**(8): 1749-70.

Toufighi, K., et al. (2005). "The Botany Array Resource: e-Northerns, Expression Angling, and promoter analyses." Plant J **43**(1): 153-63.

Tsvetkov, A. S., et al. (2007). "Microtubule-binding proteins CLASP1 and CLASP2 interact with actin filaments." Cell Motil Cytoskeleton.

Vartiainen, M. K. and L. M. Machesky (2004). "The WASP-Arp2/3 pathway: genetic insights." Curr Opin Cell Biol **16**(2): 174-81.

Wada, T., et al. (2002). "Role of a positive regulator of root hair development, CAPRICE, in Arabidopsis root epidermal cell differentiation." Development **129**(23): 5409-19.

Wada, T., et al. (1997). "Epidermal cell differentiation in *Arabidopsis* determined by a *myb* homolog, *CPC*." Science **277**: 1113-1116.

Walker, J. D., et al. (2000). "SIAMESE, a gene controlling the endoreduplication cell cycle in Arabidopsis thaliana trichomes." Development **127**(18): 3931-40.

Wasteneys, G. O. (2002). "Microtubule organization in the green kingdom: chaos or self-order?" J Cell Sci **115**(Pt 7): 1345-54.

Watanabe, T., et al. (2004). "Interaction with IQGAP1 links APC to Rac1, Cdc42, and actin filaments during cell polarization and migration." Dev Cell **7**(6): 871-83.

Whittington, A. T., et al. (2001). "MOR1 is essential for organizing cortical microtubules in plants." Nature **411**: 610-613.

Yin, H., et al. (2002). "Stu1p is physically associated with beta-tubulin and is required for structural integrity of the mitotic spindle." Mol Biol Cell **13**(6): 1881-92.

Zhang, F., et al. (2003). "A network of redundant bHLH proteins functions in all TTG1-dependent pathways of Arabidopsis." Development **130**(20): 4859-69.

Zhang, W., et al. (2004). "Phospholipase D alpha 1-derived phosphatidic acid interacts with ABI1 phosphatase 2C and regulates abscisic acid signaling." Proc Natl Acad Sci U S A **101**(25): 9508-13.

Zhang, X., et al. (2005). "The IRREGULAR TRICHOME BRANCH loci regulate trichome elongation in Arabidopsis." Plant Cell Physiol **46**(9): 1549-60.

Zimmermann, P., et al. (2004). "GENEVESTIGATOR. Arabidopsis microarray database and analysis toolbox." Plant Physiol **136**(1): 2621-32.

❖ Danksagung

Bedanken möchte ich mich bei Martin Hülskamp der mir die Möglichkeit gab sowohl meine Diplom- als auch meine Doktorabeit in seinem Lehrstuhl durchzuführen. Die vielen Jahre die ich in seiner Arbeitsgruppe gearbeitet habe werde ich sicher nicht vergessen.

So besonders wurde die Zeit natürlich auch nur durch die Anwesenheit von allen Mitarbeitern von Lehrstuhl III wobei ich die ehemaligen nicht vergessen möchte. Eigentlich (soll ich ja nicht sagen) fällt mir niemand ein den ich nicht mochte.

Mein ganz besonderer Dank gilt Christine die mir bei einem wichtigen Teil des STICHEL Projektes eine sehr große Hilfe war. Nicht vergessen darf ich Irene die mir in den letzten Monaten auch viel geholfen hat und sich auch nicht beschwerte wenn es schon wieder „einige" Kisten zum absammeln gab.

Diese Arbeit wäre mit Sicherheit nie fertig geworden wenn nicht einige beim Korrigieren der kleineren oder größeren Unpässlichkeiten geholfen hätten. Besonders möchte ich an dieser Stelle Christoph und Norman erwähnen. Fast kein fehlender Literaturhinweis entging den Augen von Martina. Auch Dierk konnte mir per Telekorrektur noch so einige unschöne Formulierungen entreissen. Weiterhin war Birger eine große Hilfe bei der Erstellung des CLASP Dendrogramms.

Auch meinen Eltern und meinen Geschwistern möchte ich an dieser Stelle danken. Ohne euch hätte alles nur halb soviel Spass gemacht.

❖ **Erklärung:**

Ich versichere, dass ich die von mir vorgelegte Dissertation selbständig angefertigt, die benutzten Quellen und Hilfsmittel vollständig angegeben und die Stellen der Arbeit − einschließlich Tabellen, Karten und Abbildungen −, die anderen Werken im Wortlaut oder dem Sinn nach entnommen sind, in jedem Einzelfall als Entlehnung kenntlich gemacht habe; dass diese Dissertation noch keiner anderen Fakultät oder Universität zur Prüfung vorgelegen hat; dass sie − abgesehen von unten angegebenen Teilpublikationen − noch nicht veröffentlicht worden ist sowie, dass ich eine solche Veröffentlichung vor Abschluss des Promotionsverfahrens nicht vornehmen werde. Die Bestimmungen der Promotionsordnung sind mir bekannt. Die von mir vorgelegte Dissertation ist von Prof. Dr. Martin Hülskamp betreut worden.

Köln, den

❖ Lebenslauf

Name:	Herrmann
Vorname:	Ullrich
Adresse:	Buchenweg 71
	50859 Köln
Geburtsdatum:	12.08.1977
Geburtsort:	Frechen
Nationalität:	deutsch
Familienstand:	ledig

Ausbildung:

1997	Abitur an der Königin Luise Schule in Köln
1997-2001	Studium der Biologie an der Universität zu Köln in Biologie
2001-2002	Diplomarbeit am Botanischen Institut der Universität zu Köln unter Betreuung von Prof. Dr. Martin Hülskamp mit dem Titel:
	„Identifikation neuer Interaktionspartner von Trichom-Entwicklungsgenen mit dem Hefe-Zwei-Hybrid-System."
ab Nov. 2002	Promotion am Botanischen Institut der Universität zu Köln unter Betreuung von Prof. Dr. Martin Hülskamp mit dem Titel:
	„Two genes involved in trichome morphogenesis: Localisation and putative function of STI and At-CLASP in *A. thaliana*."

Köln im August 2007

Ullrich Herrmann